# FIRST DENSITY CORRECTION TO THE TRANSPORT COEFFICIENTS FOR A SQUARE WELL GAS: TEMPERATURE DEPENDENCE AND BOUND STATE EFFECTS

By

GREGORY E. GARLAND

A DISSERTATION PRESENTED TO THE GRADUATE SCHOOL
OF THE UNIVERSITY OF FLORIDA IN
PARTIAL FULFILLMENT OF THE REQUIREMENTS
FOR THE DEGREE OF DOCTOR OF PHILOSOPHY

UNIVERSITY OF FLORIDA

1984

# ACKNOWLEDGEMENTS

I would like to thank Professor James W. Dufty for his continuous aid and encouragement during my years of graduate study. I am grateful for the help of many people both professionally and as friends; in particular I would like to acknowledge J. V. Sengers, P. L. Coldwell, W. B. Streett, P. A. Egelstaff, Cristina, Frances, Jackie, Bob, Dean, Norm, Mark, Don, my father and especially my mother. Appreciation is also due to the rest of the faculty, staff and my fellow graduate students in the Department of Physics, whom I will miss greatly. Grants from the National Science Foundation and Petroleum Research Fund have supported this work. Mrs. Sharon Bullivant and Mrs. Yvonne Dixon deserve much credit for typing the manuscript quickly and accurately.

## TABLE OF CONTENTS

Page

ACKNOWLEDGEMENTS....................ii

ABSTRACT....................vi

CHAPTER

I. INTRODUCTION....................1

II. THE HARD SPHERE FLUID....................11
  A. Enskog Theory of Hard Spheres....................16
  B. Sengers et al., Calculation of the First Density Correction for Hard Spheres....................18
  C. Generalized Enskog Equation....................20
  D. Modified Enskog Theory....................27

III. FORMAL DENSITY EXPANSION OF THE TRANSPORT COEFFICIENTS.32

IV. CLASSICAL SQUARE WELL GAS....................43

V. EVALUATION OF THE CROSS TERM....................55
  A. Cross Term for the Shear Viscosity....................55
  B. Cross Term for the Thermal Conductivity....................62

VI. DISCUSSION....................72

APPENDICES
  A. CLUSTER EXPANSIONS OF THE TIME CORRELATION FUNCTIONS...85
  B. COLLISION OPERATORS FOR THE SQUARE WELL POTENTIAL......98
  C. SQUARE WELL TRAJECTORIES....................101

REFERENCES....................124

BIOGRAPHICAL SKETCH....................127

## LIST OF TABLES

Page

II.1 COMPARISON OF ENSKOG THEORY TO HARD SPHERE MOLECULAR DYNAMICS........................................19

IV.1 COLLISION INTEGRALS FOR THE SQUARE WELL POTENTIAL........54

V.1 CROSS TERM FOR THE SHEAR VISCOSITY.......................69

V.2 CROSS TERM FOR THE THERMAL CONDUCTIVITY..................70

V.3 BOLTZMANN SHEAR VISCOSITY AND THERMAL CONDUCTIVITY.......71

## LIST OF FIGURES

Page

I.1 ..........5

I.2 ..........7

II.1 ..........13

II.2 ..........15

II.3 ..........24

II.4 ..........26

II.5 ..........30

V.1 ..........61

V.2 ..........68

VI.1 ..........77

VI.2 ..........80

VI.3 ..........82

C.1 ..........103

C.2 ..........107

C.3 ..........111

Abstract of Dissertation Presented to the Graduate School
of the University of Florida in Partial Fulfillment of the
Requirements for the Degree of Doctor of Philosophy

# FIRST DENSITY CORRECTION TO THE TRANSPORT COEFFICIENTS FOR A SQUARE WELL GAS: TEMPERATURE DEPENDENCE AND BOUND STATE EFFECTS

By

GREGORY E. GARLAND

April 1984

Chairman: Dr. James Dufty
Major Department: Physics

The temperature dependence of transport properties of a moderately dense square well gas is studied in order to understand the effects of attractive forces (particularly bound states). The quantum cluster expansions of the Green-Kubo time correlation functions for the thermal conductivity, shear viscosity, and self-diffusion coefficients are given, and exact expressions to zeroth (Boltzmann level) and first order in the density are obtained. Specializing to Boltzmann statistics and the classical square well potential allows calculations of the kinetic-potential parts of the first density correction. Good agreement with molecular dynamics results is found, but quantitative differences from real fluids are observed. Possible reasons for the discrepancies are discussed. The important contributions to the remaining triple collision parts are discussed. A brief description of the utility and limitations of the hard sphere model is given for comparison. In particular, the dynamic structure factor is calculated for a dense fluid of hard spheres and compared with recent neutron scattering data for Krypton and molecular dynamics simulations.

# CHAPTER I
# INTRODUCTION

The evaluation of the equilibrium and dynamic properties of dense gases and liquids relies to a large extent on theories with various degrees of phenomenology or uncontrolled approximations, as might be expected in a system with such complicated many-body interactions. For equilibrium properties (e.g., the equation of state and other thermodynamic functions) there exists a rigorous theory, the cluster expansion method[1] developed by Ursell and Mayer, for finding these properties which can be used to test the phenomenological models. The cluster expansion generates a power series in the density whose first few coefficients are in a form suitable for practical calculation. Thus expressing the result of a phenomenological model in a similar series allows one to determine which effects the model properly predicts and those for which it fails. For dynamical properties (e.g., transport coefficients) there is at present no such theory to use as a benchmark beyond the low density Boltzmann limit. Although the attempts of Bogolubov and others[2] in finding a systematic derivation of the Boltzmann transport equation at first indicated that a density expansion similar to the virial expansion might be found, further analyses indicated two complications. Dynamic properties are in general non-analytic functions of the density[3], and the cluster expansion analogous to that used for equilibrium properties must be resumed partially to give the correct expression for a dynamical property as a function of the density. As a consequence there has been no rigorous calculation of transport properties beyond the low density Boltzmann result, except for Sengers et al.[4], calculation of the first order density corrections for hard sphere transport coefficients. The main portion of this work (Chapters III, IV, and V) will concern an extension of Sengers' work to a more realistic potential, so that the effects of the attractive part of the interaction on the transport properties may be examined. It is known that the temperature dependence of properties for both real fluids and potential models with attractive parts differ strongly from hard spheres particularly at low temperatures.[5] However, there is no adequate theory of these differences outside the Boltzmann limit. For example, a recent comparison between computer simulation and phenomenological models show that it is difficult to predict even the correct sign of the first order correction to the Boltzmann transport coefficients.[6] The simplest interaction which incorporates attractive forces is the square well potential,

$$\phi(r) = \begin{cases} \infty & r < \sigma \\ -\varepsilon_0 & \sigma < r < R\sigma \\ 0 & r > R\sigma, \end{cases} \tag{1.1}$$

where r is the relative separation of the particles and $\sigma$ and $R\sigma$ are the inner and outer radii of the well. The transport properties to be considered are the shear viscosity ($\eta$), thermal conductivity ($\lambda$), and self-diffusion (nD where n is the density). [The fourth coefficient, bulk viscosity ($\kappa$), is known to be of higher order in the density than the level considered here.] The square well potential is still highly idealized when compared to a more realistic potential such as the Lennard-Jones model; however, the square well model retains many of the simplifications of the hard sphere model that allow a more detailed treatment of the calculations. At the outset the square well appears to be a good compromise between ease of calculation and introduction of the qualitative features associated with realistic potential models (e.g., finite collision times and bound states), since the square well parameters may be adjusted to give a reasonably good fit to the second virial coefficient and coefficient of shear viscosity of the Lennard-Jones model (see Figures I.1 and I.2). However, it should be noted that the parameters chosen for the virial coefficient and those for the transport coefficients are in general quite different. Further comment on the quality of the square well potential as a model for fluid behavior will be given in Chapter VI.

Calculations with the hard sphere model can generally be taken to a much greater depth than with other potentials. For example, the first non-analytic density corrections to Sengers' results have been calculated.[7] More generally, the phenomenological Enskog model[8] provides a satisfactory estimate of the transport coefficients for hard spheres over a wide range of densities. Various ad hoc modifications of the Enskog model to represent other potentials have also been suggested.[8] Thus hard spheres and models based on hard spheres are still used in many problems. The ability of hard sphere models to predict the behavior of dense gases and liquids will be examined in Chapter II. There it will be seen that agreement of hard sphere kinetic theories with computer simulations of hard spheres is generally quite good over a range of

Figure I.1. Second virial coefficient, $B_2^* = B_2/b_0$, the square well potential (———) and the Lennard-Jones potential (- - -) as function of $T^* = kT/\varepsilon_0$. $R = 1.85$; $\varepsilon_{LJ}/\varepsilon_0 - 1.72\sigma$; $\sigma_{LJ}/\sigma = 1.077$; $b_0 = 2\pi\sigma^3/3$.

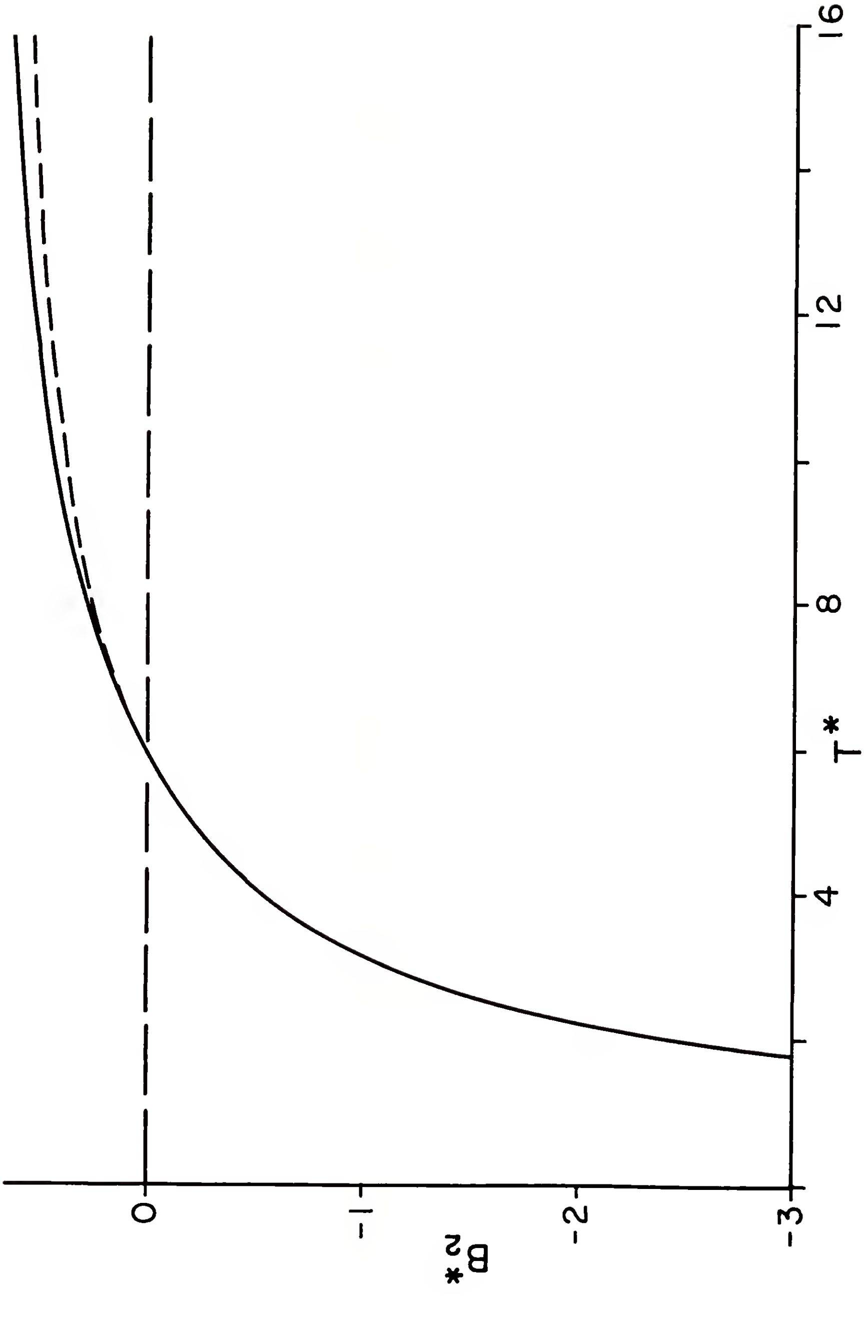
0
-1
-2
-3
$B_2^*$
4
8
12
16
$T^*$

Figure I.2. Shear viscosity, $\eta^*$, for the square well potential (-----) and the Lennard-Jones potential (o o o) as a function of $T^* = kT/\varepsilon_0$. $R = 1.96$; $\varepsilon_{LJ}/\varepsilon_0 = .717$; $\sigma_{LJ}/\sigma = 1.143$. Coefficients are normalized to hard spheres.

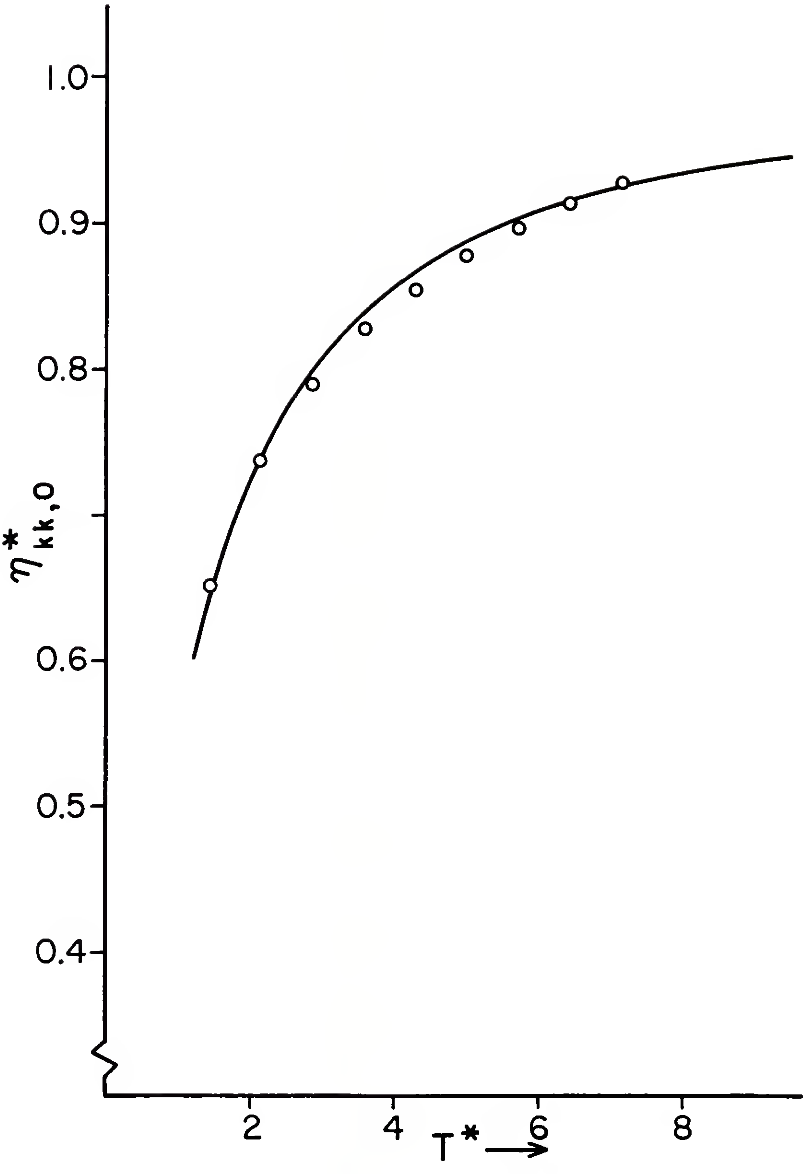
1.0
0.9
0.8
0.6
0.5
0.4
$\eta^*_{kk,0}$
2
4
6
8
$T^* \rightarrow$

densities, but that quantitative and qualitative differences can be found when compared to experimental data or other potential models.

The transport coefficients will be evaluated through their Green-Kubo formulas[9]; any general transport coefficient, $\xi = nD, \eta, \lambda, \kappa$, can be expressed as the Laplace transform of a time-correlation function:

$$\xi = \lim \frac{K_\xi}{V} \int_0^\infty dt e^{-\varepsilon t} \langle J_\xi(0) J_\xi(-t) \rangle, \tag{1.2}$$

where lim denotes $\lim_{\varepsilon \to 0} \lim_{V \to \infty}$. Here the limit $V \to \infty$ is the usual thermodynamic limit, taken with the density $n$ being constant; the constants $K_\xi$ and the fluxes $J_\xi$, which depend upon the particular transport coefficient being considered, will be defined in Chapter III. The brackets <...> denote an equilibrium grand canonical ensemble average. (There are other forms of these expressions, but all lead to the same final result.[10]) The fluxes can be separated into two parts: (1) a sum over single particle functions of the momentum, the 'kinetic' part $J_k$, and (2) a sum over two particle functions of the positions and momenta, the 'potential' part $J_\phi$.

$$J = J_k + J_\phi$$

$$J_k = \sum_\alpha a(\alpha)$$

$$J_\phi = \frac{1}{2} \sum_{\alpha \neq \beta} b(\alpha\beta). \tag{1.3}$$

As a result one may separate three contributions to the transport coefficients corresponding to the kinetic-kinetic term, the kinetic-potential cross terms, and the potential-potential terms in the time correlation function:

$$\xi = \xi_{kk} + 2\xi_{\phi k} + \xi_{\phi\phi}. \qquad (1.4)$$

This form is convenient for comparison with computer simulations[11], and to find the first density correction only the first two terms, $\xi_{kk}$ and $\xi_{\phi k}$, need be considered since the last term can be shown to be of higher order in the density. In a manner analogous to the cluster expansion methods of equilibrium statistical mechanics, a density expansion of (1.4) has been derived[12], allowing identification of both the Boltzmann result and first density correction terms. (There has been extensive discussion of the resummations of this expansion which give the non-analytic portions of the density dependence[7]; the first two terms in the series remain unchanged.) In Appendix A, an extension of this classical cluster expansion for repulsive potentials is given to include quantum effects and potentials with bound states. Accordingly this work will analyze various contributions to the first density correction to transport coefficients for a square well gas in an attempt to identify contributions due to the potential part of the fluxes, Enskog-like corrections to two body scattering, three body scattering events, and bound states contributions--in particular monomer-dimer scattering and dimer formation.

The results of the following chapters are as follows. In Chapter II applications of the hard sphere fluid are reviewed. The Enskog theory[8] is compared with molecular dynamics and the rigorous results of Sengers et al.[4] The related theory for time correlation functions, called the generalized Enskog theory[13], is reviewed and calculations of the dynamic structure factor, $S(k,\omega)$, are presented. The comparison with recent neutron scattering data[14] and molecular dynamics for hard spheres[15] and Lennard-Jones fluids[16] is discussed. The modified Enskog theory[17], and ad hoc adaptation of the Enskog theory to real fluids is also discussed. In Chapter III (and in Appendix A) the density expansion for the hydrodynamic transport coefficients is made. The quantum mechanical form of the fluxes, ensemble average, and cluster expansion is presented in a compact and general manner. The expressions giving the Boltzmann transport coefficient and its first order correction are identified for $\eta$, $\lambda$ and $nD$. The specialization to classical mechanics and the square well potential is made for these results and is given in Chapter IV. The Boltzmann contribution is evaluated over a wide range of temperatures and compared to existing results. The contribution to the first density correction by $\xi_{\phi k}$ is given for in Chapter V for $\xi = \eta, \lambda$. Both the scattering states and bound states contributions are evaluated, the results agreeing with computer simulation. Contrasts are made with the behavior of real fluids and the Enskog theory. Finally in Chapter VI these results are summarized and discussed. The large contribution from bound states for $\xi_{\phi k}$ is further analyzed. Comparison is made between the triple collision contribution to $\xi_{kk,1}$, based on estimates from molecular dynamics, for the square well potential and Sengers' hard sphere calculations.

# CHAPTER II
# HARD SPHERE FLUID

The hard sphere fluid has been a popular model both because theoretical calculations are easier with such a simple model and because for many years the only reasonably successful model for dense fluids was the Enskog model for hard spheres. The simple nature of the interaction also has led to extensive computer simulation over the fluid phase so the 'experimental' properties are well known, giving an easy method of checking theoretical models.[18] The primary objection to the hard sphere model is an essentially trivial temperature dependence. Figure II.1 illustrates the difference between the temperature dependence of transport coefficients for hard spheres and for the Lennard-Jones potential, in the Boltzmann limit. At finite densities another qualitative difference is the formation of bound states (dimerization) for potentials with attractive parts. Figure II.2 shows the fraction of dimers for the Lennard-Jones gas at $n\sigma^3 = .01$. Thus it can be argued that bound state effects such as nonomer-dimer scattering will have a significant effect at lower temperatures.

An objective of this research is to provide exact results for the first density correction to the Boltzmann results to serve for guidance and interpretation of phenomenological models of the dense gas phase. As mentioned above, the Enskog theory describes dense gas transport properties quite well over a wide range of densities. However, the only firm theoretical justification of the Enskog theory is given by comparison

Figure II.1. Boltzmann transport coefficients for the Lennard-Jones potential relative to hard spheres. Horizontal line is hard sphere limit.

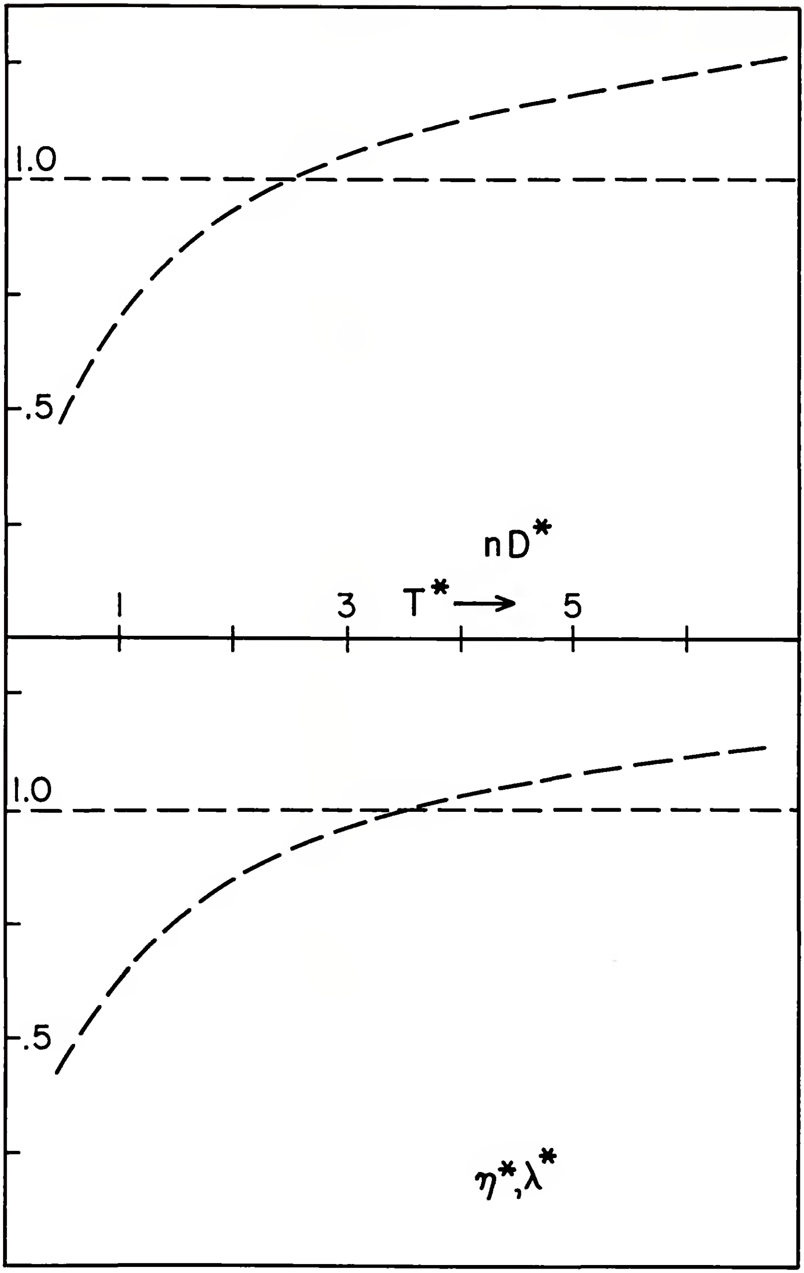
1.0
.5
nD*
1
3
T* ⟶
5
1.0
.5
η*, λ*

Figure II.2. Fraction of dimers for the Lennard-Jones potential at $n\sigma^3 = 0.1$; $\sigma = 3.405$, $\varepsilon/k = 119.8$°K potential parameters for Argon.

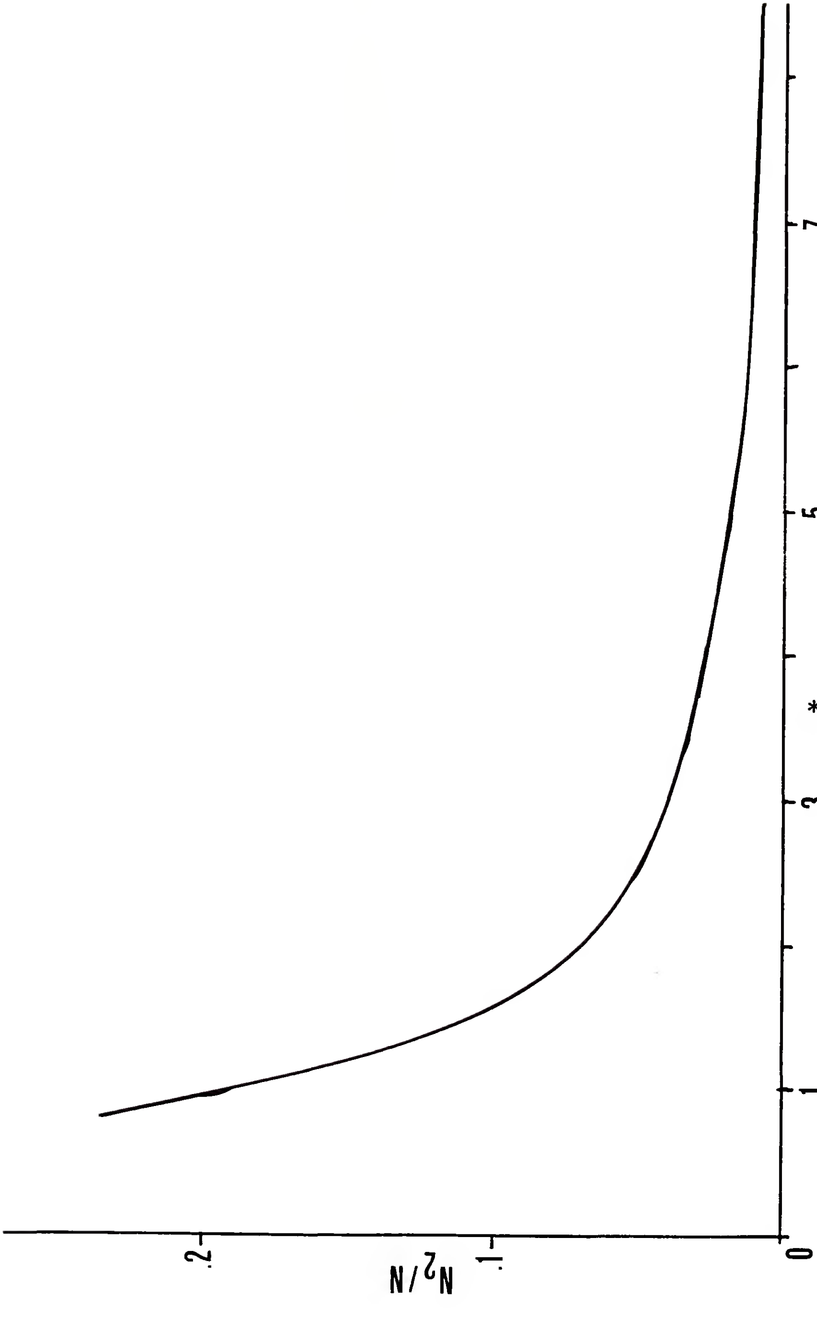

.2
.1
0
$N_2/N$
1
3
5
7
$T^*$

with Sengers et al. evaluation of the exact first density corrections. These results and a related calculation of the dynamic structure factor are reviewed briefly in order to indicate the utility of the Enskog model and its range of validity. The application of the concepts used in the Enskog theory to other potentials has been widely used, but prior to the work presented here there have been no exact results for a critical analysis of these theories. The modified Enskog theory is also briefly described, and it is shown to be inadequate for the square well model.

## A. Enskog Theory of Hard Spheres.[8]

The Enskog theory was formulated as a phenomenological modification of the Boltzmann transport equation using intuitive concepts that are well defined only for a hard sphere fluid. While retaining the simplicity of two body dynamics Enskog introduced modifications to account for the finite size of the particles, introducing the concepts of collisional transfer and excluded volume. The first is essentially the transport of a property through the effect of the interparticle potential rather than by moving particles of the fluid from one point to another (Various definitions in the literature of what is meant by collisional transfer are not exactly equivalent, so care should be exercised when comparing different works); the second is a modification of the probability of a collision due to presence of other particles in the fluid. Unlike other potentials, the instantaneous nature of the hard sphere collision allows precise definition of both the difference in the positions of the particles and of the pair correlation function at the time of the collision. The Enskog equation gives the exact binary collision dynamics for hard spheres and correctly identifies the dominant contribution from higher order collisions to first order in the density.

Comparing the theoretical prediction to simulations for hard spheres one notes the equation of state is exact for hard spheres (see (2.9)); there is also quite good agreement with the transport coefficients for densities $n^* < .1$ and only ≈ 30% error at $n^* = 0.3$ ($n^* = n\sigma^3$, where $\sigma$ is the force range). A summary of the Enskog predictions for the transport coefficients is given below

$$\eta_E = \eta_0^{H.S.}\left(\frac{1}{g(\sigma)} + .8\,\frac{2\pi}{3}\,n^* + .761\,g(\sigma)\left(\frac{2\pi}{3}\,n^*\right)^2\right)$$

$$\lambda_E = \lambda_0^{H.S.}\left(\frac{1}{g(\sigma)} + 1.2\,\frac{2\pi}{3}\,n^* + .755\,g(\sigma)\left(\frac{2\pi}{3}\,n^*\right)^2\right)$$

$$nD_E = nD_0^{H.S.}/g(\sigma).$$

$$\kappa_E = \eta_0^{H.S.}\left(1.002\,g(\sigma)\left(\frac{2\pi}{3}\,n^*\right)^2\right) \qquad (2.1)$$

Here $g(\sigma)$ is the pair correlation function at contact and $\lambda_0^{H.S.}$, $\eta_0^{H.S.}$, and $D_0^{H.S.}$ are the Boltzmann value for the transport coefficients:

$$\eta_0^{H.S.} = \frac{5}{16\sigma^2}\left(\frac{m}{\beta\pi}\right)^{1/2}$$

$$\lambda_0^{H.S.} = \frac{75\ k_B}{64m\sigma^2}\left(\frac{m}{\beta\pi}\right)^{1/2}$$

$$nD_0^{H.S.} = \frac{3}{8m\sigma^2}\left(\frac{m}{\beta\pi}\right)^{1/2} . \qquad (2.2)$$

Thus one sees that although some density dependence is included, the temperature dependence is the same as in the Boltzmann case. A comparison of the Enskog predictions for transport data from molecular dynamics[19] is shown in Table II.1.

Direct comparison of the Enskog theory to experiment does not show such good agreement; however, by using the low density transport data to define a temperature dependent hard sphere diameter, one gets reasonably good agreement with experiment[20] (~ 10% error at the critical density).

## B. Sengers et al. Calculation of the First Density Correction for Hard Spheres

As mentioned above, the simple nature of hard sphere dynamics makes theoretical calculations easier. In particular only sequences of binary collisions occur so that the binary collision expansion[23] of the kinetic equation for hard spheres is particularly useful. It can be shown that for three hard spheres interacting in three dimensions there is only a finite number of binary collisions; so the expansion terminates after a few terms. Using this, Sengers' group was able to evaluate the first density correction to the hard sphere transport coefficients.[4] The results are in good agreement with the Enskog values (~ 10%), and they were able to identify which types of collisions were included in the Enskog theory and which were neglected. A parallel of this analysis with the square well model is not possible exactly; however, some of the collision sequences for scattering by square wells can be related to similar sequences for hard spheres and may thus be considered as having the same relative importance for determining the square well transport coefficients.

TABLE II.1 Comparison of Enskog Theory to Hard Sphere Molecular Dynamics

| $n\sigma^3$ | $D/D_E{}^a$ | $D/D_E{}^b$ | $\eta/\eta_E$ | $\lambda/\lambda_E$ | $\kappa/\kappa_E$ |
|---|---|---|---|---|---|
| .0071 | 1.00 | 1.02 | 1.01 | .98 | .9 |
| .0354 | 1.01 | 1.04 | 1.01 | .99 | 1.0 |
| .0707 | 1.03 | -- | .99 | -- | -- |
| .1414 | 1.09 | 1.16 | .99 | .97 | .9 |
| .1768 | 1.13 | -- | -- | -- | -- |
| .2357 | 1.16 | 1.34 | 1.02 | 1.00 | .98 |
| .2828 | 1.17 | -- | -- | -- | -- |
| .3536 | 1.06 | 1.27 | 1.10 | 1.07 | 1.2 |
| .3928 | .95 | 1.15 | 1.10 | 1.03 | 1.1 |
| .4419 | .70 | .84 | 1.44 | 1.05 | 1.1 |
| .4714 | -- | .58 | 2.16 | 1.05 | .6 |

Note: Ratio of hard sphere transport coefficients to the values predicted by the Enskog theory. Column headed by $D/D_E{}^a$ is for 108 particle simulation; column headed by $D/D_E{}^b$ is an extrapolation to infinite system, using mainly a 500 particle simulation. Quoted uncertainities are ≈ ± .02 for $D/D_E$, ≈ ± .04 for $\eta/\eta_E$, ≈ ± .02 for $\lambda/\lambda_E$, and ≈ ± .02 for $\kappa/\kappa_E$.

Source: B. J. Alder, D. M. Gass, and T. E. Wainwright.[19]

A summary of the results of Sengers et al. is given below. These results are extrapolated to include higher order Sonine polynomial approximations in the triple collision term; $\eta_0^{H.S.}$, etc., are the hard sphere Boltzmann results, and $\sigma$ is the core radius.

$$\lambda_1/(n\sigma^3\lambda_0^{H.S.}) = \frac{4\pi}{5} - \frac{5\pi}{12}(.963 \pm .001)$$

$$\eta_1/(n\sigma^3\eta_0^{H.S.}) = \frac{8\pi}{15} - \frac{5\pi}{12}(.972 \pm .0015) \qquad (2.3)$$

$$D_1/(n\sigma^3 D_0^{H.S.}) = -\frac{5\pi}{12}(.918 \pm .002).$$

Here the density expansion is $\xi = \xi_0 + (n\sigma^3)\xi_1$. The first terms in $\lambda_1$ and $\eta_1$ are due to the potential parts of the fluxes and are given exactly by the Enskog theory.

## C. Generalized Enskog Equation[13]

A useful property of hard spheres is the instantaneous nature of the collision. This implies that one can calculate in detail the $t \to 0^+$ limit in the derivation of a kinetic equation and still retain collisional effects associated with transfer of momentum. This procedure leads to what is called the generalized Enskog equation. (For continuous potentials, it leads to a collisionless Vlasov-like equation.) This short time limit does not require a density expansion, and therefore the applicability of the kinetic equation is not limited to dilute gases. As an example the dynamic structure factor, $S(\vec{k},\omega)$, determined from the generalized Enskog theory (GET) shall be reviewed.[24]

$S(\vec{k},\omega)$, which is related to the differential cross section, is given by the Fourier transform in space and time of the density-density correlation function,

$$S(\vec{k},\omega) = \frac{1}{n}\int_{-\infty}^{\infty} dt\, e^{i\omega t} \int d\vec{r}\, e^{-i\vec{k}\cdot\vec{r}} \langle \hat{n}(0,0)\hat{n}(\vec{r},-t)\rangle, \tag{2.4}$$

with

$$\hat{n}(\vec{r},-t) = \sum_{i=1}^{N} \delta(\vec{r}-\vec{q}_i(-t)).$$

Following the usual methods of kinetic theory, one notes that the solution of (2.4) requires a formal closure of the BBGKY hierarchy by expressing the two-body reduced distribution function as a functional of the one-body reduced distribution function (see Appendix A). For the type of correlation function considered here, sums of single particle functions, this is relatively simple because there exists a set of operators $U(1\ldots s;t)$ which map the single particle function onto the reduced distribution function, (i.e., $\psi(1\ldots s;t) = U(1\ldots s;t)\delta(r-q_1)$ for this case.) Thus one can easily close the hierarchy to get the kinetic equation for $\psi(1;t)$:

$$\left(\frac{\partial}{\partial t} + \frac{\vec{p}_1}{m}\cdot\frac{\partial}{\partial \vec{q}_1}\right)\psi^{(1)}(1;t) = -n\int d\vec{x}_2 L_I(12)U(12;t)U^{-1}(1;t)\,\psi^{(1)}(1;t). \tag{2.5}$$

Here $L_I$ is the interacting part of the Liouville operator. [$L_I(12) = -\frac{\partial\,\phi(12)}{\partial r_{12,i}}\cdot\frac{\partial}{\partial r_{12,i}}$ for continuous potentials, and $L_I(12) = b_{12}$, the binary collision operator for hard spheres.[25]] The usual density expansion is obtained from a cluster expansion of

$U(12;t)U^{-1}(1;t)$; however by taking the $t \rightarrow 0^{\pm}$ limit of $U(12;t)U^{-1}(1;t)$, one gets the generalized Enskog equation. As in the Enskog theory this procedure retains static correlation between the particles and binary collision dynamics, and thus one can consider the GET as giving a valid approximation to the time correlation functions over the same range of densities as the Enskog theory. For $S(k,\omega)$ the Fourier transformed form of (2.4) leads to the following expression:

$$S(\vec{k},\omega)/S(k) = 2 \operatorname{Re} (1, R(k,\omega)\, 1). \tag{2.6}$$

The scalar product is defined with a Maxwell-Boltzmann weighting function $f_0(\vec{v})$:

$$(a,b) = \int d\vec{v}\, f_0(\vec{v})\, a^*b, \tag{2.7}$$

and the operator $R(\vec{k},\omega)$ by

$$R(k,\omega) = \left[-i\omega + ik\cdot\vec{v} - B(\vec{k})\right]^{-1} , \tag{2.8}$$

with $B(\vec{k})$ being the generalized Enskog operator defined by equation (2.5) of reference (24). (The transport coefficients obtained from (2.8) are the same as those from the Enskog theory.) One notes that $B(\vec{k})$, derived from the right hand side of (2.5), does not depend on $\omega$ since the $t \rightarrow 0$ limit was taken, but it still generates dynamics due to the discontinuous potential.

Due to the complicated form of $B(k)$, one usually proceeds by choosing a kinetic model for $R(k,\omega)$. This involves finding the matrix elements of

Figure II.3. Dynamic structure factor $S(k,\omega)$ vs. k for $\omega$ = 0,1,2 meV. Kinetic theory (——); neutron scattering data for Krypton (ooo) at T = 297°K, $n\sigma^3 = .47$.

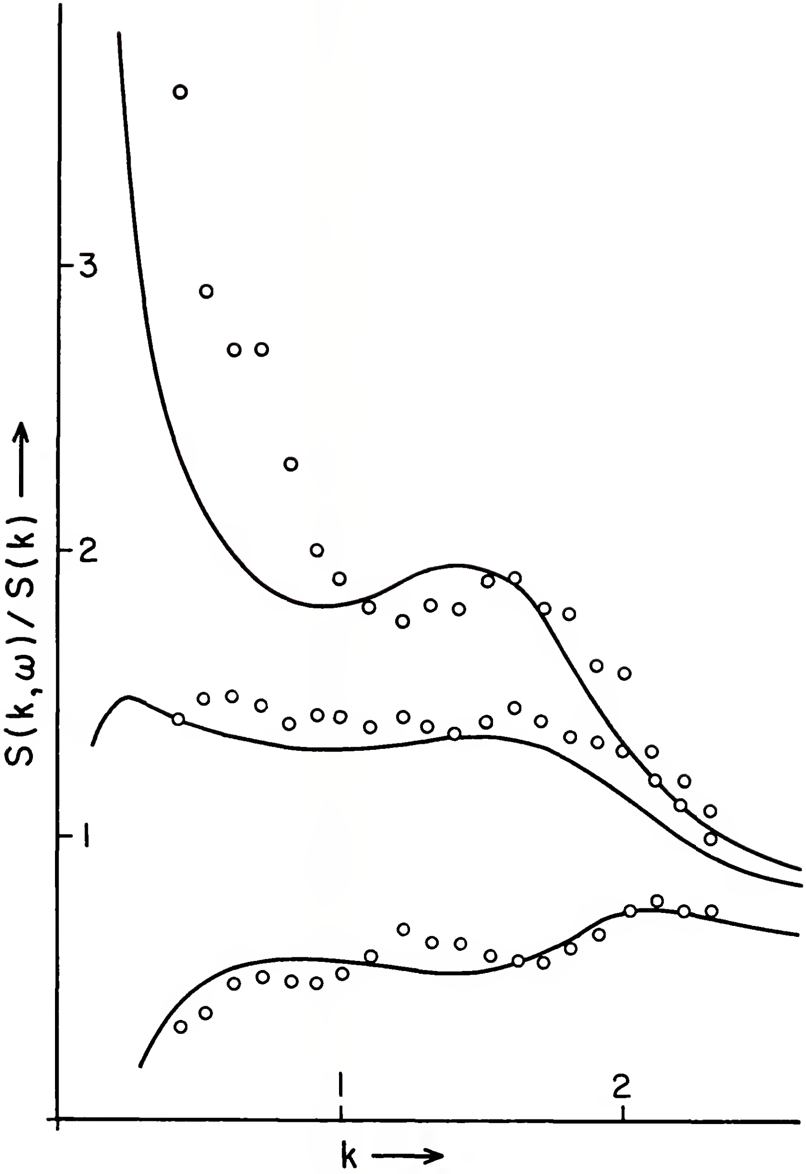
S(k,ω)/S(k)
3
2
1
1
2
k

Figure II.4. Full width at half maximum (FWHM) vs. k. Kinetic theory (——); Krypton data (ooo); Lennard-Jones molecular dynamics (•••); hard sphere molecular dynamics (ΔΔΔ).

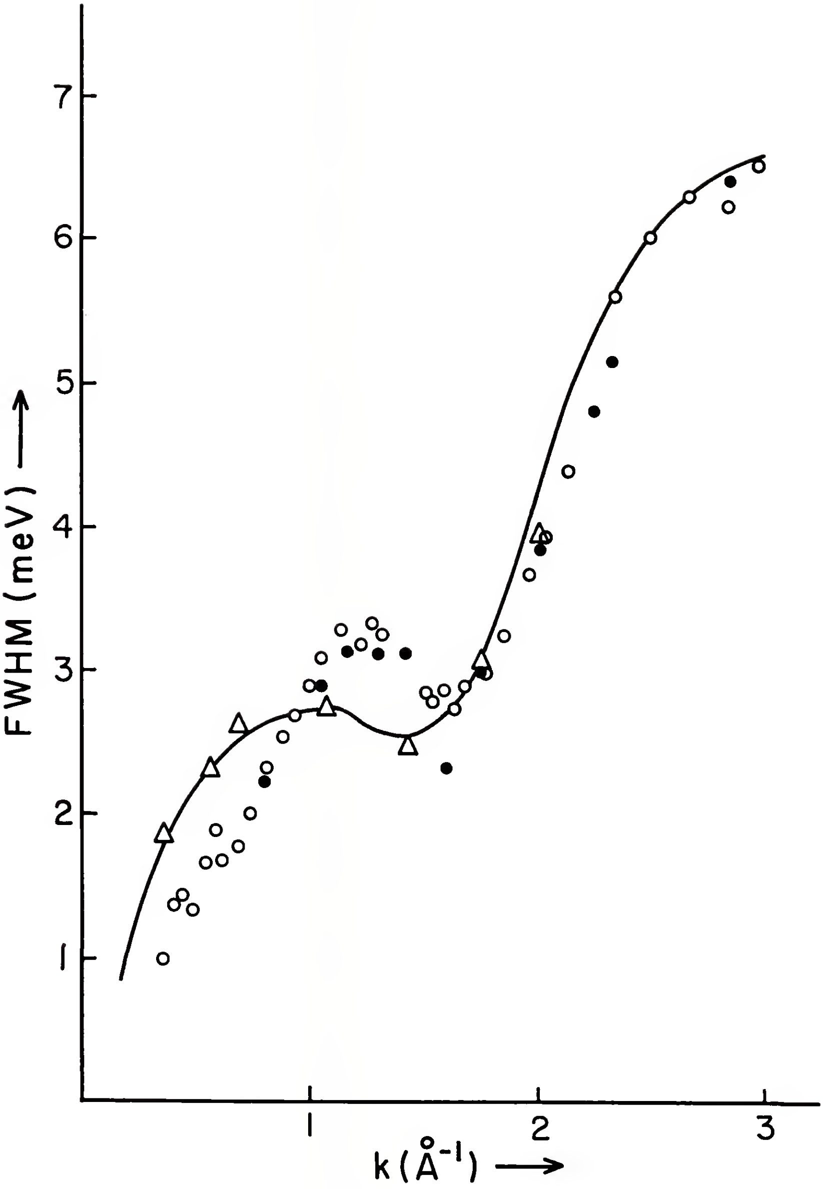
FWHM (meV) →
1
2
3
4
5
6
7
k (Å⁻¹) →
1
2
3

R with respect to a finite set of orthogonal functions, $\{u_\alpha\}$, which guarantee that some set of desired properties of the correlation function is given, while representing the behavior outside the space spanned by $\{u_\alpha\}$ in terms of a single parameter. By choosing the $\{u_\alpha\}$ so the hydrodynamic limit of $S(k,\omega)$ is given correctly, very good agreement is found with the molecular dynamic results of Alder et al.[15] for hard spheres, and fair agreement is found with the neutron scattering data of Eglestaff et al.[14] These results are shown in figures II.3 and II.4, and one sees that there are noticeable discrepancies between the Krypton data and the GET at small k and $\omega$ values. Included in figure II.4 are the molecular dynamic results of Ullo and Yip for the Lennard-Jones potential.[16] The full Lennard-Jones model is closer to the experimental data over a larger range of k values although some differences are seen at higher density in the small k range ($k < 1\ \text{Å}^{-1}$). The truncated Lennard-Jones potential (no attractive forces) behaves more like the hard sphere kinetic model at small k; therefore, the differences between the GET and experiment are due to the potential model not containing attractive forces.

## D. Modified Enskog Theory.

From the results of the Enskog theory one can make various phenomenological modifications for real fluids. For example if one assumes that the processes the Enskog theory includes are the important ones for real fluids as well, then one can claim the form of the transport coefficients is the same, with the low density result and $g(\sigma)$ to be found from experimental data. The pair correlation function at contact cannot be unambiguously defined for other potentials, however, an ad hoc method of defining g through the equation of state has been extensively tested. One knows that for hard spheres the equation of state is related to $g(\sigma)$ by

$$\frac{1}{T}\left[\left(\frac{\partial PV/T}{\partial T}\right) - 1\right] = -\frac{2\pi}{3}\, g(\sigma)n^*. \tag{2.9}$$

By using experimental data on the left hand side, Hanley et al.[17] have made comparisons of the predictions of the modified Enskog theory (MET) with experiment. Their results show the MET agrees quite well with experiment at low densities over a wide range of temperature and has an error of ~10% at densities one or two times the critical density. They also find that the first density correction ($\xi_1$, if $\xi = \xi_0 + \xi_1 n + \ldots$) predicted by the MET agrees with experiment if experimental virial coefficients and low density transport data are used. On the other hand if the virial coefficients and Boltzmann transport coefficient for a Lennard-Jones potential are used, then poor agreement is found. This is attributed to the failure of the MET for the Lennard-Jones fluid to predict the triple collision contribution for real fluids to $\xi_1$ correctly. Presumably then, computer simulations for a model fluid would be well given by the MET for that model. However, Michels and Trappeniers[6] have compared their molecular dynamics simulation for the square well fluid to the MET, and they conclude that it does not give even the correct sign of the first density correction. It is not known if the same result holds for continuous potentials such as the Lennard-Jones model.

In figure II.5 the MET value for the first density correction to nD for the square well is compared to molecular dynamics and the predictions

Figure II.5. Comparison of modified Enskog theory (- - -), repeated ring theory (———, with bound states; - o - o - without bound states), and molecular dynamics ($\Delta$) for the first density correction to self diffusion for the square well. Horizontal dashed line is the hard sphere limit.

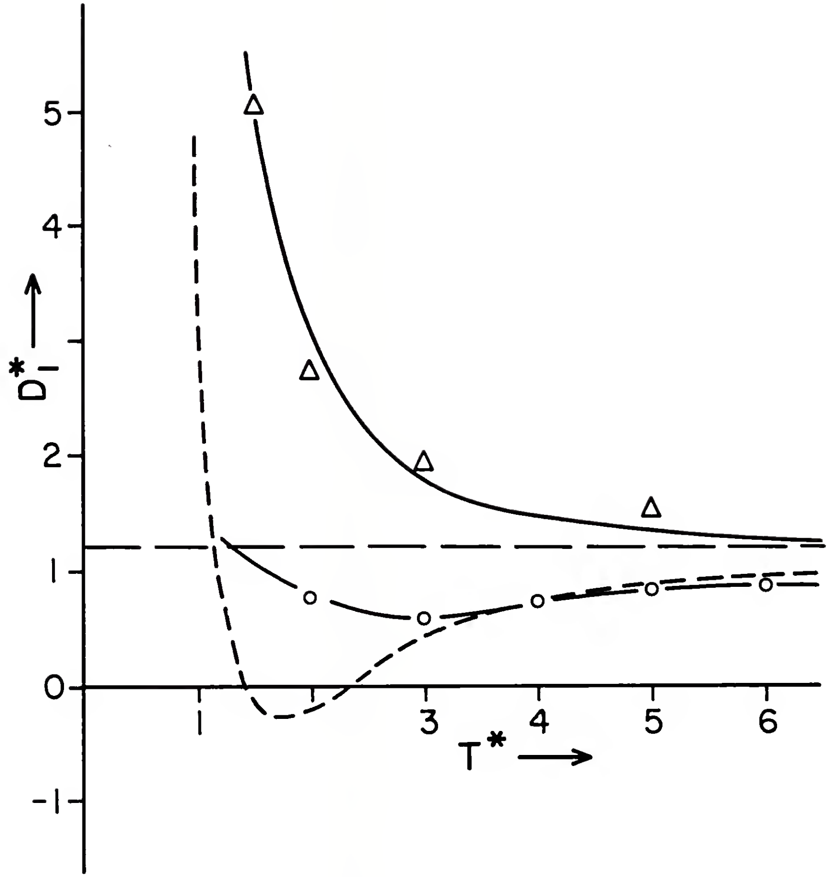
5
4
2
1
0
-1
$D_1^*$
1
3
4
5
6
$T^*$

of a 'repeated-ring' model.[21] It is noted that the MET result is similar to that of Hoffman and Curtiss[22], while the primary difference between the Hoffman-Curtiss model and the repeated ring calculation is that the repeated ring properly includes the effects of bounds states. Thus it may be seen that bound states or contributions due the attractive part of the well are important in dense gases.

From the examples above one can see that the hard sphere model can give qualitatively correct behavior for dynamic properties of gases, and the agreement between hard sphere molecular dynamics and theory is generally very good. However, the $S(\vec{k},\omega)$ calculation and the failure of the square well MET results show that attractive forces and bound states effects play an important role in the calculation of dynamic properties. An alternative dense gas theory must then take into account effects which are not included in or properly calculated by models based on hard spheres.

# CHAPTER III

# FORMAL DENSITY EXPANSION OF THE TRANSPORT COEFFICIENT

The density expansion of time correlation function for the transport coefficients has been discussed previously for classical mechanical systems by several authors.[26] The generalization given here for quantum mechanical systems follows in an obvious way from the classical results; McLennan[10] and Boercker and Dufty[27] have considered the special case of correlations between sums of single particle functions for quantum systems previously. The transport coefficients considered here are of the general form

$$\Lambda = \mathrm{Re} \lim \frac{K_\Lambda}{V} \int_0^\infty dt e^{-\varepsilon t} \langle J_\Lambda \cdot J_\Lambda(-t) \rangle , \tag{3.1}$$

where $K_\Lambda$ is a constant depending upon the particular transport coefficient considered and the brackets $\langle \ldots \rangle$ denote a grand canonical ensemble average. The transport coefficients $\Lambda$ for a simple fluid are the shear viscosity ($\eta$), the thermal conductivity ($\lambda$), the bulk viscosity ($\kappa$), and self diffusion ($nD$, where $n$ is the number density). In the definitions of $J_\Lambda$ given below and in the correlation function $J_\Lambda \cdot J_\Lambda(-t)$, it is assumed that repeated Latin indices are summed over ($i,j$, etc. = $x,y,z$):

$$\text{Self-diffusion:} \quad K_D = \frac{1}{3m^2}$$

$$J_D = \sqrt{N}\, p_{1i} \quad , \tag{3.2a}$$

Shear viscosity: $K_\eta = \frac{\beta}{10}$ (3.2b)

$$J_\eta = \{T_{ij}\}_{Tr},$$

Thermal conductivity: $K_\lambda = \frac{k_B\beta^2}{3}$ (3.2c)

$$J_\lambda = S_i - \frac{h}{\rho} P_i \quad ,$$

Bulk viscosity: $K_\kappa = \frac{\beta}{9}$ (3.2d)

$$J_\kappa = T_{ii} - \tilde{T}_{ii} .$$

In (3.2d) $\tilde{T}_{kk}$ is the time average of $T_{kk}$. McLennan has shown $\tilde{T}_{kk}$ is given by[28]

$$\tilde{T}_{kk} = 3\left(pV + \left(\frac{\partial p}{\partial u}\right)_n (H - \langle H\rangle) + \left(\frac{\partial p}{\partial n}\right)_u (N - \langle N\rangle)\right). \qquad (3.3)$$

In (3.2) and (3.3), m is the particle mass, N is the number of particles, $\beta = \frac{1}{k_B T}$ with $k_B$ being Boltzmann's constant and T the temperature, $\rho$ is the mass density, h is the enthalpy density (h = u + p, with u the energy density and p the pressure), and H is the Hamiltonian operator. The braces $\{..\}_{Tr}$ denote the traceless part of $T_{ij}$:

$$\{Tr\}_{Tr} = T_{ij} - \frac{\delta_{ij}}{3} T_{kk}, \qquad (3.4)$$

with $\delta_{ij}$ being the Kronecker delta function. The stress tensor $T_{ij}$, energy flux $S_i$ and total momentum $P_i$ are defined by

$$T_{ij} = \frac{1}{m} \sum_{\alpha} p_{\alpha i} p_{\alpha j} - \frac{1}{2} \sum_{\alpha \neq \beta} \frac{\partial \phi(\alpha\beta)}{\partial r_{\alpha\beta,i}} r_{\alpha\beta,j}$$

$$S_i = \frac{1}{2m^2} \sum_{\alpha} p_{\alpha}^{2} p_{\alpha i} + \frac{1}{4m} \sum_{\alpha \neq \beta} \{ \phi(\alpha\beta)(p_{\alpha i} + p_{\beta i})$$

$$- (p_{\alpha j} + p_{\beta j}) \frac{\partial \phi(\alpha\beta)}{\partial r_{\alpha\beta,j}} r_{\alpha\beta,i} \} \tag{3.5}$$

$$P_i = \sum_{\alpha} p_{\alpha i} \; .$$

Here $\alpha,\beta$ are particle labels, $p_\alpha$ is the momentum operator, $r_{\alpha\beta} = r_\alpha - r_\beta$ is the relative position operator, and $\phi(\alpha,\beta)$ in the pair potential. The operation indicated by $[a,b]_+$ denotes the anti-commutator ab + ba. It is seen that the fluxes in general have two parts: (1) a 'kinetic' part consisting of sums of single particle function of the momentum, $J_k$; (2) a 'potential' part consisting of sums of two particle functions of the momenta and relative position, $J_\phi$; i.e.,

$$J = J_k + J_\phi$$

$$J_k = \sum_{\alpha} a(\alpha)$$

$$J_\phi = \frac{1}{2} \sum_{\alpha \neq \beta} b(\alpha\beta)$$

There exist several other definitions for the quantum formulation of the time correlation functions for the transport coefficients; however, they are all equivalent for the transport coefficients considered here.[10]

From the definition of J one can write the transport coefficient as a sum of three terms,

$$\Lambda = \Lambda_{kk} + 2\Lambda_{\phi k} + \Lambda_{\phi\phi} , \qquad (3.6)$$

called the kinetic, cross, and potential terms, respectively. This form is convenient for comparison with molecular dynamics since each term in (3.6) can be calculated separately. It will be shown below that $\Lambda_{kk}$ is of lowest order in the density (leading term $\sim n^0$) and gives the usual Boltzmann result. The first density correction to $\Lambda$ (order $\sim n^1$) then consists of the second term in the expansion of $\Lambda_{kk}$ plus the lowest order term in $\Lambda_{\phi k}$, while $\Lambda_{\phi\phi}$ is formally of higher order in n. The contribution from $\Lambda_{\phi k}$ depends upon two body dynamics only and will be evaluated in Chapter IV. The contribution from $\Lambda_{kk}$ involves three body dynamics.

The details of the density expansion of each term in (3.6) are given in Appendix A. Compact and general expressions can be found if the statistics of the system are included in the density operator, thus the reduced distribution function and cluster functions can be defined in a manner closely related to the classical calculations.[27] It is to be noted that the cluster expansion of the density operator then implies that both $n\sigma^3$ (where $\sigma$ characterizes the force range) and $n\tau^3$ (where $\tau = h(\frac{\beta}{2\pi m})^{1/2}$ is the thermal wavelength) are small parameters. This grand canonical average will therefore have the form

$$\langle A\rangle = \sum_{N\geq 0} \frac{z^N}{N!\Xi} \operatorname*{Tr}_{1..N} \rho_N A_N ,$$

$$\rho_N = N!\hat{P}_N \lambda^{3N} e^{-\beta H_N} ,$$

$$\Xi = \sum_{N\geq 0} \frac{z^N}{N!} \operatorname*{Tr}_{1..N} \rho_N \, . \tag{3.7}$$

Here the trace is taken over a complete set of states in the N-particle space, while the operator $\hat{P}_N$ projects onto the properly symmetrized subspace for identical particles; the activity is defined by $\lambda^3 z = e^{\beta\mu}$, where $\mu$ is the chemical potential. In a manner analogous to the classical case, reduced distribution functions corresponding to the kinetic and potential parts of the fluxes can be found, and each of the terms in (3.6) can be represented as a trace over the coordinates of one and two particles involving the one- and two-body reduced distribution functions:

$$\Lambda_{kk} = \text{Re} \lim \frac{n}{V} \operatorname*{Tr}_{1} a(1)\, \psi_k^{(1)}(1;\varepsilon)$$

$$\Lambda_{\phi k} = \text{Re} \lim \frac{n^2}{2V} \operatorname*{Tr}_{1,2} b(12)\psi_k^{(2)}(12;\varepsilon)$$

$$\Lambda_{\phi\phi} = \text{Re} \lim \frac{n^2}{2V} \operatorname*{Tr}_{1,2} b(12)\psi_\phi^{(2)}(12;\varepsilon) \tag{3.8}$$

Here $\psi_k^{(s)}$ and $\psi_\phi^{(s)}$ are the kinetic and potential parts of the s-particle reduced distribution function, $\psi^{(s)}$, defined by

$$\psi^{(s)}(1..s;\varepsilon) = \int_0^\infty dt e^{-\varepsilon t} \tilde{\psi}^{(s)}(1..s;t)$$

$$n^s \tilde{\psi}^{(s)}(1..s;t) = \sum_{N\geq s} \frac{z^N}{(N-s)!\,\Xi} \operatorname*{Tr}_{s+1...N} \rho_N \, J_N(-t). \tag{3.9}$$

The density expansions of $\psi_k^{(1)}$, $\psi_k^{(2)}$, and $\psi_\phi^{(2)}$ therefore give the density expansion for $\Lambda$. The results of Appendix A imply for each term in (3.8) that

$$\Lambda_{kk} = \Lambda_{kk,0} + n\,\Lambda_{kk,1} + \cdots$$

$$\Lambda_{\phi k} = 0 + n\,\Lambda_{\phi k,1} + \cdots$$

$$\Lambda_{\phi\phi} = 0 + 0 + n^2\Lambda_{\phi\phi,2} + \cdots \tag{3.10}$$

Thus the cluster expansion for $\psi_\phi^{(2)}$ is not needed for the first density correction. Also as in the classical case, $\psi_k^{(1)}$ is determined from the first equation of the BBGKY hierarchy:

$$(\varepsilon + L(1))\psi_k^{(1)}(1) + n\,\mathrm{Tr}_2\, L_I(12)\Psi(12;\varepsilon|\psi_k^{(1)}(\cdot)) = \tilde{\psi}_k^{(1)}(1;t=0). \tag{3.11}$$

Here $\Psi$ is the expression for $\psi_k^{(2)}$ as a functional of $\psi_k^{(1)}$ as given by the cluster expansion,

$$\psi_k^{(2)}(12;\varepsilon) = \Psi(12;\varepsilon|\psi_k^{(1)}(\cdot)). \tag{3.12}$$

The Liouville operator in (3.11) is defined by

$$L = \sum_\alpha L(\alpha) + \sum_{\alpha<\beta} L_I(\alpha\beta) = \frac{i}{\hbar}\left[H,\ \right]_- , \tag{3.13}$$

where $[A,B]_-$ is the commutator of A and B, AB − BA. Since $\Psi$ is a linear operator on $\psi_k^{(1)}$, (3.11) may be formally solved for $\psi_k^{(1)}$:

$$\psi_k^{(1)}(1;\varepsilon) = (\varepsilon + L(1) + \hat{M}')^{-1}\,\tilde{\psi}_k^{(1)}(1;t=0)$$

$$\hat{M}'f(1) \equiv n \operatorname*{Tr}_{2} L_T(12)\Psi(12;\varepsilon|f(\cdot)). \qquad (3.14)$$

Direct substitution of the density expansion of $\Psi$ from Appendix A gives the density expansion for $\hat{M}'$. Noting that only the $\varepsilon \to 0$ limit of (3.14) is required in (3.8) or (3.10) and that $\tilde{\psi}_k^{(1)}$ is independent of $r_1$, equation (3.14) can be rewritten as

$$g(1) = \hat{M}^{-1}h(1), \qquad (3.15a)$$

with

$$g(1) \equiv \lim_{\varepsilon \to 0} D^{-1}(1)\, n\psi_k^{(1)}(1;\varepsilon),$$

$$h(1) = D^{-1}(1)\, \tilde{\psi}_k^{(1)}(1;t=0),$$

$$\text{and } \hat{M} = \lim_{\varepsilon \to 0} D^{-1}(1)\hat{M}'D(1). \qquad (3.15b)$$

Here $D(1) = \lambda^3 e^{-\beta H(1)}$. The density expansion of $\hat{M}$ (from $\Psi$) and $h(1)$ (from a cluster expansion of (3.9)) identifies the density expansion for $g(1)$. Letting

$$g(1) = g^{(0)}(1) + n\, g^{(1)}(1) + \ldots$$

$$h(1) = h^{(0)}(1) + n\, h^{(1)}(1) + \ldots$$

$$\hat{M} = \hat{M}_1 + n\, \hat{M}_2 + \ldots , \qquad (3.16)$$

then the lowest order terms in (3.10) will be given by

$$\Lambda_{kk,0} = \mathrm{Re} \lim_{V\to\infty} \frac{1}{V} \mathop{\mathrm{Tr}}_{1} D(1)\, a^{(0)}(1)\, g^{(0)}(1)$$

$$\Lambda_{kk,1} = \mathrm{Re} \lim_{V\to\infty} \frac{1}{V} \mathop{\mathrm{Tr}}_{1} D(1)\, (a^{(1)}(1)\, g^{(0)}(1) + a^{(0)}(1)\, g^{(1)}(1))$$

$$\Lambda_{\phi k,1} = \mathrm{Re} \lim_{V\to\infty} \frac{1}{2V} \mathop{\mathrm{Tr}}_{1,2}\, b^{(0)}(12)\, \Psi_1(12;|D(1)g^{(0)}(1)). \qquad (3.17)$$

Here $a^{(0)}$, $a^{(1)}$, and $b^{(0)}$ are the lowest order terms in the density expansion of the fluxes (this density dependence is only through thermodynamic functions), and $\Psi_1$ is the first term in the density expansion of $\Psi$ $\left[\text{specifically, } \Psi_1(12|f) = \lim_{\varepsilon\to 0} D(12)\varepsilon R(12;\varepsilon)(1+\overline{P}_{12})D^{-1}(1)f(1)\right]$, equation (A.27). The solutions to

$$M_1 g^{(0)}(1) = h^{(0)}(1)$$

and

$$M_1 g^{(1)}(1) = - M_2 g^{(0)}(1) + h^{(1)}(1) \qquad (3.18)$$

give $g^{(0)}(1)$ and $g^{(1)}(1)$. Defining the scalar product (a,b) allows a more compact expression for the kinetic parts of (3.16):

$$(a,b) \equiv \lim_{V\to\infty} \frac{1}{V} \mathop{\mathrm{Tr}}_{1} D(1)a^{\dagger}(1)b(1) \qquad (3.19)$$

where the dagger, †, denotes the hermitian adjoint. Thus

$$\Lambda_{kk,0} = \mathrm{Re}\ (a^{(0)}(1),g^{(0)}(1))$$

$$\Lambda_{kk,1} = \mathrm{Re}\ \left[(a^{(0)}(1),g^{(1)}(1)) + (a^{(1)}(1),g^{(0)}(1))\right]$$

$$\Lambda_{\phi k,1} = \mathrm{Re}\,\frac{1}{2V}\,\underset{1,2}{\mathrm{Tr}}\; b^{(0)}(12)\;\Psi(12|D(1)g^{(0)}(1)) \;. \qquad (3.20)$$

Using the definitions (3.2) of each transport coefficient in (3.20) gives the specific equations which must be evaluated.

For the shear viscosity, $\eta = \eta_{kk,0} + n(\eta_{kk,1} + 2\eta_{\phi k,1}) + \ldots$:

$$\eta_{kk,0} = \frac{\beta}{10}\,(D_{ij}, \tilde{D}^{(0)}_{ij})$$

$$\eta_{kk,1} = \frac{\beta}{10}\,(D_{ij}, \tilde{D}^{(1)}_{ij})$$

$$\eta_{\phi k,1} = \frac{\beta}{10V}\,\underset{1,2}{\mathrm{Tr}}\,\left[(L_I(12)r_{12,i}p_{12,j}) \bullet \Psi_1(12|D(1)\;\tilde{D}^{(0)}_{ij})\right]. \qquad (3.21)$$

Here

$$D_{ij} = \{p_{1i}p_{1j}\}_{Tr} \;,$$

$$\tilde{D}^{(0)}_{ij} = \hat{M}_1^{-1}\; D_{ij} \;,$$

and

$$\tilde{D}^{(1)}_{ij} = -\,\hat{M}_1^{-1}\;\hat{M}_2\hat{M}_1^{-1}\;D_{ij} \;. \qquad (3.22)$$

For the thermal conductivity, $\lambda = \lambda_{kk,0} + n(\lambda_{kk,1} + 2\lambda_{\phi k,1}) + \ldots$ :

$$\lambda_{kk,0} = \frac{k_B\beta^2}{3}\;(S_i^{(0)}(1), \tilde{S}_i^{(0)}(1))$$

$$\lambda_{kk,1} = \frac{k_B\beta^2}{3}\;(S_i^{(0)}(1), \tilde{S}_i^{(1)}(1))$$

$$\lambda_{\phi k,1} = \frac{k_B\beta^2}{6V} \mathop{\mathrm{Tr}}_{1,2} \{(\frac{1}{4m} [\phi(12),(p_{1i} + p_{2i})]_+$$

$$+ \frac{1}{8m} [[(p_{1j} + p_{2j}), L_I(12)p_{12,j}]_+, r_{12},i]_+) \tag{3.23}$$

$$\times \Psi_1(1,2|p(1)\tilde{S}_i^{(0)}(1))\}.$$

Here

$$S_i^{(0)}(1) = \frac{1}{m} p_{1,i} (\frac{p_1^2}{2m} - h^{(0)})$$

$$\tilde{S}_i^{(0)}(1) = \hat{M}_1^{-1} S_1^{(0)}(1)$$

$$\tilde{\tilde{S}}_i^{(0)}(1) = \hat{M}_1^{-1}\hat{M}_2\hat{M}_1^{-1} S_i^{(0)}(1). \tag{3.24}$$

Note that $h^{(0)}$ is the first term in the density expansion for the enthalpy per particle. One might expect there would be a term involving the second order term in the enthalpy, $h^{(1)}$, however it vanishes due to orthogonality conditions.

Finally, for the self-diffusion coefficient, $(nD) = (nD)_0 + n(nD)_1 + \ldots$:

$$(nD)_0 = \frac{1}{3m^2} (p_{1i},\tilde{P}_i^{(0)}(1))$$

$$(ND)_1 = \frac{1}{3m^2} (p_{1i},\tilde{P}_i^{(1)}(1)) \tag{3.25}$$

with

$$\tilde{p}_i^{(0)}(1) = \hat{M}_{s1}^{-1} p_{1i}$$

$$\tilde{p}^{(1)}(1) = \hat{M}_{s1}^{-1}\hat{M}_{s2}\hat{M}_{s1}^{-1} p_{1i} \quad . \tag{3.26}$$

Here $M_s$ is the collision operator for self correlations defined in Appendix A.

The classical limit of these equations for η, λ and nD will be considered in Chapter IV. The classical limit agrees with the results of Ernst et al.[26], and the quantum operator $M_2$ agrees with that of McLennan.[10]

# CHAPTER IV
## CLASSICAL SQUARE WELL GAS

The square well potential defined by (1.1) simplifies the calculation of the transport coefficients since (1) the time evolution of the system can be written in a closed form, and (2) the discontinuous nature of the potential reduces the initial conditions to be considered to surfaces at $\sigma$ and $R\sigma$. From Appendix B and equations (A.26) the classical expressions for the collision operators, $\hat{M}_1$ and $\hat{M}_2$ , may be written in the following forms:

$$M_1 g(1) = -\lim_{\varepsilon\to 0} f_0^{-1}(1)\int d\vec{p}_2 d\vec{r}\ \theta(12)\varepsilon R(12)\ f_0(12)(1+\sigma\overline{P}_{12})\ g(1).$$

$$\hat{M}_2 g(1) = f_0^{-1}(1)\int d\vec{p}_2 d\vec{p}_3 d\vec{r}_{21} d\vec{r}_{31}\ \theta(12)\big[\varepsilon R(123)W(123) - \varepsilon R(12)W(12)$$

$$\times\ (\varepsilon R(13)W(13) + \varepsilon R(23)W(23) - 1)(1+\sigma\overline{P}_{12}+\sigma\overline{P}_{13})f_0(2)f_0(3)g(1). \qquad (4.1)$$

The classical W-functions are $W(1...s) = \exp(-\beta \sum_{i<j} \phi(ij))$, and the $\theta$-operator is given by $\dfrac{\partial\phi(r)}{\partial r_i}\dfrac{\partial}{\partial p_i}$ for continuous potentials; it will be assumed that the potential is continuous at this point, and later the limit to a square well potential will be used. Then the transport coefficients may be written as the following: (1) For the shear viscosity:

$$\eta_{kk,0} = \frac{\beta}{10} \int d\vec{p}_1 \; f_0(1) D_{ij}(1) \tilde{D}_{ij}(1)$$

$$\eta_{kk,1} = \frac{\beta}{10} \int d\vec{p}_1 \; f_0(1) \tilde{D}_{ij}(1) \; M_2 \tilde{D}_{ij}(1)$$

$$\eta_{\phi k,1} = - \frac{\beta}{40} \lim_{\varepsilon \to 0} \int d\vec{p}_1 d\vec{p}_2 d\vec{r} \; (r_i \theta(12) p_j) \varepsilon R(12;\varepsilon)$$

$$\times f_0(12)(1+\overline{P}_{12}) \tilde{D}_{ij}(1). \tag{4.2}$$

Here $f_0(1)$ and $f_0(12)$ are the low density one- and two-body distribution functions:

$$f_0(12) = f_0(1) f_0(2) \; e^{-\beta\phi(12)}$$

$$f_0(1) = \left(\frac{2\pi}{\beta m}\right)^{-3/2} e^{-\beta \frac{p_1^2}{2m}} , \tag{4.3}$$

and $\vec{r} = \vec{r}_2 - \vec{r}_1$ and $\vec{p} = \frac{1}{2} (\vec{p}_2 - \vec{p}_2)$ are the relative position and momentum. $D_{ij}(1) = \{p_{1i} p_{1j}\}_{Tr}$ is the classical kinetic part of the momentum flux; $\tilde{D}_{ij}(1)$ is the solution to

$$\hat{M}_1 \tilde{D}_{ij} = D_{ij} , \tag{4.4}$$

where $\hat{M}_1$ is seen to reduce to the classical Boltzmann operator. The potential part of the momentum flux has been written as

$$r_i \frac{\partial \phi}{\partial r_j} \equiv r_i \;\; \theta(12) p_j \; . \tag{4.5}$$

This allows the cross term to be written in the suggestive form

$$\eta_{\phi k,1} = \frac{\beta}{40} \lim_{\varepsilon \to 0} \int d\vec{p}_1 d\vec{p}_2 d\vec{r} (r_i p_j \varepsilon \theta(12) R(12) f_0(12)(1+\overline{P}_{12}) \tilde{D}_{ij}(1), \qquad (4.6)$$

where the combination of operators $\lim\limits_{\varepsilon \to 0} \varepsilon\theta(12)R(12)$ can be evaluated in the same manner as in the Boltzmann case (see Chapter V). The solutions to (4.1) depend upon the evaluation of $\tilde{D}_{ij}$. The solution to equation (4.4) for $\tilde{D}_{ij}$ is usually given in terms of successive Sonine polynomial approximations[12]; here the first Sonine polynomial approximation which is known to accurate to within a few percent will be used; i.e.,

$$\tilde{D}_{ij} \approx a_{\eta,0} D_{ij} \qquad (4.7)$$

where this in turn implies from (4.2) and (4.4)

$$\eta_{kk,0} = \beta^{-1} a_{\eta,0}$$

where $a_{\eta,0}$ is given by (4.19) below. For the other transport coefficients similar results follow:

(2) For the thermal conductivity:

$$\lambda_{kk,0} = \frac{k_B \beta^2}{3} \int d\vec{p}_1 f_0(\vec{p}_1) \; S_i(1) \cdot \tilde{S}_i(1)$$

$$\lambda_{kk,1} = \frac{k_B \beta^2}{3} \int d\vec{p}_1 f_0(\vec{p}_1) \tilde{S}_i(1) \cdot \hat{M}_2 \tilde{S}_i(1)$$

$$\lambda_{\phi k,1} = \lim_{\varepsilon \to 0} \frac{k_B \beta^2}{12 m^2} \int d\vec{p}_1 d\vec{p}_2 d\vec{r} \; \phi(r) P_i f_0(12) \cdot \varepsilon R(12)(1+\overline{P}_{12}) \tilde{S}_i(1)$$

$$+ \lim_{\varepsilon \to 0} \frac{k_B \beta^2}{12 m^2} \int d\vec{p}_1 d\vec{p}_2 d\vec{r}\ r_i (\vec{P}\cdot\vec{p})\theta(12)\cdot\varepsilon R(12) f_0(12)(1+\overline{P}_{12})\tilde{S}_i(1). \tag{4.8}$$

Here $S_i$ is the low density form of the kinetic part of the heat flux

$$S_i(1) = \left(\frac{p_1^2}{2m} - \frac{5}{2\beta}\right) p_{1i}\ , \tag{4.9}$$

and $\tilde{S}_i(1)$ is given by

$$\tilde{S}_i(1) = \hat{M}_1^{-1} S_i(1). \tag{4.10}$$

In the first Sonine polynomial approximation, $\tilde{S}_i$ is given by

$$\tilde{S}_i(1) \approx a_{\lambda,0} S_i(1)$$

where the first of equation (4.6) and equation (4.10) then give

$$\lambda_{kk,0} = \frac{5k_B}{2m\beta} a_{\lambda,0}, \tag{4.11}$$

when $a_{\lambda,0}$ is given by (4.19). Again the potential part of the flux that depends upon the force, usually written in the form $(\vec{P}\cdot(\partial\phi(r)/\partial\vec{r})$ has been eliminated in favor of $\theta(12)(\vec{P}\cdot\vec{p})r_i$ .

(3) For self-diffusion:

$$(nD)_0 = \frac{1}{3m^2} \int d\vec{p}_1\ f_0(1) p_{1i}\cdot\tilde{P}_{1i}$$

$$(nD)_1 = \frac{1}{3m^2} \int d\vec{p}_1\ f_0(1)\tilde{P}_{1i}\cdot\hat{M}_{2s}\tilde{P}_{1i}\quad . \tag{4.12}$$

Here $\tilde{P}_{1i}$ is given by the inverse of the Lorentz-Boltzmann operator, $\hat{M}_{1s}$, acting on $p_1$, and $\hat{M}_{2s}$ in the triple collision operator for self correlations,

$$\tilde{P}_{1i} = \hat{M}_{1s}^{-1} P_{1i} \ . \qquad (4.13)$$

$\hat{M}_{1s}$ and $\hat{M}_{2s}$ are given by (4.3) and (4.4) with $\sigma = 0$. In the first Sonine polynomial approximation,

$$\tilde{P}_{1i} \approx a_D P_{1i}$$

with

$$(nD)_0 = (m\beta)^{-1} a_D, \qquad (4.14)$$

where $a_D$ is define in (4.19) below. Equation (4.2), (4.8) and (4.12) for the Boltzmann term and cross term depend upon the evaluation of the operators $\varepsilon R(12)$ and $\theta(12)\varepsilon R(12)$ acting on single particle functions of the momenta. For scattering states, it is easy to see that the $\lim_{\varepsilon \to 0} \varepsilon R(12) g(1) \equiv \lim_{t \to \infty} g(1;-t)$ if $g(-t) \to$ a constant as $t \to \infty$. For bound states this identity no longer holds, and more care must be taken in the evaluation of the limit $\varepsilon \to 0$. In addition, the $\theta(ij)$ operator for the square well is undefined and must be evaluated in the context of a limit of a continuous potential. The presence of the $\theta$ operator restricts the integral to those portions of phase space where the force is non-zero, and since the $\theta$ operator always occurs in conjunction with the resolvent R, the following identity can be used:

$$\theta(ij)R(ij) = 1 + R_0^{-1}(ij)R(ij). \qquad (4.15)$$

The use of (4.15) and Gauss' theorem reduces the integration over the relative coordinate to the surface bounding the space $\frac{\partial\phi(r)}{\partial r_i} \neq 0$, plus some integrals which vanish or $\varepsilon \to 0$,[29] i.e., integrals of the form

$$\lim_{\varepsilon\to 0} \int d\vec{p}_1 d\vec{p}_2 \int d\vec{r}\; h(12)\varepsilon\theta(12)R(12)g(12)$$

$$= \lim_{\varepsilon\to 0} \int d\vec{p}_1 d\vec{p}_2 \int_{V_s} d\vec{r}\; h(12)\; \varepsilon\; (1 - R_0^{-1}(12)R(12))g(12)$$

$$= \lim_{\varepsilon\to 0} - \int d\vec{p}_1 d\vec{p}_2 \int_{V_s} d\vec{r}\; h(12)\left(\frac{2}{m}\, p_i\, \frac{\partial}{\partial r_i}\right) \varepsilon R(12)g(12)$$

$$= \lim_{\varepsilon\to 0} - \int d\vec{p}_1 d\vec{p}_2 \int_{S} d\hat{r}\; |r|^2 h(12)\; \frac{2}{m}(\vec{p}\cdot\hat{r})\varepsilon R(12)g(12), \qquad (4.16)$$

where $V_s$ is the volume where $\frac{\partial\phi}{\partial r_i} \neq 0$ and $S$ is the surface bounding that volume. Thus one can see that the square well integrals for the Boltzmann and cross terms can be expressed in terms of integrals over the surfaces $|\vec{r}| = \sigma^+$, $R\sigma^+$ and $R\sigma^-$ if it is viewed as the limit of a continuous potential.

To illustrate the evaluation of integrals of the type given by (4.16), the Boltzmann term will be considered. In order to emphasize the difference with hard spheres, the low density square well coefficients will be expressed in the dimensionless form

$$\eta_0^* = \eta_{kk,0}/\eta_0^{HS} \qquad \lambda_0^* = \lambda_{kk,0}/\lambda_0^{HS} \qquad D_0^* = D_{kk,0}/D_0^{HS} \qquad (4.17)$$

where the hard sphere Boltzmann transport coefficients are given by (2.4). It is well known that the integrals for the Boltzmann coefficients can be reduced to expressions involving two dimensional integrals over the relative momentum and impact parameter. Remembering that the Sonine polynomial approximation in the lowest order term in equations (4.2), (4.8) and (4.12) gives

$$\eta_0^* = a_{\eta,0}/\eta_0^{HS}$$

$$\lambda_0^* = \frac{5}{2}\frac{k_B}{m\beta}\, a_{\lambda,0}/\lambda_0^{HS}$$

$$(nD)_0^* = \frac{1}{m\beta}\, a_{D,0}/(nD)_0^{HS} \quad , \tag{4.18}$$

where

$$a_{\eta,0} = \frac{10\ m^2}{\beta^2}\left(\int d\vec{p}_1 f_0(1) D_{ij}(1)\hat{M}_1 D_{ij}(1)\right)^{-1}$$

$$a_{\lambda,0} = \frac{15m}{2\beta^3}\left(\int d\vec{p}_1 f_0(1) S_i(1)\hat{M}_1 S_i(1)\right)^{-1}$$

$$a_{D,0} = \frac{3m}{\beta}\left(\int d\vec{p}_1 f_0(1) p_{1i}\hat{M}_{1s} p_{1i}\right)^{-1} . \tag{4.19}$$

The expressions for the shear viscosity and thermal conductivity reduce to the integral,

$$\eta_0^* = \lambda_0^* = \left[\Omega^{(2,2)}(T^*)\right]^{-1} \quad , \tag{4.20}$$

while the self diffusion coefficient can be expressed as

$$(nD)_0^* = \left[\Omega^{(1,1)}(T^*)\right]^{-1} \quad . \tag{4.21}$$

Here $T^* \equiv \frac{kT}{\varepsilon_0}$, while the $\Omega$-integrals are given by

$$\Omega^{(1,1)}(T^*) = -\frac{\beta}{8\sigma^2}\left(\frac{\beta}{m\pi}\right)^{1/2} \int d\vec{p}_1 d\vec{p}_2 d\vec{r}\; p_{1i}\left[\lim_{\varepsilon\to 0} \theta(12)\varepsilon R(12) f_0(12)\right] p_{1i}$$

$$\Omega^{(2,2)}(T^*) = -\frac{\beta}{32m\sigma^2}\left(\frac{\beta}{m\pi}\right)^{1/2} \int d\vec{p}_1 d\vec{p}_2 d\vec{r}\{p_{1i}p_{1j}\}_{Tr}\left[\lim_{\varepsilon\to 0} \theta(12)\right.$$

$$\left.\times\; \varepsilon R(12) f_0(12)(1+\bar{P}_{12})\right]\{p_{1i}p_{1j}\}_{Tr} \qquad (4.22)$$

Taking the $\Omega^{(2,2)}$ integral as an example, it is reduced to a two dimensional integral through the steps outlined after (4.14). Using (4.16) and doing the integral over total momentum $\vec{P} = \vec{p}_1 + \vec{p}_2$ gives

$$\Omega^{(2,2)}(T^*) = -\frac{\beta}{32\sigma^2 m}\left(\frac{\beta}{m\pi}\right)^{1/2} \int d\vec{p}\; f_0(p) \int d\hat{r}\; \frac{2}{m}(\vec{p}\cdot\hat{r})\{p_i p_j\}_{Tr}$$

$$\times \lim_{\varepsilon\to 0} \left\{\left[R^2\sigma^2 \varepsilon\tilde{R}(r,p)\; 2\{p_i p_j\}_{Tr}\right]_{R\sigma^+}\right.$$

$$+ \left[\sigma^2 e^{1/T^*} \varepsilon\tilde{R}(r,p) 2\{p_i p_j\}_{Tr}\right]_{\sigma^+}$$

$$\left.- \left[R^2\sigma^2\; e^{1/T^*} \varepsilon\tilde{R}(r,p) 2\{p_i p_j\}_{Tr}\right]_{R\sigma^-}\right\}. \qquad (4.23)$$

The brackets $[\ldots]_r$ indicate the functions inside are to be evaluated at initial conditions given by $|r| = R\sigma^+$, $\sigma^+$, and $R\sigma^-$ respectively. The operator $\tilde{R}(\vec{r},\vec{p})$ is the resolvent operator for relative position and momentum (i.e., $\tilde{R}(r,p) = (\varepsilon + \frac{2}{m} p_i \frac{\partial}{\partial r_i} - \frac{\partial\phi(r)}{\partial r_i}\frac{\partial}{\partial p_i})^{-1}$ for continuous potentials), and the low density distribution function for relative momentum is $f_0(p) = (\frac{\beta}{\pi m})^{3/2}\; e^{-\beta p^2/m}$.

To evaluate (4.23), it is noted that for initial conditions at $R\sigma^+$ all particles scatter free so that $\vec{p}$ goes to its asymptotic value after a finite time; therefore the relation $\lim_{\varepsilon\to 0} \varepsilon\tilde{R}(r,p)f(p) = \lim_{t\to\infty} f(p;-t)$ can be used. For initial conditions at $\sigma^+$ and $R\sigma^-$ for scattering states the same argument holds, however there is a cancellation between the two integrals so that the sum is zero. For example, for initial conditions given by $R\sigma^-$ on the forward hemisphere $(\vec{p}\cdot\hat{\sigma} > 0)$ which miss the core (the trajectory leading to $\vec{p}_9$ in Appendix C) scatter into the same momentum state for particles starting on the back hemisphere ($\vec{p}_8$ with impact parameter greater than $\sigma$) and thus cancel each other due to opposite signs. Similarly for impact parameters less than $\sigma$, particles starting at $R\sigma^-$ are cancelled by particles at $\sigma^+$ which scatter into the same final state.

It has long been argued that bound states give no contribution to the Boltzmann coefficient; for the square well this can be explicitly proven.[29] For bound trajectories starting at $\sigma^+$ and $R\sigma^-$, operator $\lim_{\varepsilon\to 0} \varepsilon\tilde{R}\{p_ip_j\}_{Tr}$ can be evaluated by

$$\Omega^{(2,2)}_{B.S.} \sim \int d\vec{p}\int_{R\sigma^-,\sigma^+} d\hat{r}(\vec{p}\cdot\hat{r})\{p_ip_j\}_{Tr} \lim_{\varepsilon\to 0} \varepsilon\tilde{R}\{p_ip_j\}_{Tr}$$

$$\sim \int d\vec{p}\int_{R\sigma^-,\sigma^+} d\hat{r}(\vec{p}\cdot\hat{r})\{\lim_{\varepsilon\to 0} \varepsilon \int_0^\infty dt e^{-\varepsilon t}\{p_ip_j\}_{Tr}\{p_i(-t)p_j(-t)\}_{Tr}. \qquad (4.24)$$

Here it is implicitly assumed that (4.24) is to be integrated only over that part of phase space giving bound trajectories. By explicitly writing out the time dependence of $\{p_ip_j\}_{Tr}$ and taking the Laplace transform, one gets an infinite series which can be summed into a closed form before the limit $\varepsilon \rightarrow 0$ can be taken. Taking the limit then proves there is no contribution from bound states.

Thus the $\Omega^{(2,2)}$ integral is given by

$$\Omega^{(2,2)}(T^*) = \frac{-\beta R^2}{8m^2}\left(\frac{\beta}{m\pi}\right)^{1/2} \int d\vec{p}\, f_0(\vec{p}) \int_{R\sigma^+} d\hat{r}\,(\vec{p}\cdot\hat{r}) \times \{p_i p_j\}_{Tr}\{p_i^* p_j^*\}_{Tr} \tag{4.25}$$

where $p_i^*$ is the asymptotic value of $p_i$. Since the dynamics is fully specified by the magnitude of $\vec{p}$ and relative angle $(\vec{p}\cdot\hat{r})$, (4.25) can immediately be written as

$$\Omega^{(2,2)}(T^*) = -\frac{1}{m}\left(\frac{\beta\pi}{m}\right)^{3/2} R^2 \int_0^\infty p^7 dp\, f_0(p) \int_{R\sigma^+} \sin\theta \cos\theta\, d\theta \left[\frac{(\vec{p}\cdot\vec{p}^*)^2}{p^4} - \frac{1}{3}\right] \tag{4.26}$$

Changing variables to reduced momentum $y = \sqrt{(\beta/m)}\, p$ and reduced impact parameter $x = \frac{b}{\sigma} = R \sin\theta$, and denoting $\vec{p}\cdot\vec{p}^*/p^2$ by $\cos\Theta(x,y)$, gives for $\Omega^{(2,2)}$ the result:

$$\Omega^{(2,2)}(T^*) = \int_0^\infty y^7 dy\, e^{-y^2} \int_0^R x dx (1 - \cos^2\Theta(x,y)). \tag{4.27}$$

As seen in Appendix C, if $x$ is less than a critical value, $a$, then $\cos\Theta$ is given by the function $L_4(x,y)$; for larger values $\cos\Theta$ is given by $L_2(x,y)$. Thus $\Omega^{(2,2)}$ may be written as a sum of two terms:

$$\Omega^{(2,2)}(T^*) = I_1(T^*) + I_2(T^*)$$

with

$$I_1(T^*) = \int_0^{\gamma} y^7 dy e^{-y^2} \int_0^R xdx(1 - L_4{}^2(x,y))$$

$$I_2(T^*) = \int_{\gamma}^{\infty} y^7 dy e^{-y^2} \{\int_0^a xdx(1 - L_4{}^2(x,y))$$

$$+ \int_a^R xdx(1 - L_2{}^2(x,y))\}. \qquad (4.28)$$

Here $\gamma$ is the critical momentum where all trajectories hit the core, $\gamma = (T^*(R^2-1))^{1/2}$, and $a = (1 - \frac{1}{y^2 T^*})^{1/2}$. Similar results can be found for $\Omega^{(1,1)}(T^*)$:

$$\Omega^{(1,1)}(T^*) = I_{1D}(T^*) + I_{2D}(T^*)$$

$$I_{1D}(T^*) = 2\int_0^{\gamma} y^5 dy e^{-y^2} \int_0^R xdx(1 - L_4(x,y))$$

$$I_{2D}(T^*) = 2\int_{\gamma}^{\infty} y^5 dy e^{-y^2} \{\int_0^a xdx(1 - L_4(x,y))$$

$$+ \int_a^R xdx(1 - L_2(x,y))\}. \qquad (4.29)$$

These integrals have been evaluated over a range of temperatures and agree with the results of Holleran and Hulbert[30] and Brush and Lawrence.[31] Table IV.1 gives a listing of the $\Omega^{(1,1)}$ and $\Omega^{(2,2)}$ integrals for R = 1.5. Direct calculation of (4.29) for high temperatures can be compared to perturbation theory for the square well gas[32] which gives the $\Omega^{(1,1)}$ integral as a series in $\frac{1}{T^*}$, (i.e. $\Omega^{(1,1)} = 1 + c_1/T^* + \ldots$). The linear approximation given by the perturbation appears to be reasonable only for $\frac{1}{T^*} < .1$; at $\frac{1}{T^*} = .1$ the error between $\Omega^{(1,1)} - 1$ as given by (4.29) and by $c_1/T^*$ is ~ 20%.

TABLE IV.1 COLLISION INTEGRALS FOR THE SQUARE WELL POTENTIAL

| $T^*$ | $\Omega^{(1,1)}(T^*)$ | $\Omega^{(2,2)}(T^*)$ |
|---|---|---|
| .5 | 1.481 | 1.746 |
| 1.0 | 1.331 | 1.477 |
| 1.5 | 1.247 | 1.330 |
| 2.0 | 1.192 | 1.247 |
| 2.5 | 1.156 | 1.195 |
| 3.0 | 1.132 | 1.159 |
| 3.5 | 1.111 | 1.132 |
| 4.0 | 1.096 | 1.113 |
| 4.5 | 1.085 | 1.098 |
| 5.0 | 1.076 | 1.085 |
| 5.5 | 1.069 | 1.076 |
| 6.0 | 1.063 | 1.066 |
| 6.5 | 1.058 | 1.060 |
| 7.0 | 1.054 | 1.054 |
| 7.5 | 1.050 | 1.049 |
| 8.0 | 1.046 | 1.045 |
| 8.5 | 1.044 | 1.041 |
| 9.0 | 1.041 | 1.037 |
| 9.5 | 1.038 | 1.034 |
| 10.0 | 1.036 | 1.032 |
| 20.0 | 1.0174 | 1.0172 |
| 50.0 | 1.0065 | 1.0061 |
| 100.0 | 1.0031 | 1.0028 |
| 200.0 | 1.0015 | 1.0014 |

# CHAPTER V

# EVALUATION OF THE CROSS TERMS FOR THE CLASSICAL SQUARE WELL GAS

The first density correction to the transport coefficients consists of two terms: a kinetic piece, $\Lambda_{kk,1}$ , which depends upon three-body dynamics, and the potential kinetic cross term, $\Lambda_{\phi k,1}$, which depends upon two-body dynamics. The calculation of $\Lambda_{kk,1}$ for the square well would be even more difficult than for hard spheres. However, estimates of its value can be found from molecular dynamics or from model kinetic equations, such as the repeated-ring theory for self-diffusion (see for example Figure II.5). The cross term can be evaluated in detail for $\eta$ and $\lambda$, allowing determination of the importance of bound states relative to scattering states, as follows.

## A. Cross Term for Shear Viscosity

From equation (4.6) the cross term for the shear viscosity can be written as

$$\eta^*_{\phi k,1} = \lim_{\varepsilon\to 0} \frac{\beta^2}{\sigma^3 20 m\Omega^{(2,2)}} \int d\vec{p}_1 d\vec{p}_2 d\vec{r}(r_i p_j)\theta(12)\varepsilon R(12) \tag{5.1}$$

$$\times f_0(12)(1 + \overline{P}_{12})\{p_{1j} p_{1i}\}_{Tr} ,$$

where $\eta^*_{\phi k,1} = \eta_{\phi k,1}/\sigma^3 \eta_0^{H.S.}$, and the first Sonine polynomial approximation has been used. Proceeding by changing to relative and center of momentum coordinates leads to

$$\eta^*_{\phi k,1} = \lim_{\varepsilon\to 0} \frac{\beta^2}{\sigma^3 20 m\Omega^{(2,2)}} \int d\vec{p}_1 d\vec{p}_2 d\vec{r}(r_i p_j)\theta(12)\varepsilon R(12)$$

$$\times f_0(p)e^{-\beta\phi(r)} 2\{p_i p_j\}_{Tr}. \tag{5.2}$$

Making the transformation given by (4.14) gives

$$\eta^*_{\phi k,1} = \lim_{\varepsilon\to 0} \frac{\beta^2}{\sigma^3 5m^2\Omega^{(2,2)}} \int d\vec{p}\; f_0(p) \int d\hat{r}(\vec{p}\cdot\hat{r})\{[|r|^2(r_i p_j)e^{-\beta\phi(r)}$$

$$\times \varepsilon\tilde{R}(r,p)\{p_i p_j\}_{Tr}]_{\sigma^+}$$

$$+ [|r|^2(r_i p_j)e^{-\beta\phi(r)}\varepsilon\tilde{R}(r,p)\{p_i p_j\}_{Tr}]_{R\sigma^+}$$

$$- [|r|^2(r_i p_j)e^{-\beta\phi(r)}\varepsilon\tilde{R}(r,p)\{p_i p_j\}_{Tr}]_{R\sigma^-} . \tag{5.3}$$

The brackets $[\ldots]_{r_i}$ indicate the function is to be evaluated for initial conditions at $|r| = r_i$. To evaluate the operation of $\varepsilon\tilde{R}(r,p)$, the integrals are separated into the phase space for scattering states and bound states; i.e.,

$$\eta^*_{\phi k,1} = \eta^*_{\phi k,1}(S.S.) + \eta^*_{\phi k,1}(B.S.) \tag{5.4}$$

All particles with initial separations $|\vec{r}| = R\sigma^+$ will contribute to the scattering states; for initial conditions at $|\vec{r}| = R\sigma^-$ or $\sigma^+$ the scattering states are given by the condition $\frac{(\vec{p}\cdot\hat{r})^2}{m} > \varepsilon_0$. The bound state contribution is given by complementary portion of the integrals over $|\vec{r}| = R\sigma^-$ and $\sigma^+$. For the scattering states $\varepsilon\tilde{R}(r,p)\{p_i p_j\}_{Tr}$ in the limit $\varepsilon \to 0$ is equal to the asymptotic value of $\{p_i(-t)p_j(-t)\}_{Tr}$.

Denoting $\{p_i^* p_j^*\}_{Tr}$ as

$$\lim_{t\to\infty} \{p_i(-t)p_j(-t)\}_{Tr} = \{p_i^* p_j^*\}_{Tr} , \qquad (5.5)$$

the scattering states part can be written as

$$\eta^*_{\phi k,1}(S.S.) = \frac{8\sqrt{\pi}}{5\Omega^{(2,2)}} \left(\frac{\beta}{m}\right)^{7/2} \int p^6 dp \; e^{-\beta p^2/m} \int d\theta \sin\theta \cos\theta$$

$$\left\{ R^3 \left[ \left(\frac{\hat{r}\cdot\vec{p}^*}{p}\right)\left(\frac{\vec{p}\cdot\vec{p}^*}{p^2}\right) - \frac{1}{3}\left(\frac{\hat{r}\cdot\vec{p}}{p}\right)\frac{p^{*2}}{p^2}\right]_{R\sigma^+} \right.$$

$$+ e^{1/T^*}\left[ \left(\frac{\hat{r}\cdot\vec{p}^*}{p}\right)\left(\frac{\vec{p}\cdot\vec{p}^*}{p^2}\right) - \frac{1}{3}\left(\frac{\hat{r}\cdot\vec{p}}{p}\right)\frac{p^{*2}}{p^2}\right]_{\sigma^+}$$

$$\left. - R^3 e^{1/T^*}\left[ \left(\frac{\hat{r}\cdot\vec{p}^*}{p}\right)\left(\frac{\vec{p}\cdot\vec{p}^*}{p^2}\right) - \frac{1}{3}\left(\frac{\hat{r}\cdot\vec{p}}{p}\right)\frac{p^{*2}}{p^2}\right]_{R\sigma^-} \right\}. \qquad (5.6)$$

The limits of the integrals for various initial conditions can be identified from the dynamics given in Appendix C, and the functions $\left(\frac{\hat{r}\cdot\vec{p}^*}{p}\right)$ and $\frac{\vec{p}\cdot\vec{p}^*}{p^2}$ can be identified with one of the $K_i$'s or $L_i$'s there.

Changing to reduced variables $y = \sqrt{\beta/m}\; p$ and $x = R\sin\theta$ allows $\eta^*_{\phi k,1}(S.S.)$ to be written as a sum of six integrals corresponding to different initial conditions:

$$\eta^*_{\phi k,1}(S.S.) = \frac{8\sqrt{\pi}}{5\Omega^{(2,2)}} \{J_{1\eta} + J_{2\eta} + e^{1/T^*}(J_{3\eta} + J_{4\eta} + J_{5\eta} + J_{6\eta})\}, \qquad (5.7)$$

where

$$J_{1\eta} = R \int_0^{Y} y^6 dy e^{-y^2} \int_0^{R} x dx (K_4 L_4 + \frac{1}{3} K_0)$$

$$J_{2\eta} = R \int_{\gamma}^{\infty} y^6 dy e^{-y^2} \{\int_0^a xdx(K_4L_4 + \frac{1}{3} K_0) + \int_0^R xdx(K_4L_4 + \frac{1}{3} K_0)\}$$

$$J_{3\eta} = \int_{1/\sqrt{T^*}}^{R\gamma} y^6 dy e^{-y^2} \int_0^{R\alpha} xdx(K_6L_6 - K_7L_7 - \frac{2}{3} \alpha^2 K_0')$$

$$J_{4\eta} = \int_{R\gamma}^{\infty} y^6 dy e^{-y^2} \int_0^1 xdx(K_6L_6 - K_7L_7 - \frac{2}{3} \alpha^2 K_0')$$

$$J_{5\eta} = -R \int_{1/\sqrt{T^*}}^{R\gamma} y^6 dy e^{-y^2} \int_0^{R\alpha} xdx(K_{11}L_{11} - K_8L_8 - \frac{2}{3} \alpha^2 K_0)$$

$$J_{6\eta} = -R \int_{1/\sqrt{T^*}}^{\infty} y^6 dy e^{-y^2} \{\int_0^1 xdx(K_{11}L_{11} - K_8L_8 - \frac{2}{3} \alpha^2 K_0)$$

$$+ \int_1^{R\alpha} xdx(K_9L_9 - K_8L_8 - \frac{2}{3} \alpha^2 K_0)\}. \qquad (5.8)$$

Here $\gamma$ and $a$ have the same meaning as in Chapter IV, $\gamma = (T^*(R^2-1))^{-1/2}$, $a = (1 + 1/(y^2T^*))^{1/2}$. Also, $y = 1/\sqrt{T^*}$ is the value below which all trajectories starting inside the well are bound, $y = R\gamma$ is the value where all trajectories starting inside the well with impact parameter $x > 1$ are bound, and finally $x = R\alpha$ (where $\alpha = (1 - 1/(y^2T^*))^{1/2}$) is the impact parameter where for a given value of $y$ all states starting inside the well with $x > R\alpha$ are bound. The bound state part of $\eta^*_{\phi k,1}$ is given by the portion of phase space not covered by integrals $J_{3\eta} - J_{6\eta}$. The action of $\lim_{\varepsilon \to 0} \varepsilon \tilde{R}(r,p)$ for bound states has been evaluated in Appendix C, so that $\eta^*_{\phi k,1}(\text{B.S.})$ can be written

$$\eta^*_{\phi k,1}(\text{B.S.}) = \frac{8\sqrt{\pi}}{5\Omega^{(2,2)}} e^{1/T^*} \{\int_0^{1/\sqrt{T^*}} y^6 dy e^{-y^2} \int_0^1 xdx \frac{1}{3} (1-x^2)^{1/2}$$

$$+ \int_{1/\sqrt{T^*}}^{R\gamma} y^6 dy e^{-y^2} \int_{R\alpha}^1 xdx \frac{1}{3}(1-x^2)^{1/2}$$

$$-R \int_{0}^{1\sqrt{T^*}} y^6 dy e^{-y^2} \int_{0}^{1} x dx \, \frac{1}{3} \left(1 - \frac{x^2}{R^2}\right)^{1/2}$$

$$-R \int_{1/\sqrt{T^*}}^{R\gamma} y^6 dy e^{-y^2} \int_{R\alpha}^{1} x dx \, \frac{1}{3} \left(1 - \frac{x^2}{R^2}\right)^{1/2}$$

$$-R \int_{0}^{R\gamma} y^6 dy e^{-y^2} \int_{1}^{R} x dx \, \frac{1}{3} \left(1 - \frac{x^2}{R^2}\right)^{1/2}$$

$$-R \int_{R\gamma}^{\infty} y^6 dy e^{-y^2} \int_{R\alpha}^{R} x dx \, \frac{1}{3}\left(1 - \frac{x^2}{R^2}\right)^{1/2} \} . \tag{5.9}$$

This result may be simplified into contribution from negative energy states and positive energy states. The positive energy states are bound classically but not quantum mechanically. Thus,

$$\eta^*_{\phi k,1}(B.S.) = \frac{8\sqrt{\pi}}{45\Omega^{(2,2)}} e^{-1/T^*} (X_1 + X_2 + X_3) \tag{5.10}$$

where

$$X_{1\eta} = (-R^3) \int_{1/\sqrt{T^*}}^{\infty} y^6 dy e^{-y^2} (1-\alpha^2)^{3/2}$$

$$X_{2\eta} = (1-R^3) \int_{0}^{1/\sqrt{T^*}} y^6 dy e^{-y^2}$$

$$X_{3\eta} = \int_{1/\sqrt{T^*}}^{R\gamma} y^6 dy e^{-y^2} (1-R^2\alpha^2)^{3/2} . \tag{5.11}$$

Here $X_2$ gives the contribution from negative energy states. In Table V.1, (5.7) and (5.10) are given for several R values and various values of T*. These results are plotted in Figure V.1 for R = 1.5 for comparison with hard spheres and molecular dynamics. The large deviation from the hard sphere result even for the scattering states shows an important dependence

Figure V.1. Comparison of $\eta^*_{\phi k,1}$ and molecular dynamics (ΔΔΔ). Scattering states only (- - -); scattering states plus bound states (-----). Horizontal line is hard sphere limit.

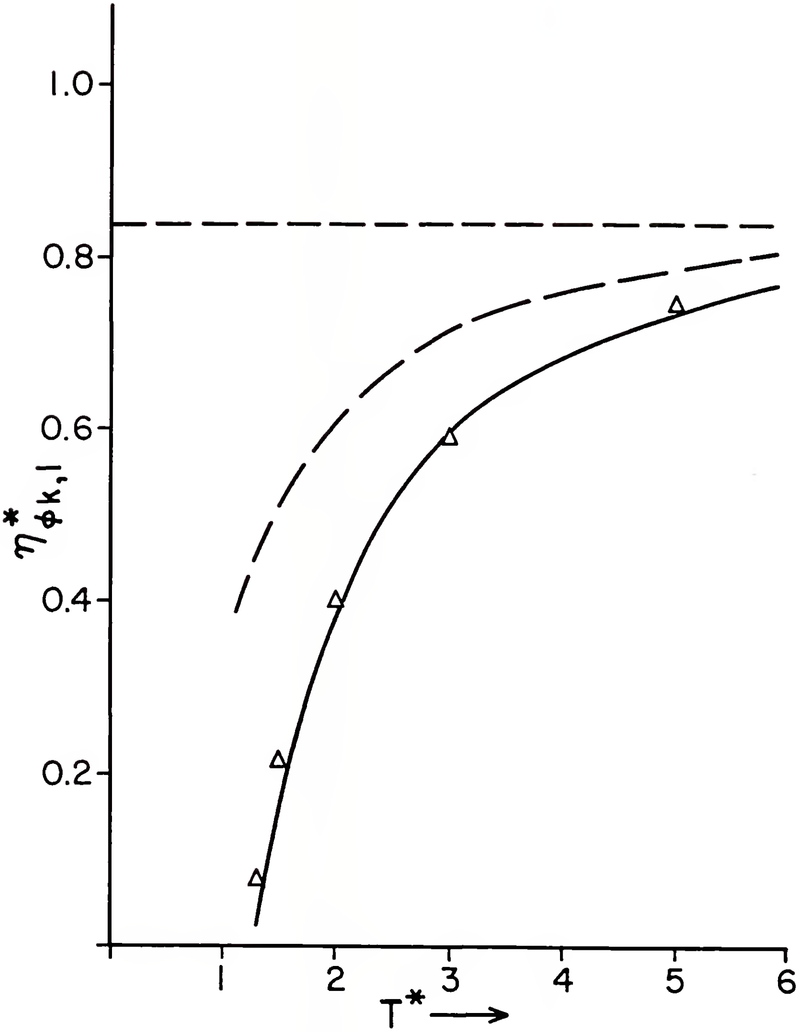
1.0
0.8
0.6
0.4
0.2
$\eta^*_{\phi k,1}$
1
2
3
4
5
6
$T^* \longrightarrow$

on potential model. Further, there is a significant dependence on the bound states (i.e., approximately 30% at $T^* = 2.0$; using the Boltzmann shear viscosity parameters this corresponds to ~ 300° K for Argon). This important effect has been seen to be due mainly to the positive energy bound states.

## B. Cross Term for the Thermal Conductivity

The cross term for the thermal conductivity (equation (4.8)) can be written as the sum of two integrals:

$$\lambda^*_{\phi k,1} = I_1 + I_2, \tag{5.12}$$

where

$$I_1 = \lim_{\epsilon \to 0} \frac{\beta^3}{m\sigma^3 30\Omega^{(2,2)}} \int d\vec{P}d\vec{p}d\vec{r}\ \phi(r)\ P_i\ \epsilon R(12)\ f_0(12)\big(S_i(1) + S_i(2)\big)$$

$$I_2 = \lim_{\epsilon \to 0} \frac{\beta^3}{m\sigma^3 30\Omega^{(2,2)}} \int d\vec{P}d\vec{p}d\vec{r}\ (\vec{P}\cdot\vec{p})r_i\Theta(r,p)\epsilon R(12)f_0(12)\big(S_i(1) + S_i(2)\big). \tag{5.13}$$

Here $\lambda^*_{\phi k,1} = \lambda_{\phi k,1}/\sigma^3\lambda_0^{H.S.}$, and the first Sonine polynomial approximation has been used. The second integral $I_2$ can be handled in the same manner as the shear viscosity cross term, leading to equations similar to (5.7) and (5.10); i.e.,

$$I_2 = I_2(S.S.) + I_2(B.S.). \tag{5.14}$$

Here the scattering states contribution is given by

$$I_2(\mathrm{S.S.}) = \frac{8\sqrt{\pi}}{15\ \Omega^{(2,2)}}\{J_{1\lambda} + J_{2\lambda} + e^{1/T^*}(J_{3\lambda} + J_{4\lambda} + J_{5\lambda} + J_{6\lambda})\}, \tag{5.15}$$

where

$$J_{1\lambda} = R\int_0^{\gamma} y^4 dy\ e^{-y^2}\int_0^R xdx[2y^2L_4K_4 + (4y^2 - 5)K_0]$$

$$J_{2\lambda} = R\int_{\gamma}^{\infty} y^4 dy\ e^{-y^2}\{\int_0^a xdx[2y^2L_4K_4 + (4y^2 - 5)K_0]$$

$$+ \int_a^R xdx[2y^2L_2K_2 + (4y^2 - 5)K_0]\}$$

$$J_{3\lambda} = \int_{1/\sqrt{T^*}}^{R\gamma} y^4 dy\ e^{-y^2}\int_0^{R\alpha} xdx[2y^2(L_6K_6 - L_7K_7)$$

$$+ (4y^2\alpha^2 - 5)K_0']$$

$$J_{4\lambda} = \int_{R\gamma}^{\infty} y^4 dy\ e^{-y^2}\int_0^1 xdx[2y^2(L_6K_6 - L_7K_7)$$

$$+ (4y^2\alpha^2 - 5)K_0']$$

$$J_{5\lambda} = -R\int_{1/\sqrt{T^*}}^{R\gamma} y^4 dy\ e^{-y^2}\int_0^{R\alpha} xdx[2y^2(L_{11}K_{11} - L_9K_9)$$

$$+ (4y^2\alpha^2 - 5)K_0]$$

$$J_{6\lambda} = -R\int_{R\gamma}^{\infty} y^4 dv\ e^{-y^2}\{\int_0^1 xdx[2v^2(L_{11}K_{11} - L_9K_9)$$

$$+(4y^2\alpha^2 - 5)K_0]$$

$$+ \int_1^{R\alpha} x\,dx\left[2y^2(L_8K_8 - L_9K_9) \qquad + (4y^2\alpha^2 - 5)K_0\right]\Big\}. \qquad (5.16)$$

The parameters and functions in (5.16) are the same as those in (5.8). Similarly the bound states contribution may be written

$$I_2(\text{B.S.}) = \frac{56\sqrt{\pi}}{135\ \Omega^{(2,2)}}\, e^{1/T^*}(X_{1\lambda} + X_{2\lambda} + X_{3\lambda}),$$

where

$$X_{1\lambda} = (-R^3)\int_{1/\sqrt{T^*}}^{\infty} y^4 dy\ e^{-y^2}(y^2 - 15/14)(1-\alpha^2)^{3/2}$$

$$X_{2\lambda} = (1 - R^3)\int_0^{1/\sqrt{T^*}} y^4 dy\ e^{-y^2}(y^2 - 15/14)$$

$$X_{3\lambda} = \int_{1/\sqrt{T^*}}^{R\gamma} y^4 dy\ e^{-y^2}(y^2 - 15/14)(1 - R^2\alpha^2)^{3/2}. \qquad (5.18)$$

In (5.18) $X_2$ gives the contribution of negative energy states to $I_2$.

The first integral in (5.13) is of a different type from that found for the shear viscosity, and it is identically zero for hard spheres. However, since the operator $\varepsilon R(12)$ acts on a function of the energy and momenta only, the property $\lim_{\varepsilon\to 0} \varepsilon R(12)g(12) = \lim_{t\to\infty} g(12;-t)$ can be used to evaluate the integral. Doing the center of momentum integral gives

$$I_1 = \frac{\beta}{6\sigma^3\Omega^{(2,2)}} \int d\vec{p}\,d\vec{r}\,f_0(p)\phi(r)e^{-\beta\phi(r)} \lim_{\varepsilon\to 0} \varepsilon\tilde{R}(r,p)\left(\frac{\beta p^2}{m} - \frac{3}{2}\right) \qquad (5.19)$$

The combination $\phi(r)\ e^{-\beta\phi(r)}$ restricts the $d\vec{r}$ integral to points initially within the force range. The action of the resolvent operator on the function of $p^2$ leaves it unchanged for bound states and replaces $p^2$ by $\alpha^2 p^2$ for scattering states. The $d\vec{r}$ integral is seen to be the volume of that portion of the well where scattering occurs (for the contribution to $I_1$ from scattering states) or the volume of that portion of the well where the initial conditions lead to bound states (for the bound state contribution to $I_1$). Changing to reduced variables x and y shows that $I_1$ can be written as

$$I_1 = \frac{2\sqrt{\pi}}{3\Omega^{(2,2)}} \frac{e^{1/T^*}}{T^*} \left(I_1(\text{S.S.}) + I_1(\text{B.S.})\right) \tag{5.20}$$

with

$$\begin{aligned} I_1(\text{S.S.}) = & \int_{1/\sqrt{T^*}}^{R\gamma} y^2 dy \left(\frac{3}{2} - \alpha^2 y^2\right) e^{-y^2} F_1(R\alpha) \\ & + \int_{R\gamma}^{\infty} y^2 dy \left(\frac{3}{2} - \alpha^2 y^2\right) e^{-y^2} F_2(R\alpha), \end{aligned} \tag{5.21}$$

and

$$\begin{aligned} I_1(\text{B.S.}) = & \frac{4}{3} \int_0^{1/\sqrt{T^*}} y^2 dy \left(\frac{3}{2} - y^2\right) e^{-y^2} (R^3 - 1) \\ & + \int_{1/\sqrt{T^*}}^{R\gamma} y^2 dy \left(\frac{3}{2} - y^2\right) e^{-y^2} \left(\frac{4}{3}(R^3 - 1) - F_1(R\alpha)\right) \\ & + \int_{R\gamma}^{\infty} y^2 dy \left(\frac{3}{2} - y^2\right) e^{-y^2} \left(\frac{4}{3}(R^3 - 1) - F_2(R\alpha)\right). \end{aligned} \tag{5.22}$$

In (5.21) and (5.22) the functions $F_1$ and $F_2$ give the volume of the space corresponding to scattering for the square well,

$$\begin{aligned} F_1(x) = & \frac{2R^3}{3} \left(2 - \left(2 + \frac{x^2}{R^2}\right)\left(1 - \frac{x^2}{R^2}\right)^{1/2}\right) \\ & + 2x^2 R\left(1 - \frac{x^2}{R^2}\right)^{1/2} - 2x^2(1 - x^2)^{1/2} \end{aligned}$$

$$-\frac{2}{3}\left(2-(2+x^2)(1-x^2)^{1/2}\right)$$

$$F_2(x) = \frac{2R^3}{3}\left(2-(2+\frac{x^2}{R^2})(1-\frac{x^2}{R^2})^{1/2}\right)$$

$$+\ 2x^2R(1-\frac{x^2}{R^2})^{1/2}-\frac{4}{3}\ . \qquad (5.23)$$

A graph of $\lambda^*_{\phi k,1}$ is shown in figure (V.2) for R = 1.5. A collection of $\lambda^*_{\phi k,1}$ for various values of R is included in Table V.2. For completeness a table of $\eta^*_{kk,0}$ and $\lambda^*_{kk,0}$ for different R values is also included (Table V.3). It should be noted that the inclusion of the bound states leads to qualitatively different behavior from that seen for the shear viscosity; this should be contrasted with the scaled Enskog and modified Enskog theories of chapter II, which predict the same behavior for $\lambda_{\phi k,1}$ and $\eta_{\phi k,1}$.

Figure V.2. Cross term for the thermal conductivity $\lambda^*_{\phi k,1}$; (- - -) scattering states only; (——) scattering plus bound states.

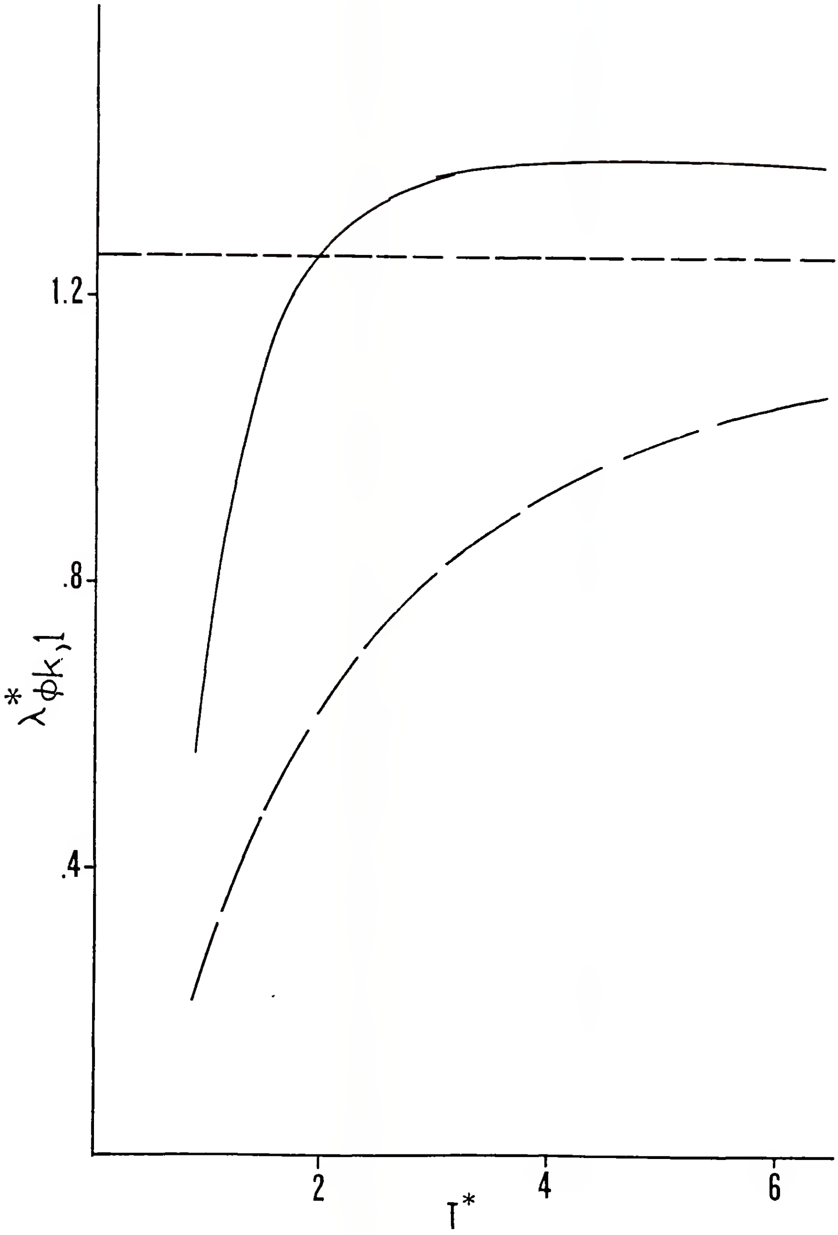
1.2
.8
.4
$\lambda^*_{\phi k,1}$
2
4
6
$T^*$

TABLE V.1 CROSS TERM FOR THE SHEAR VISCOSITY

| R→ | 1.4 | 1.5 | 1.6 | 1.7 | 1.8 | 1.9 | 2.0 |
|---|---|---|---|---|---|---|---|
| $T^*$↓ | | | | | | | |
| 0.5 | -2.574 | -3.312 | -4.058 | -4.823 | -5.615 | -6.436 | -7.271 |
| 1.0 | -0.151 | -0.393 | -0.654 | -0.936 | -1.234 | -1.554 | -1.889 |
| 1.5 | .283 | .142 | -0.014 | -0.186 | -0.373 | -0.576 | -0.794 |
| 2.0 | .469 | .372 | .264 | .143 | .010 | -0.136 | -0.296 |
| 2.5 | .571 | .501 | .421 | .331 | .230 | .118 | -0.005 |
| 3.0 | .636 | .582 | .534 | .450 | .370 | .280 | .183 |
| 3.5 | .678 | .637 | .587 | .531 | .466 | .393 | .313 |
| 4.0 | .711 | .677 | .636 | .589 | .535 | .475 | .408 |
| 5.0 | .750 | .727 | .699 | .666 | .627 | .583 | .534 |
| 6.0 | .776 | .758 | .738 | .712 | .683 | .649 | .611 |
| 7.0 | .792 | .779 | .762 | .743 | .720 | .693 | .663 |
| 8.0 | .803 | .793 | .780 | .764 | .746 | .724 | .700 |
| 9.0 | .811 | .802 | .792 | .779 | .764 | .746 | .726 |
| 10.0 | .817 | .810 | .802 | .790 | .778 | .763 | .746 |

Note: Table entries are normalized by $\eta^*_{\phi k,1} = \eta_{\phi k,1}/(\sigma^3\eta_o^{H.S.})$ .

TABLE V.2 CROSS TERM FOR THE THERMAL CONDUCTIVITY

| R → <br> $T^*$ ↓ | 1.4 | 1.5 | 1.6 | 1.7 | 1.8 | 1.9 | 2.0 |
|---|---|---|---|---|---|---|---|
| 0.5 | -1.529 | -2.198 | -2.814 | -3.396 | -3.964 | -4.526 | -5.078 |
| 1.0 | .753 | .707 | .683 | .675 | .675 | .683 | .694 |
| 1.5 | 1.088 | 1.127 | 1.182 | 1.248 | 1.325 | 1.409 | 1.500 |
| 2.0 | 1.212 | 1.272 | 1.346 | 1.430 | 1.524 | 1.628 | 1.740 |
| 2.5 | 1.269 | 1.336 | 1.413 | 1.502 | 1.599 | 1.704 | 1.818 |
| 3.0 | 1.301 | 1.367 | 1.443 | 1.529 | 1.623 | 1.727 | 1.841 |
| 3.5 | 1.318 | 1.382 | 1.454 | 1.537 | 1.628 | 1.727 | 1.836 |
| 4.0 | 1.329 | 1.390 | 1.458 | 1.535 | 1.623 | 1.717 | 1.822 |
| 5.0 | 1.335 | 1.390 | 1.452 | 1.524 | 1.600 | 1.686 | 1.781 |
| 6.0 | 1.336 | 1.386 | 1.443 | 1.505 | 1.575 | 1.653 | 1.736 |
| 7.0 | 1.335 | 1.380 | 1.430 | 1.488 | 1.552 | 1.620 | 1.698 |
| 8.0 | 1.332 | 1.373 | 1.410 | 1.471 | 1.530 | 1.593 | 1.664 |
| 9.0 | 1.328 | 1.365 | 1.408 | 1.456 | 1.509 | 1.568 | 1.633 |
| 10.0 | 1.326 | 1.359 | 1.400 | 1.444 | 1.492 | 1.547 | 1.606 |

Note: Table entries are normalized by $\lambda^*_{\phi k,1} = \lambda_{\phi k,1}/(\sigma^3\lambda_o^{H.S.})$ .

## TABLE V.3 BOLTZMANN SHEAR VISCOSITY AND THERMAL CONDUCTIVITY

| R → | 1.4 | 1.5 | 1.6 | 1.7 | 1.8 | 1.9 | 2.0 |
|---|---|---|---|---|---|---|---|
| $T^*$ ↓ | | | | | | | |
| 0.5 | .642 | .579 | .528 | .486 | .451 | .421 | .394 |
| 1.0 | .718 | .678 | .644 | .615 | .588 | .564 | .541 |
| 1.5 | .780 | .751 | .726 | .703 | .682 | .662 | .643 |
| 2.0 | .823 | .801 | .781 | .763 | .746 | .730 | .714 |
| 2.5 | .853 | .836 | .820 | .806 | .792 | .778 | .764 |
| 3.0 | .876 | .862 | .849 | .837 | .825 | .813 | .802 |
| 3.5 | .893 | .881 | .870 | .860 | .850 | .840 | .830 |
| 4.0 | .907 | .897 | .887 | .878 | .870 | .861 | .853 |
| 5.0 | .925 | .918 | .911 | .905 | .898 | .891 | .885 |
| 6.0 | .939 | .933 | .928 | .922 | .917 | .912 | .906 |
| 7.0 | .949 | .944 | .939 | .935 | .931 | .926 | .922 |
| 8.0 | .956 | .952 | .948 | .944 | .941 | .937 | .934 |
| 9.0 | .961 | .957 | .954 | .951 | .948 | .945 | .942 |
| 10.0 | .966 | .962 | .960 | .957 | .954 | .952 | .949 |

Note: Table entries are normalized by $\eta^*_{kk,0} = \eta_{kk,0}/\eta_0^{H.S.} = \lambda^*_{kk,0} = \lambda_{kk,0}/\lambda_0^{H.S.}$ .

# CHAPTER VI
# DISCUSSION

The contribution to the first density correction to transport coefficients has been seen to consist of a kinetic-potential cross term and a kinetic-kinetic term involving three body dynamics. The cross term for shear viscosity and thermal conductivity have been calculated in detail for the square well potential and are seen to have a strong temperature dependence both in the scattering states and the bound states, as compared to the hard sphere value (Figure V.1 and V.2). The kinetic terms have not been calculated yet for an potential other than hard spheres. However, estimates of its temperature dependence for $\eta^*_{kk,1}$ and $(nD)^*_1$ may be found from the square well molecular dynamics data of Michels and Trappeniers.[6,11] The kinetic part for shear viscosity ranges from ~ -1.1 at T* = 5.0 to ~ -1.8 at T* = 1.32, compared to the hard sphere value of -1.26. (The uncertainty in $\eta^*_{kk,1}$ for the square well is large enough so that it is not possible to say whether or not $\eta^*_{kk,1}$ has a maximum value and approaches the hard sphere limit from above.) The self diffusion value is seen to range from ~ -1.5 at T* = 5.0 to ~ -5.0 at T* = 1.5, compared to a value of -1.2 for hard spheres. (It is seen that the first density correction terms and the Boltzmann transport coefficient all have similar temperature dependence. This may account for the reasonable agreement found between scaled hard sphere theories and experiment.[20]) As already noted by Michels and Trappeniers,[6] the sign of the first density correction of η for the square gas will change sign at around T* ~ 3.0. This behavior has not been observed in experimental results on simple fluids. However, the lack of data in the low density and low temperature region leaves the possibility open. For example, the measurements of Haynes[33] for the first density correction for Argon and Fluorine above the critical temperature show a tendency to decrease as the temperature is lowered.

As mentioned in Chapter II, the triple collision operator as defined by (B.4) has been calculated in detail for hard spheres. To see the connection between the result here and the hard sphere calculations of Hoegy and Sengers[4], note that the operator $\hat{M}_2$ can be written (in the classical limit) in the form

$$\hat{M}_2 y(1) = -\frac{\varepsilon}{2} f_0^{-1}(1) \int d\vec{x}_2 d\vec{x}_3 \{R_0^{-1}(123)(R(123) - R_0(123))W(123)$$

$$- \sum_{\alpha} R_0^{-1}(\alpha)(R(\alpha) - R_0(\alpha))W(\alpha) - \sum_{\alpha_1} \sum_{\alpha_2 \neq \alpha_1} R_0^{-1}(\alpha_1)(R(\alpha_1) - R_0(\alpha_1))$$

$$\times W(\alpha_1)[f_{\alpha_2} + R_0^{-1}(\alpha_2)(R(\alpha_2) - R_0(\alpha_2)W(\alpha_2))]\}$$

$$\times f_0(1)f_0(2)f_0(3)\ (1 + \sigma\bar{P}_{12} + \sigma\bar{P}_{13})y(1). \qquad (6.1)$$

Here α denotes the pair (i,j), i,j = 1,2,3 and the sum is over distinct pairs; $f_{\alpha_2}$ is the Mayer f-function. For the special case of hard spheres, it can be shown that the operator can be written as Mayer f-functions times operators which generate sequences of binary collisions.

$$\hat{M}_2 y(1) = -f_0^{-1}(1) \int d\vec{x}_2 d\vec{x}_3 \{\sum_{\gamma} f_{\alpha} f_{\beta} \bar{T}_{\gamma} + \sum_{\beta,\gamma} f_{\alpha} \bar{T}_{\beta} R_0 T_{\gamma} + \ldots\} \qquad (6.2)$$

where the $\bar{T}_\alpha$'s and $T_\alpha$'s are the binary collision operators for hard spheres. (See ref. (34) for a discussion of the properties of hard spheres which allow a simplification of this result.) In this way the dominant collision sequences can be identified. For hard spheres the term proportional to only one binary collision among three particles, modified by the excluded volume correction due to the Mayer f-functions, gives better than 90% of the triple contribution to $\Lambda_{kk,1}$. This term can be identified exactly with the Enskog correction due to three body interactions. The next most important term comes from two binary collisions among three particles modified by the excluded volume of the non-interacting particle. Next in importance are the 'ring' events, sequences of three binary collisions among three particles, while all four binary collision scattering events are of negligible importance. Due to the dominance of the Enskog term, attempts have been made to derive a similar expression from (6.1) by a binary collision expansion of the full square well operator. That is, an expression where the dynamics of the interacting particles is modified by static correlations. However the relationships between the T-operators and the Mayer f-functions for hard spheres which allow one to factor the f-functions to the left of the binary collision operators in (6.2) do not hold true for other potentials. In equation (6.2), for example, the first term is obtained from terms like $\overline{T}_\gamma\ (1 + f_\gamma)f_\alpha f_\beta$; for hard spheres $\overline{T}_\gamma f_\gamma = 0$, but not for other potentials. The Enskog approach is also seen to be inadequate for the consideration of bound state effects, as seen in the calculation of the repeated ring theory for self-diffusion.[29] There the effects due to bound states are a major contribution to the first density correction. Thus for fluids with attractive forces it may not be reasonable to attempt to separate static and dynamic correlations between the particles. From the above discussion it is seen that it is not clear how to derive an Enskog-like piece from the triple collision operator for the square well potential considered here, although several 'Enskog-like' models have been suggested previously for evaluation of the triple collision operator.[17]

The dependence of the self-diffusion coefficient for the square well is known not to be the same as the diffusion coefficient for the Lennard-Jones or for experimental data. In Figure VI.1 the addition of the square well gives poorer agreement with experiment than the Enskog theory, although the decrease in the self diffusion coefficient for the square well relative to hard spheres is what one would expect. This effect and the strong temperature dependence found for the cross terms may be due to the inappropriateness of the square well as a model for real fluids, or due to using classical mechanics to calculate the bound state contributions to the transport coefficients. These cases will be considered below.

For the first case it has already been noted that the square well parameters for a fluid as determined from P-V-T data and those determined from transport phenomena are sometimes quite different, while those from a smooth potential such as the Lennard-Jones model are close. While this indicates that one may not be able to map fluid behavior for the square well onto experimental results, it does not explain why there would be qualitative difference in the behavior of the square well fluid as compared to other fluids with attractive potentials. High temperature effects due to the hard core have been seen, e.g. the second virial coefficient exhibits a maximum for real fluids due to penetration of the core while the square well monotonically approaches its hard core value. Another effect associated with the discontinuous potential is the

Figure VI.1. Comparison of nD for the square well (ΔΔΔ), Enskog theory (---), and Lennard-Jones and experimental data (——).

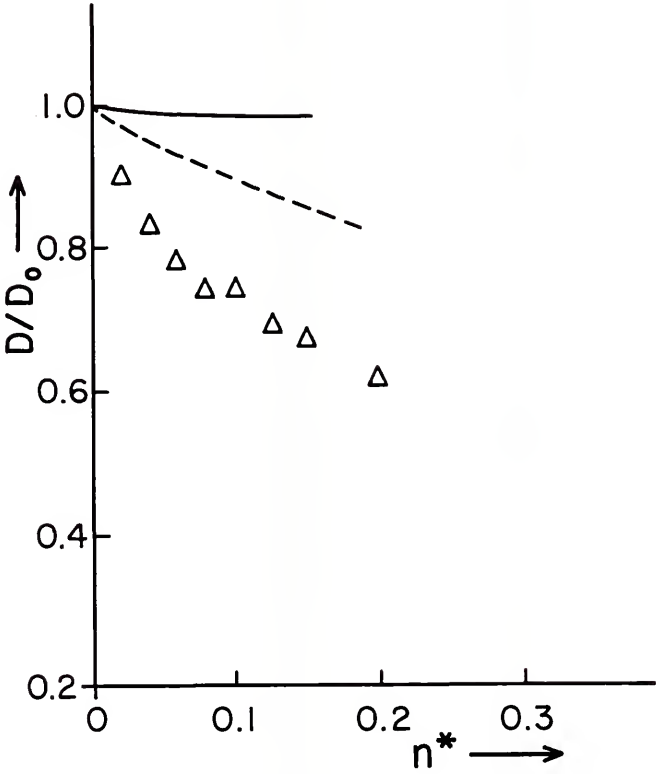
1.0
0.8
0.6
0.4
0.2
$D/D_o$
0
0.1
0.2
0.3
n*

existence of high energy bound states; i.e., no matter what the angular momentum between the two particles is, there is always a region of phase space where the particles are bound together. It is also well known that the square well model (nor other two body potentials) cannot match both second virial and third virial coefficients of experimental data due to the lack of three body forces.[34] In fact the Lennard-Jones and square well predictions for the third virial coefficient do not agree (Figure (VI.2) even though the second virial coefficients do. However, inclusion of three-body forces may not resolve the discrepancy between the square well molecular dynamics and experiment, since the Lennard-Jones molecular dynamics data for self-diffusion does agree with experiment.

The close agreement between the results presented here and the molecular dynamics results can lead one to argue that the disagreement with experiment is due to using classical mechanics for the bound states. Quantum effects would be most notable in the negative energy states which are bound in both classical and quantum systems, and in the metastable states which are bound classically due to the centrifugal barrier but not bound in quantum mechanics. Figures II.2, V.1 and V.2 both exhibit large effects due to bound states; for the shear viscosity, $\eta^*_{\phi k,1}$, almost all the bound state effects are due to the metastable states. The fraction of monomers and dimers can be estimated from the calculations of Stogryn and Hirschfelder[35] (see figure VI.3). It is seen that the square well has approximately twice the fraction of dimers as the Lennard-Jones for the same state conditions. Furthermore, the square well parameters used in figure (VI.2), found from PVT data, have a much shallower well depth than those found for the shear viscosity (see figures I.1 and I.2) so that using the square well to model a

Figure VI.2. Third virial coefficient for square well (-----) and Lennard-Jones (- - -) potentials. Potential parameters as in Figure I.1.

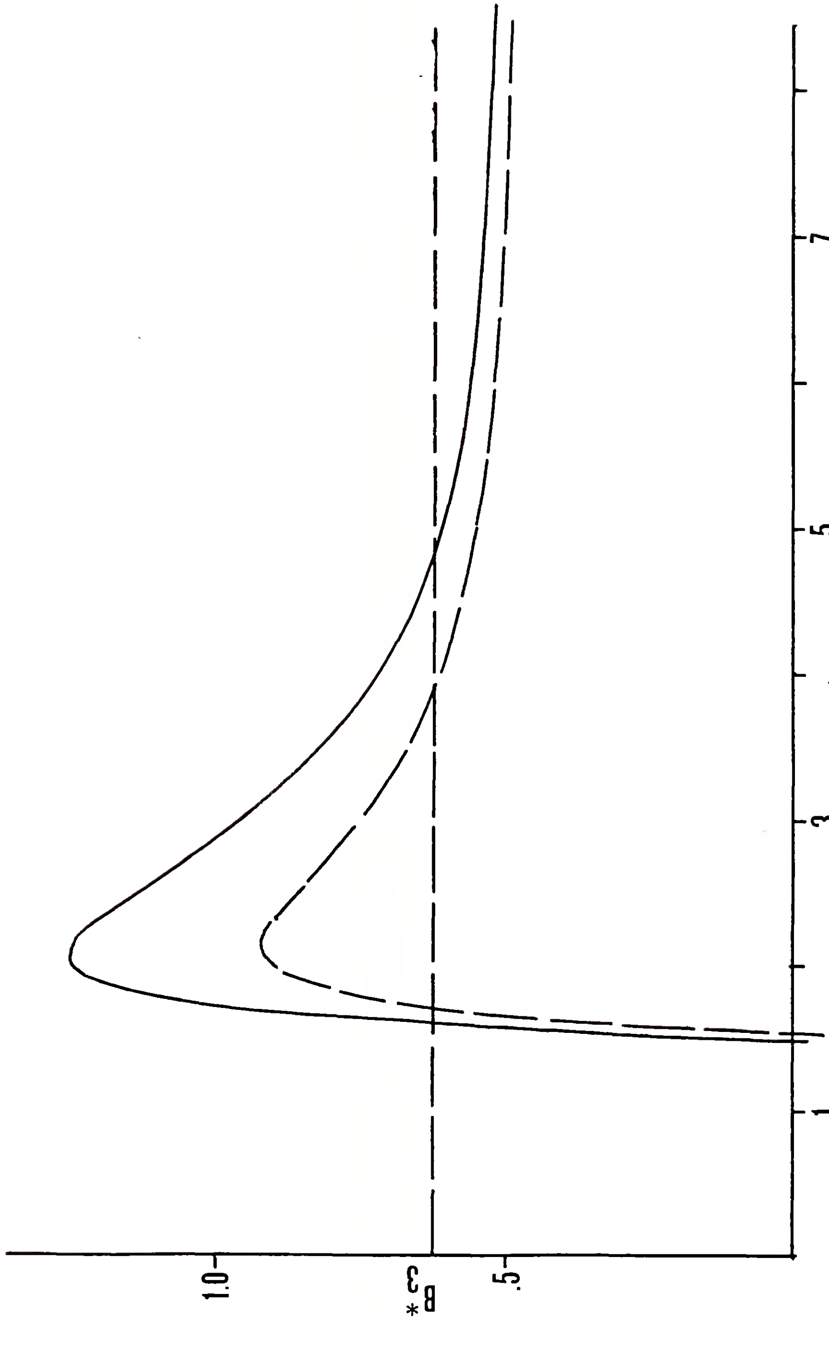
1.0
$B_3^*$
.5
1
3
5
7
T*

Figure VI.3. Fraction of Monomers ($N_1/N$) as a function of temperature at $n\sigma^3 = .01$; Lennard-Jones (- - -), square well (---). Potential parameters same as Figure I.1.

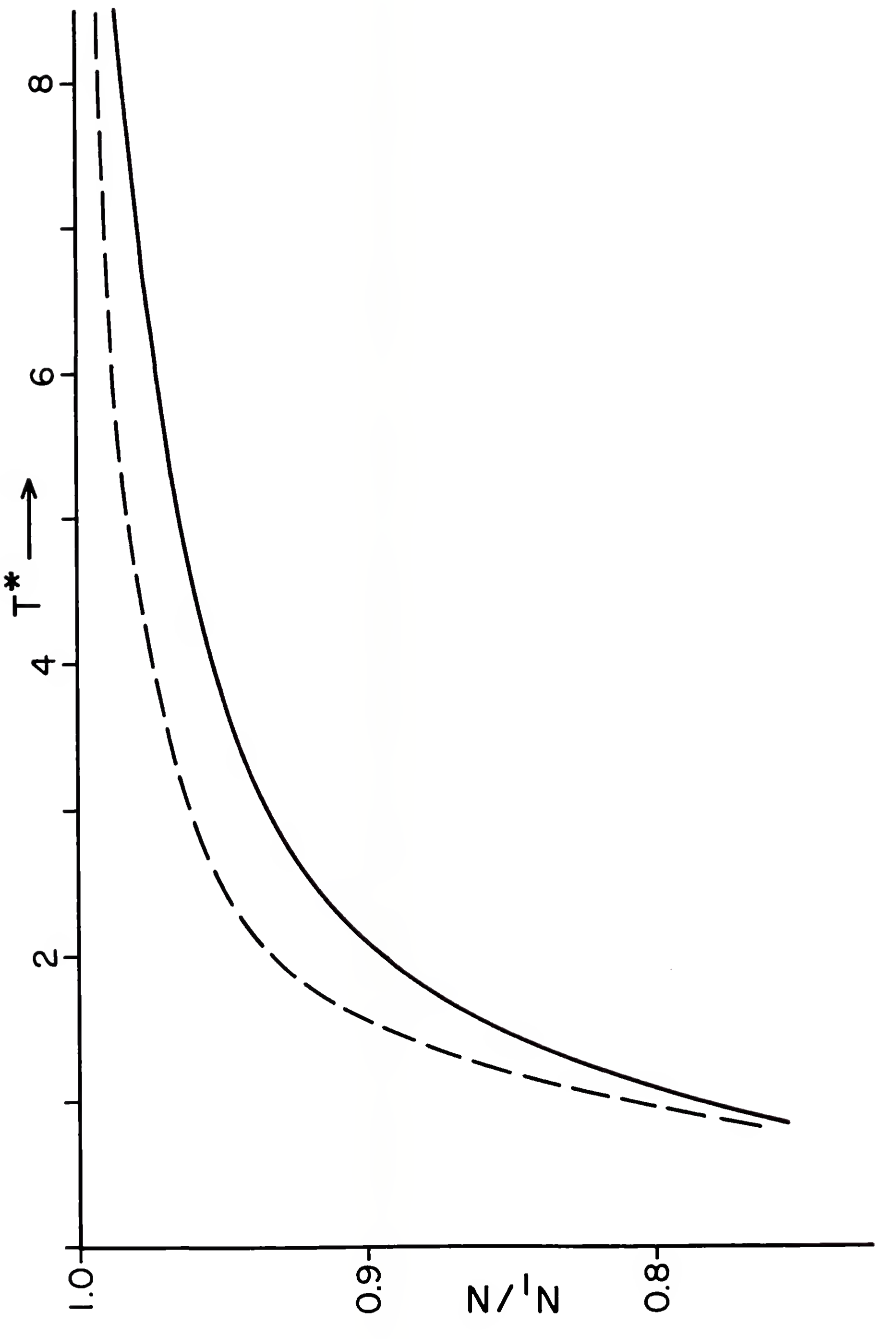
T* ⟶
2
4
6
8
1.0
0.9
0.8
$N_1/N$

transport property leads to a much larger fraction of dimers. Unfortunately it is not possible to predict what overall effect quantum mechanics would have on these states, so the use of quantum mechanics may have no effect on the discrepancy. (The thermal wavelength $\lambda$ is typically of the order $.1\sigma$, so one would not expect quantum effects to be important.)

In summary this work has presented calculations comparing the hard sphere fluid and square well fluid to experimental data and molecular dynamics. It is seen that the hard sphere fluids cannot describe in detail the behavior of real fluids due to the lack of an attractive well. The success of the repeated ring theory for self diffusion indicates a generalization of it for a more general type of transport coefficient would be a useful approach to the evaluation of higher density effects in fluids. (The form of such a generalization is not known at the present time.) The square well calculations agree well with molecular dynamics for square wells; although differences still exist with real fluids. The resolution of these differences would imply either (1) the square well fluid behaves in a manner qualitatively different from fluids with continuous potentials or (2) that it is necessary to use quantum calculations for descriptions of the behavior of dense fluids. These points could be investigated by both theoretical calculation and low density computer simulation of continuous potentials for comparison with the square well or by quantum calculations for the square well. Some investigation of molecular dynamics for the Lennard-Jones model has been done.[36] The slow decay of the time correlation functions at low density appears to be the major obstacle in the way of extensive use of computer simulations at low density. the latter case turns out to agree with the experimental data, it would indicate that the square well potential emphasizes the difference between classical and quantum systems much more than continuous potentials. For the former case, it would indicate that effects important here are sensitive to the detailed form of the potential. It is indeed possible that both effects are important, and that a much better understanding of the mechanisms of transport phenomena in dense gases is necessary.

# APPENDIX A
# CLUSTER EXPANSIONS OF THE TIME CORRELATION FUNCTIONS

The density expansion of the quantum Green-Kubo formulas is obtained in the same manner as for classical systems[12]:

(1) The activity expansion for n, $\psi^{(1)}$, and $\psi^{(2)}$ is obtained from a cluster expansion of a generating function.

(2) The expansion for n is inverted to give the activity as a series in n, which is then used to obtain $\psi^{(1)}$ and $\psi^{(2)}$ or a series in the density.

(3) It is observed that the reduced distribution functions separate naturally into kinetic and potential parts, corresponding to $J_k$ and $J_\phi$, and it is seen that the lowest order terms in $\psi_\phi$ are well defined from the cluster expansion.

(4) The kinetic parts are seen to be ill-defined for $\varepsilon \to 0$ (or $t \to \infty$), hence the behavior of $\psi_k$ is to be determined from a closure the BBGKY hierarchy.

(1) Consider a time correlation function of the form

$$\Lambda = \lim_{\substack{\varepsilon \to 0 \\ V \to \infty}} \frac{1}{V} \int dt\, e^{-\varepsilon t} \langle J_\Lambda J_\Lambda(-t) \rangle \tag{A.1}$$

with

$$J_\Lambda = \Big(1 + \sigma \sum_{\alpha \neq 1}^{N} \overline{P}_{\alpha 1}\Big) a(1) + \frac{\sigma}{2} \sum_{\alpha \neq \beta} b(\alpha\beta). \tag{A.2}$$

and $J_\Lambda(-t) = e^{-L_N t} J_\Lambda(0)$.

The ensemble average is given by (3.6) and the Liouville operator is defined by (3.12). $\overline{P}_{\alpha\beta}$ is the permutation operator for labels $\alpha$ and $\beta$, and $\sigma = 0$ for self correlations. The reduced distribution function $\psi^{(s)}(1..s;\varepsilon)$ are given by (3.9) and the density n is given by

$$n = \lim_{V \to \infty} \frac{1}{V} \langle N \rangle$$

$$= \lim_{V \to \infty} \frac{1}{V} \sum_{N \geq 0} \frac{N\varepsilon^N}{N!\Xi} \operatorname*{Tr}_{1..N} \rho_N. \tag{A.3}$$

It is more convenient to consider the cluster expansion of the reduced density operators defined by

$$n^s F^{(s)}(1..x;\alpha) \equiv \sum_{N \geq s} \frac{\varepsilon^N}{(N-s)!\Xi(\alpha)} \operatorname*{Tr}_{s+1..N} D_N(1..N,\alpha) \tag{A.4}$$

rather than (A.3) and (3.8) separately. Here $D_N(1..N,\alpha)$ is given by

$$D_N(1..N,\alpha) \equiv N! \hat{P}_N \lambda^{3N} e^{-\beta H_N} e^{\alpha J_N(-t)} \tag{A.5}$$

with $\Xi(\alpha) \equiv \sum_{N \geq 0} \frac{\varepsilon^N}{N!} \operatorname*{Tr}_{1-N} D(1..N,\alpha)$.

Here $\alpha$ is a c-number parameter, so that it is seen that $F^{(s)}$ is related to $\psi^{(s)}$ and n by

$$\tilde{\psi}^{(s)}(1..s;t) = \left. \frac{\partial F^{(s)}(1..s;\alpha)}{\partial\alpha} \right|_{\alpha=0}$$

$$n = \lim_{V \to \infty} \frac{1}{V} \operatorname*{Tr}_{1} n F^{(1)}(1;\alpha=0) \tag{A.6}$$

The Husimi-Ursell cluster operators[12], $U(1..s|r..t)$, are the most convenient for expansion of (A.4). They are defined by

$$
\begin{aligned}
D_N(1..N;\alpha) &= U(1..s)\, D_{N-s}(s+1..N;\alpha) \\
&+ \sum_{i=s+1}^{N} U(1..s|i)\, D_{N-s-1}\left(\{j = s+1..N|j\neq i\}_j\,\alpha\right) \\
&+ \sum_{\substack{i<j \\ s+1}}^{N} U(1..s|ij)\, D_{N-s-2}\left(\{k = s+1..N|k\neq i,j\}_j\,\alpha\right) \\
&+ \dots \quad . \qquad \text{(A.7)}
\end{aligned}
$$

By setting N=1,2, etc., the cluster functions can be found in terms of $D_i$'s:

$$
\begin{aligned}
U(1) &= D_1(1;\alpha) \\
U(1|2) &= D_2(12;\alpha) - D_1(1;\alpha)D_1(2;\alpha) \\
U(12) &= D_2(12;\alpha) \qquad \text{(A.8)} \\
U(12|3) &= D_3(123;\alpha) - D_2(12;\alpha)\, D_1(3;\alpha)
\end{aligned}
$$

etc.

Using (A.7) in (A.4) gives

$$n^s\, F^{(s)}(1..s;\alpha) = \sum_{N\geq s} \frac{\varepsilon^N}{(N-s)!\,\Xi(\alpha)} \Big\{ U(1..s) \operatorname*{Tr}_{s+1..N} D_{N-s}(j+1..N,\alpha)$$

$$+ \sum_{i=s+1}^{N} \operatorname*{Tr}_{i}\, U(1..s|i) \operatorname*{Tr}_{\{j\}} D_{N-s-1}(\{j=s+1..N|j\neq i\},\alpha)$$

$$+ \dots \Big\}$$

$$= \varepsilon^s U(1..s) + \varepsilon^{s+1} \operatorname*{Tr}_{s+1} U(1..s|s+1)$$

$$+ \frac{1}{2}\,\varepsilon^{s+2} \operatorname*{Tr}_{s+1,s+2} U(1..s|s+1,s+2) + \dots$$

$$\therefore\ n^s\, F^{(s)}(1..s,\alpha) = \sum_{\ell\geq s}^{\infty} \frac{\varepsilon^\ell}{(\ell-s)!} \operatorname*{Tr}_{s+1..\ell} U(1..s|s+1..\ell) \qquad (A.9)$$

From (A.9) the activity expansion for n and $\psi^{(S)}$ can be found from (A.8):

$$n^s\, \tilde{\psi}^{(s)}(1..s;t) = \sum_{\ell\geq s} \frac{\varepsilon^\ell}{(\ell-s)!} \operatorname*{Tr}_{s+1..\ell} \left.\frac{\partial U(1..s|s+\ell)}{\partial\alpha}\right|_{\alpha=0}$$

$$n = \lim_{V\to\infty} \frac{1}{V} \sum_{\ell\geq 1} \frac{\varepsilon^\ell}{(\ell-1)!} \operatorname*{Tr}_{1..\ell} U(1|2..\ell)\Big|_{\alpha=0} \ . \qquad (A.10)$$

Denoting $\left.\frac{\partial U}{\partial\alpha}\right|_{\alpha=0}$ as U', it will be assumed that the cluster operators are evaluated at $\alpha=0$ from here on. (Note that $D_1(1;\alpha=0)$ is defined such that $\frac{1}{V}\operatorname*{Tr}_{1} D_1(1;\alpha=0) = 1$.)

(2) Inverting the equation for n to get $\varepsilon$ as a power series in the density gives

$$\varepsilon = n - \lim_{V\to\infty} \frac{n^2}{V} \operatorname*{Tr}_{1,2} U(1|2) + \dots \qquad (A.11)$$

Substituting into the activity expansion for $\tilde{\psi}^{(1)}$ and $\tilde{\psi}^{(2)}$ gives (for convenience the $\lim_{V \to \infty}$ will be assumed)

$$\tilde{\psi}^{(1)}(1;t) = U'(1) + n\left(\mathrm{Tr}_{2}\ U'(1|2) - \frac{U'(1)}{V}\ \mathrm{Tr}_{2,3}\ U(2|3)\right)$$

$$+ \ldots$$

$$\tilde{\psi}^{(2)}(12;t) = U'(12) + n\left(\mathrm{Tr}_{3}\ U'(12|3) - 2\,\frac{U'(12)}{V}\ \mathrm{Tr}_{3,4}\ U(3|4)\right)$$

$$+ \ldots \quad . \tag{A.12}$$

For fluxes of the form given by (A.2), the U' and U operators in (A.12) are (with $D(1..s) \equiv D_s(1..s;\alpha)\Big|_{\alpha=0}$ )

$$U'(1) = D(1)\ e^{-L(1)t}\ a(1)$$

$$= D(1)\ a(1) \tag{A.13}$$

$$U'(1|2) = D(12)\ e^{-L(12)t}\left[\left(a(1) + \sigma a(2)\right) + \sigma b(12)\right]$$

$$= \left(D(1)\ D(2)\ a(2) + D(1)\ a(1)\ D(2)\right)$$

$$U(1|2) = D(12)\ e^{-L(12)t} - D(1)\ D(2)$$

$$U'(12) = D(12)\ e^{-L(12)t}\left[a(1) + \sigma a(2) + \sigma b(12)\right]$$

$$U'(12|3) = D(123)\ e^{-L(123)t}\left[a(1) + \sigma\left(a(2) + a(3)\right)\right.$$

$$+ \sigma\big(b(12) + b(13) + b(23)\big)\Big]$$

$$- D(12)\ e^{-L(12)t}\big[a(1) + \sigma a(2) + \sigma b(12)\big]\ D(3)$$

$$- D(12)\ D(3)\ a(3)$$

Therefore the first terms in the density expansion for $\tilde{\psi}^{(1)}$ and $\tilde{\psi}^{(2)}$ are given by

$$\tilde{\psi}^{(1)}(1;t) = D(1)\ \Big(1 - \frac{1}{V}\ \mathop{\mathrm{Tr}}_{2,3}\ U(2|3)\Big)\ a(1)$$

$$+ n\ \mathop{\mathrm{Tr}}_{2}\ \big[D(12)\ e^{-L(12)t} - D(1)\ D(2)\big]\ (1 + \sigma\overline{P}_{12})\ a(1)$$

$$+ n\ \mathop{\mathrm{Tr}}_{2}\ D(12)\ e^{-L(12)t}\ \sigma b(12) \qquad \text{(A.14)}$$

$$\tilde{\psi}^{(2)}(12;t) = D(12)\ e^{-L(12)t}\ \Big(1 - \frac{2}{V}\ \mathop{\mathrm{Tr}}_{3,4}\ U(3|4)\Big)(1 + \sigma\overline{P}_{12})\ a(1)$$

$$+ n\ \mathop{\mathrm{Tr}}_{3}\ \big(D(123)\ e^{-L(123)t} - D(12)\ D(3)\ e^{-L(12)t}\big)$$

$$(1 + \sigma\ \overline{P}_{12} + \sigma\overline{P}_{13})\ a(1)$$

$$+ D(12)\ e^{-eL(12)t}\ \Big(1 - \frac{2}{V}\ \mathop{\mathrm{Tr}}_{3,4}\ U(3|4)\Big)\ \sigma b(12)$$

$$+ n\ \mathop{\mathrm{Tr}}_{3}\ \big\{D(123)\ e^{-L(123)t}\ \sigma(1 + \overline{P}_{13} + \overline{P}_{23})\ b(12)$$

$$- D(12)\ D(3)\ e^{-L(12;t)}\ \sigma b(12)\big\}$$

The integral $\frac{1}{V} \operatorname{Tr}_{\alpha,\beta} U(\alpha|\beta)$ is proportional to the second coefficient:

$$\frac{1}{V} \operatorname{Tr}_{1,2} \left( D(12) - D(1)\ D(2) \right) = -\ 2nB_2 \tag{A.15}$$

(3) From the form of (A.14) the potential and kinetic parts of the reduced distribution functions can be identified:

$$\begin{aligned} \tilde{\psi}_k^{(1)}(1;t) &= (1 + 2nB_2)\ D(1)\ a(1) \\ &\quad + n \operatorname{Tr}_2 \left[ D(12)\ e^{-L(12)t} - D(1)\ D(2) \right] (1 + \sigma\, \overline{P}_{12})\ a(1) \end{aligned} \tag{A.16}$$

$$\begin{aligned} \tilde{\psi}_k^{(2)}(12;t) &= D(12)\ e^{-L(12)t}\ (1 + 4nB_2)\ (1 + \sigma\overline{P}_{12})\ a(1) \\ &\quad + n \operatorname{Tr}_3 \left[ D(123)\ e^{-L(123)t} - D(12)\ D(3)\ e^{-L(12)t} \right] \\ &\qquad \times (1 + \sigma\overline{P}_{12} + \sigma\overline{P}_{13})\ a(1) \end{aligned}$$

and

$$\tilde{\psi}_\phi^{(1)}(1;t) = \operatorname{Tr}_2 D(12)\ e^{-L(12)t}\ \sigma b(12)$$

$$\begin{aligned} \tilde{\psi}_\phi^{(2)}(12;t) &= D(12)\ e^{-L(12)t}\ (1 + 4nB_2)\ \sigma b(12) \\ &\quad + n \operatorname{Tr}_3 \left[ D(123)\ e^{-L(123)t}\ (1 + \overline{P}_{13} + \overline{P}_{23})\ \sigma \right. \\ &\qquad \left. - D(12)\ D(3)\ e^{-L(12)t}\ \sigma \right] b(12). \end{aligned} \tag{A.17}$$

Since it is desired to work with the Laplace transformed correlation functions, the transform of (A.16) and (A.17) gives:

$$\psi_k^{(1)}(1;\varepsilon) = \frac{1}{\varepsilon}\,(1 + 2nB_2)\; D(1)\; a(1)$$

$$+ \, n \mathop{\mathrm{Tr}}_{2} \left[ D(12)\; R(12;\varepsilon) - \frac{1}{\varepsilon}\, D(1)\; D(2) \right] (1 + \sigma\overline{P}_{12})\; a(1)$$

$$\psi_k^{(2)}(12;\varepsilon) = D(12)\; R(12;\varepsilon)\; (1 + 4nB_2)\; (1 + \sigma\overline{P}_{12})\; a(1) \qquad \text{(A.18)}$$

$$+ \, n \mathop{\mathrm{Tr}}_{3} \Big[ \big( D(123)\; R(123;\varepsilon) - D(12)\; D(3)\; R(12;\varepsilon) \big)$$

$$(1 + \sigma\overline{P}_{12} + \sigma\overline{P}_{13}) \Big]\; a(1)$$

and

$$\psi_\phi^{(1)}(1;\varepsilon) = \mathop{\mathrm{Tr}}_{2}\; D(12)\; R(12;\varepsilon)\; \sigma b(12)$$

$$\psi_\phi^{(2)}(12;\varepsilon) = D(12)\; R(12;\varepsilon)\; (1 + 4nB_2)\; \sigma b(12)$$

$$+ \, n \mathop{\mathrm{Tr}}_{3} \Big[ D(123)\; R(123;\varepsilon)\; (1 + \overline{P}_{13} + \overline{P}_{23})$$

$$- \, D(12)\; D(3)\; R(12;\varepsilon) \Big]\; \sigma b(12) \qquad \text{(A.19)}$$

The singular nature of the kinetic parts as $\varepsilon \to 0$ is clearly indicated in (A.18), however the potential terms in (A.19) (or (A.17)) are seen to have well defined behavior for small $\varepsilon$ (or $t \to \infty$). This is due to both the density operators D(ij..) and the flux terms b(ij) being short ranged functions of position, so that only those portions of phase space where the particles are within the force range of each other both at $t = 0$ $(\varepsilon \to \infty)$ and time $t \sim \frac{1}{\varepsilon}$ will contribute to the integral (A.1).

(4) From Chapter III, it is seen that the density expansion of $\psi_k^{(1)}$ and $\psi_k^{(2)}$ is needed for evaluation of the first and second terms of the density series for $\Lambda$. Since (A.18) is not well defined for $\varepsilon \to 0$, the BBGKY hierarchy will be used to find the small $\varepsilon$ behavior of the correlation function. It is known from the classical results that the explicit singular behavior of $\psi_k^{(2)}$ at $\varepsilon \to 0$ can be removed by expressing $\psi_k^{(2)}$ as a functional of $\psi_k^{(1)}$:

$$\psi_k^{(2)}(12;\varepsilon) = \Psi\left(12;\varepsilon \middle| \psi_k^{(1)}(\cdot)\right). \tag{A.20}$$

Then determining $\psi_k^{(1)}$ or a series in the density from the first BBGKY equation (Laplace transformed) –

$$\begin{aligned} \left(\varepsilon + L(1)\right) \psi_k^{(1)}(1;\varepsilon) - \tilde{\psi}_k^{(1)}(1;t = 0) \\ = - n\int dx_2\, L_I\, \Psi\left(12;\varepsilon \middle| \psi_k^{(1)}(\cdot)\right) \end{aligned} \tag{A.21}$$

– will give the kinetic terms in a series well defined for $\varepsilon \to 0$. Equation (A.20) easily be found from (A.18) by solving the first equation of (A.18) for $a(1)$ in terms of $\psi_k^{(1)}(1;\varepsilon)$, and then substituting this result into the second equation; i.e., let $\frac{1}{\varepsilon} D(1)a(1) = \sum_{i=0}^{\infty} \alpha_i n^i$, and equate powers of $n$ on both sides of (A.18) to define the $\alpha_i$'s. This gives

$$a(1) = (1 - 2nB_2)\, \varepsilon\, D^{-1}(1)\, \psi_k^{(1)}(1;\varepsilon)$$

$$- n\varepsilon D^{-1}(1) \operatorname*{Tr}_{2}\{[D(12)\ \varepsilon R_2(12;\varepsilon) - D(1)\ D(2)]$$

$$(1 + \sigma\overline{P}_{12})\ D^{-1}(1)\}\psi_k^{(1)}(1;\varepsilon) + \dots \quad (A.22)$$

The expression of $\psi_2^{(k)}$ as a functional of $\psi_k^{(1)}$ is thus given by

$$\psi_k^{(2)}(12;\varepsilon) = \Psi\ (12;\varepsilon|\psi_k^{(1)}(\cdot))$$

$$= D(12)\varepsilon R(12;\varepsilon)(1 + \sigma\overline{P}_{12})\ D^{-1}(1)\ \psi_k^{(1)}(1;\varepsilon)$$

$$+ n\ \{D(12)\varepsilon R(12;\varepsilon)(1 + \sigma\overline{P}_{12})\ 2B_2\ D^{-1}(1)\ \psi_k^{(1)}(1;\varepsilon)$$

$$- D(12)\varepsilon R(12;\varepsilon)(1 + \sigma\overline{P}_{12})\ D^{-1}(1) \operatorname*{Tr}_{3}[D(13)$$

$$\times\ \varepsilon R_2(13;\varepsilon) - D(1)\ D(3)]\ (1 + \sigma\overline{P}_{13})\ D^{-1}(1)\ \psi_k^{(1)}(1,\varepsilon)$$

$$+ \operatorname*{Tr}_{3}[D(123)\varepsilon R(123;\varepsilon) - D(12)\ D(3)\ \varepsilon R(12;\varepsilon)]$$

$$\times\ (1 + \sigma\overline{P}_{12} + \sigma\overline{P}_{13})\ D^{-1}(1)\ \psi_k^{(1)}(1;\varepsilon)\}$$

$$+ \dots .$$

The equation above can be written so that the terms which reduce to the classical result and those which are purely quantum mechanical may be identified:

$$\Psi(12;\varepsilon|\psi_k^{(1)}(\cdot))\ D(12)\ \varepsilon R(12;\varepsilon)\ (1 + \sigma\overline{P}_{12})\ D^{-1}(1)\ \psi_k^{(1)}(1;\varepsilon)$$

$$+ n \operatorname*{Tr}_{3} \Big[ D(123)\ \varepsilon R(123;\varepsilon) - D(12)\ D(3)\ \varepsilon R(12;\varepsilon) \Big( W(13)\ \varepsilon R(13)$$

$$+ W(23)\ \varepsilon R(23) - 1 \Big)\ (1 + \sigma \overline{P}_{12} + \sigma \overline{P}_{13}) \Big] D^{-1}_{(1)}\ \psi_k^{(1)}(1,\varepsilon)$$

$$+ n\ D(12)\ \varepsilon R(12)\ (1 + \sigma \overline{P}_{12})\ Q(2)\ D^{-1}_{(1)}\ \psi_k^{(1)}(1;\varepsilon)$$

$$+ \ldots \quad . \tag{A.23}$$

Here

$$W(ij) = D^{-1}(i)\ D^{-1}(j)\ D(ij)$$

$$\text{and} \quad Q(i) = 2B_2 + D^{-1}(i) \operatorname*{Tr}_{j} \big( D(ij) - D(i)\ D(j) \big). \tag{A.24}$$

From (A.24) it is easily seen that the operator Q(i) vanishes for classical mechanics. The first two terms in (A.24) give the classical result if the replacements

$$D(1..S) \rightarrow f_0(1)\ ..\ f_0(S)\ e^{-\beta \sum_{i<j} \phi(ji)}$$

$$W(1..S) \rightarrow e^{-\beta \sum_{i<j} \phi(ij)} \tag{A.25}$$

$$R(1..s;\varepsilon) \rightarrow \big(\varepsilon + L_{cl.}(1..s)\big)^{-1}$$

$$\text{and} \quad \operatorname*{Tr}_{1..s} \rightarrow \int d\vec{q}_1\ d\vec{p}_1\ \ldots\ d\vec{q}_s\ d\vec{p}_s\ .$$

Here $f_0$ is the Maxwell-Boltzmann distribution, $\phi(ij)$ is the interparticle potential, and $L_{cl.} = \sum_{\alpha=1}^{s} \frac{\vec{p}_{\alpha i}}{m} \cdot \frac{\partial}{\partial q_{\alpha i}} + \sum_{\alpha<\beta}^{s} L_I(\alpha\beta)$ (note $L_I(\alpha\beta) = -\frac{\partial\phi(\alpha\beta)}{\partial q_{\alpha\beta,i}} \frac{\partial}{\partial p_{\alpha\beta,i}}$ for continuous potentials).

Using (A.23) in (A.21) identifies the terms in Equations (3.13) to (3.19). The density expansion of $\hat{M}$ in Equation (3.15) is thus

$$\hat{M}_1 f_{(1)} = \lim_{\varepsilon \to 0} D^{-1}_{(1)} \mathrm{Tr}_2\, L_I(12)\, \Psi_1\big(12;\varepsilon \big| D(1)\, f(1)\big)$$

$$\hat{M}_2 f_{(1)} = \lim_{\varepsilon \to 0} D^{-1}(1)\, \mathrm{Tr}_2\, L_I \Psi_2\big(12;\varepsilon \big| D(1)\, f(1)\big), \tag{A.26}$$

where from (A.24) $\Psi_1$ and $\Psi_2$ are given by

$$\Psi_1(12;\varepsilon|\cdot) = D(12)\, \varepsilon R(12,\varepsilon)\, (1 + \sigma\overline{P}_{12})\, D^{-1}(1)\, (\cdot)$$

$$\begin{aligned} \Psi_2(12;\varepsilon|\cdot) = {} & \mathrm{Tr}_3 \Big[D(123)\, \varepsilon R(123;\varepsilon) - D(12)\, D(3)\, \varepsilon R(12;\varepsilon) \\ & \times \big(W(13)\, \varepsilon R(13;\varepsilon) + W(23)\, \varepsilon R(23;\varepsilon) - 1\big) \\ & \times (1 + \sigma\overline{P}_{12} + \sigma\overline{P}_{13})\Big]\, D^{-1}(1)\, (\cdot) \\ & + \lim_{\varepsilon \to 0} D(12)\, \varepsilon R(12;\varepsilon)\, (1 + \sigma\overline{P}_{12})\, Q(2)\, D^{-1}(1)\, (\cdot) \end{aligned} \tag{A.27}$$

As mentioned previously the operators for self correlations is given by $\sigma \to 0$ above; i.e.

$$M_{1s} f(1) = \lim_{\varepsilon \to 0} D^{-1}(1)\, \mathrm{Tr}_2\, L_I(12)\, D(12)\, \varepsilon R(12;\varepsilon)\, f(1)$$

$$M_{2s} f(1) = \lim_{\varepsilon \to 0} D^{-1}(1)\, \mathrm{Tr}_{2,3}\, \{L_I(12)\, [D(123)\, \varepsilon R(123;\varepsilon) -$$

$$D(12)\ D(3)\ \varepsilon R(12;\varepsilon)\ \left(W(13)\ \varepsilon R(13;\varepsilon) + W(23)\ \varepsilon R(23;\varepsilon) - 1\right)\Big]$$

$$f(1)\Big\} + \lim_{\varepsilon \to 0} D^{-1}(1) \operatorname*{Tr}_{2} D(12)\ \varepsilon R(12;\varepsilon)\ Q(2)\ f(1). \qquad (A.28)$$

# APPENDIX B
## COLLISION OPERATORS FOR THE SQUARE WELL POTENTIAL

The form of the operators given in Appendix A are well known for continuous potentials. For discontinuous potentials the interacting part of the Liouville operator, $L_I(i,j)$, must be defined so that there is not explicit reference to the force, or the collision operators must be written without explicit reference to the $L_I$'s.

For the second case the following identities are used:

$$\sum_{\substack{i<j\\1}}^{s} L_I(i,j)R(1..s) = -R_0^{-1}(1..s)(R(1..s) - R_0(1..s))$$

$$\mathop{\mathrm{Tr}}_{2,3} L_I(12)R(123)\chi(123) = \mathop{\mathrm{Tr}}_{2,3} L_I(13)R(123)\chi(123)$$

$$\mathop{\mathrm{Tr}}_{2,3} L_I(23)R(123)\chi(123) \equiv 0. \tag{B.1}$$

Here the $\varepsilon$ dependence of the operator will not be exhibited explicitly. $\chi(123)$ in (B.1) is any function invariant under interchange of particles and $R_0 = (\varepsilon+L_0)^{-1}$ is the resolvent operator for free streaming. From Appendix A the first and second terms in the density expansion of $\hat{M}(\varepsilon)$ are

$$\hat{M}_1 f(1) = D^{-1}(1) \mathop{\mathrm{Tr}}_{2} L_I(12)\varepsilon R(12)D(12)(1+\sigma\bar{P}_{12})f(1)$$

$$\hat{M}_2 f(1) = D^{-1}(1) \mathop{\mathrm{Tr}}_{2,3} \{L_I(12)[D(123)\varepsilon R(123)$$

$$-D(12)D(3)\varepsilon R(12)\left[W(13)\varepsilon R(13)+W(23)\varepsilon R(23) - 1\right](1+\sigma\overline{P}_{12}+\sigma\overline{P}_{13})\left]f(1)\right\}$$

$$+ D^{-1}(1) \operatorname*{Tr}_{2} L_I(12)D(12)\varepsilon R(12)(1+\sigma\overline{P}_{12})O(2)f(1). \qquad (B.2)$$

In the limit $\varepsilon \to 0$, the first equation in (B.2) gives the Boltzmann collision operator for quantum systems if f(1) is diagonal in momentum representation. The second equation, for $\hat{M}_2$, is equivalent to the results of McLennan[10] for the triple collision term, if McLennan's activity expansion is converted to a density expansion. Using the first equation of (B.1) in $\hat{M}_1$ gives the following result for $\hat{M}_1$:

$$\hat{M}_1 f(1) = -D^{-1}(1) \operatorname*{Tr}_{2} R_0^{-1}(12)\varepsilon(R(12) - R_0(12))D(12)(1+\sigma\overline{P}_{12})f(1). \qquad (B.3)$$

$\hat{M}_2$ may be written in a more symmetric form by using the second and third identities of (B.1), then eliminating the $L_I$'s gives

$$\hat{M}_2 f(1) = -D^{-1}(1) \operatorname*{Tr}_{2,3} \Big\{\tfrac{1}{2} R_0^{-1}(123)\varepsilon(R(123) - R_0(123))D(123)$$

$$-R_0^{-1}(12)\varepsilon(R(12) - R_0(12)D(12)D(3)\left[W(13)\varepsilon R(13)\right.$$

$$\left.+ W(23)\varepsilon R(23) - 1\right](1+\sigma\overline{P}_{12} + \sigma\overline{P}_{23})f(1)$$

$$-D^{-1}(1) \operatorname*{Tr}_{2} R_0^{-1}(12)\varepsilon(R(12) - R_0(12))D(12)(1+\sigma\overline{P}_{12})O(2)f(1) \qquad (B.4)$$

The interacting part of the Liouville operator $L_I$, is defined to be the commutator with potential, $\phi_{ij}$. This holds true even for discontinuous potentials; however one must be careful when taking the commutator with momentum operators since the relation $\left[p_\alpha, \cdot\right] \to \frac{h}{i}\frac{\partial}{\partial r_\alpha}$ cannot be used. For the classical limit this implies that the usual expression for $L_I$,

$$L_I(ij) = -\theta_{ij} = -\frac{\partial\phi(ij)}{\partial \vec{r}_{ij}} \cdot \frac{\partial}{\partial \vec{p}_{ij}}$$

is not appropriate. In the classical limit the interacting part of the Liouville operator $L_I(ij)$ for discontinuous potentials generates finite changes in the momentum in the limit $t \to 0$; i.e. $\lim_{t \to 0^+} e^{-L(ij)t} F(ij) \neq F(ij)$. The exact form for the interaction term depends upon whether the $t \to 0$ limit is taken from the positive or negative side, whether the streaming is forward or backward in time, and whether the probability distribution operator, $\rho$, are acted upon by the time evolution operator. Since this work does not explicitly use the interaction operator, it will not be considered further.

# APPENDIX C
# SQUARE WELL TRAJECTORIES

The dynamics for a binary collision of particles interacting via a square well can be found in a straight-forward manner using conservation of energy and conservation ofangular momentum for each partial collision at the core or the outer edge of the well. Depending upon the initial conditions, a trajectory must be one of seven distinct scattering trajectories or six distinct bound state trajectories (Figures C.1 and C.2). In Figures C.1 and C.2 and the following, $\vec{p}$ and $\vec{r} = |r|\hat{r}$ denote the initial relative momentum and position of the particles, and $\vec{p}_i$ stand for the relative momentum of the particles after a partial collision at $\vec{r}_i$. The dynamics are to be calculated backward in time, and most functions will be expressed in reduced units of

$$\text{temperature} \qquad T^* = \frac{k_B T}{\varepsilon_0}$$

$$\text{impact parameter} \qquad x = b/\sigma$$

$$\text{momentum} \qquad y = \left(\frac{\beta}{m}\right)^{1/2} p \qquad (C.1)$$

where b is the initial impact parameter and $-\varepsilon_0$ is the depth of the well. To solve the dynamics it is useful to know the four types of partial collisions shown in Figure C.3.

Figure C.1. Scattering states for square well binary collisions.

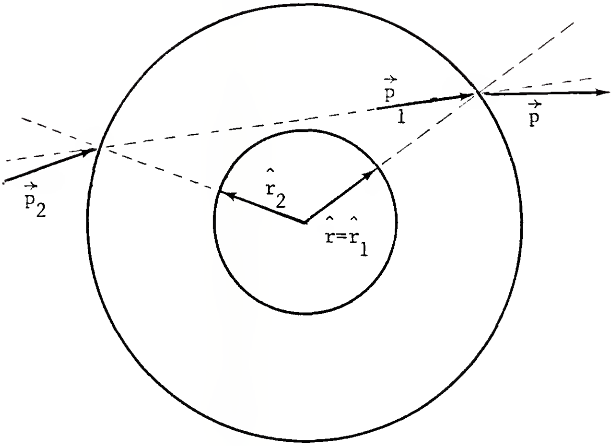
$\vec{p}_1$
$\vec{p}$
$\vec{p}_2$
$\hat{r}_2$
$\hat{r}=\hat{r}_1$

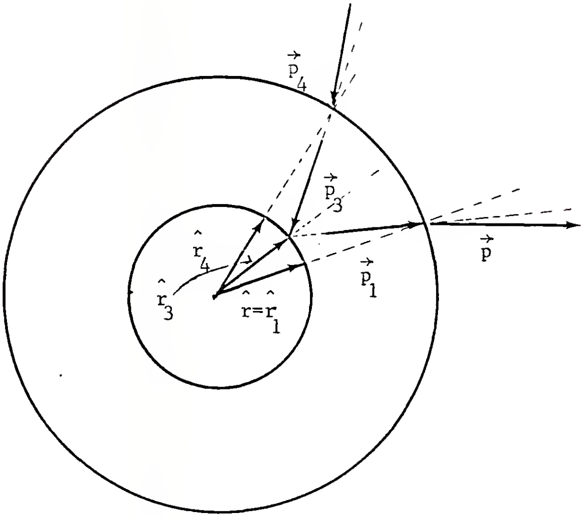
$\vec{p}_4$
$\vec{p}_3$
$\vec{p}$
$\hat{r}_4$
$\hat{r}_3$
$\vec{p}_1$
$\hat{r}=\hat{r}_1$

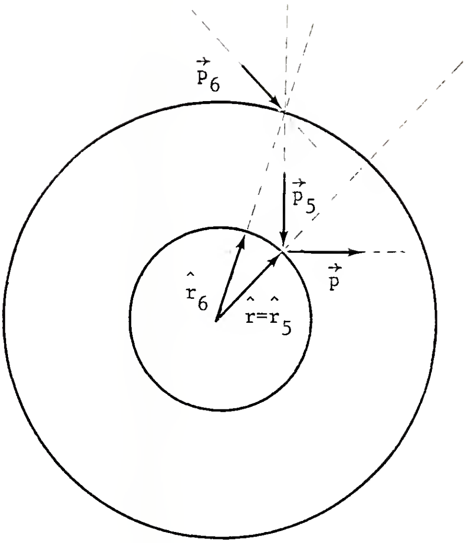
$\vec{p}_6$
$\vec{p}_5$
$\vec{p}$
$\hat{r}_6$
$\hat{r}=\hat{r}_5$

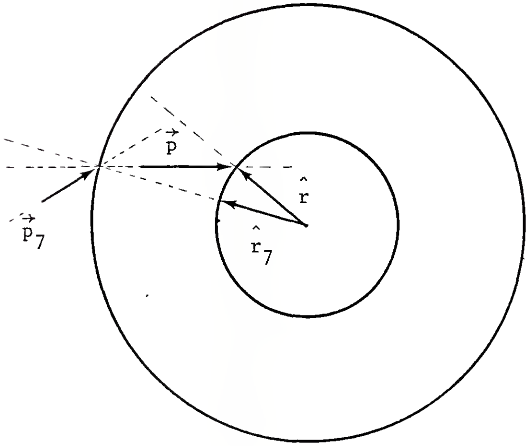
$\vec{p}$
$\hat{r}$
$\vec{p}_7$
$\hat{r}_7$

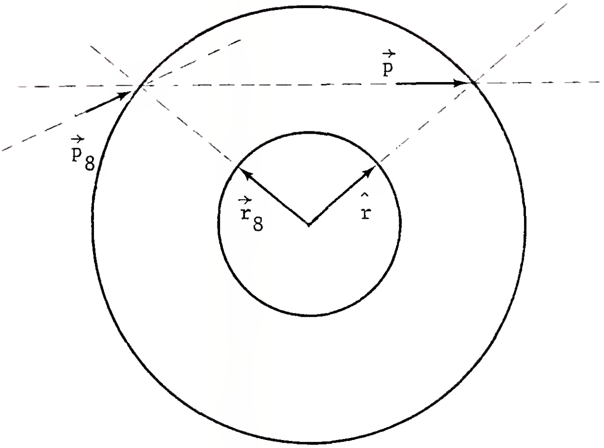
$\vec{p}$
$\vec{p}_8$
$\vec{r}_8$
$\hat{r}$

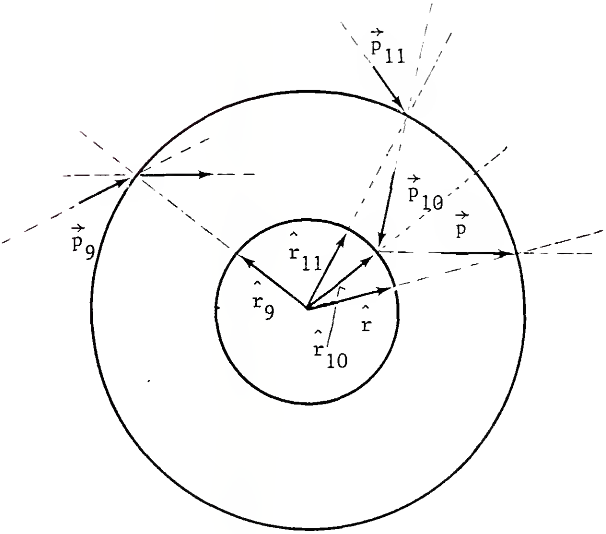
$\vec{p}_{11}$
$\vec{p}_{10}$
$\vec{p}$
$\vec{p}_9$
$\hat{r}_{11}$
$\hat{r}_9$
$\hat{r}$
$\hat{r}_{10}$

Figure C.2. Bound state trajectories for the square well.

I.

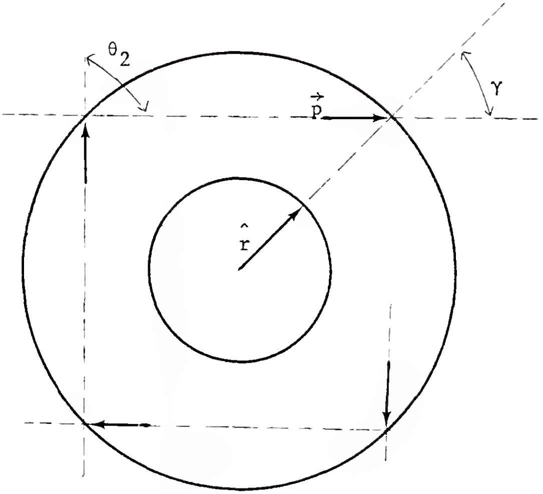

II.

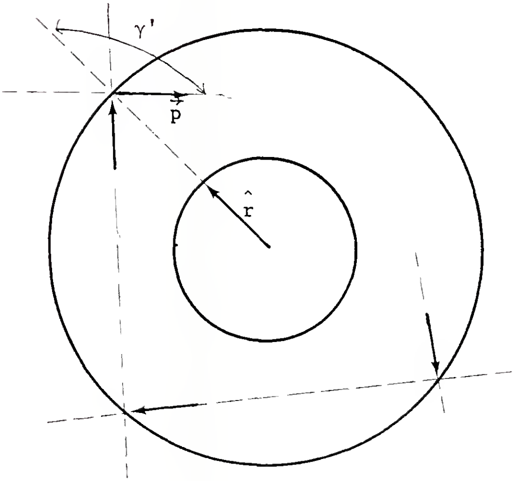

III.

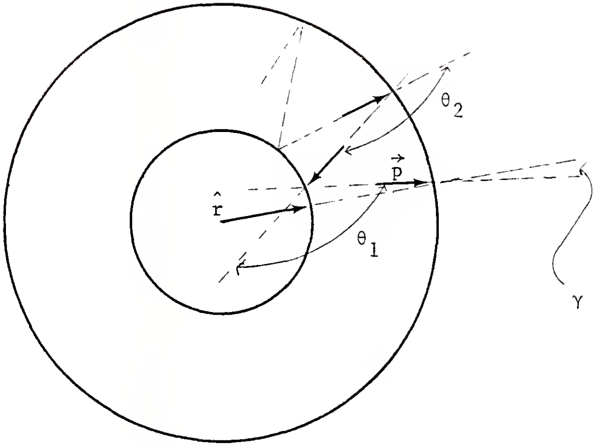

IV.

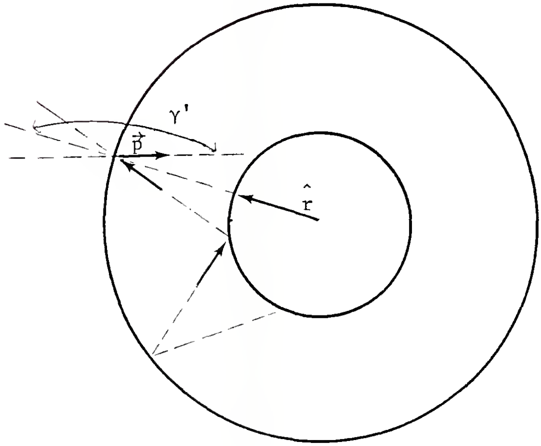

V.

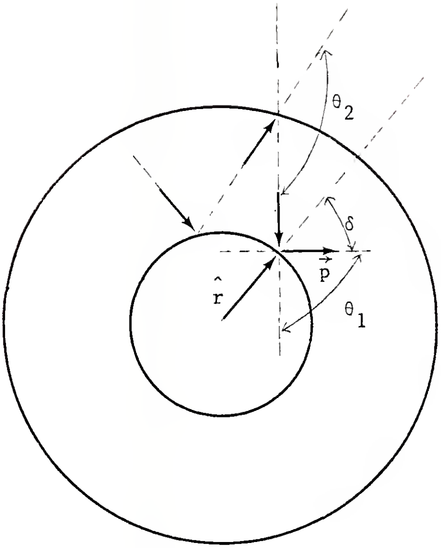

VI.

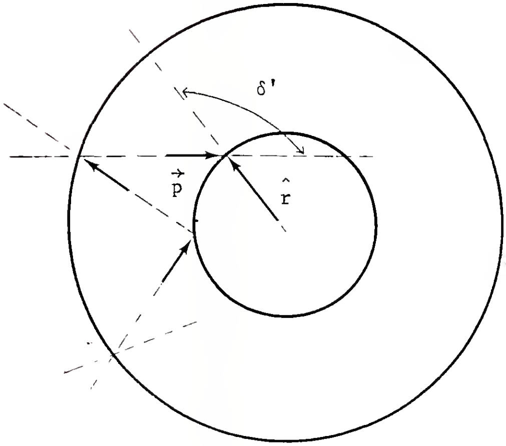

Figure C.3. Partial Collisions at $\sigma^+$, $R\sigma^+$ and $R\sigma^-$ for the square well.

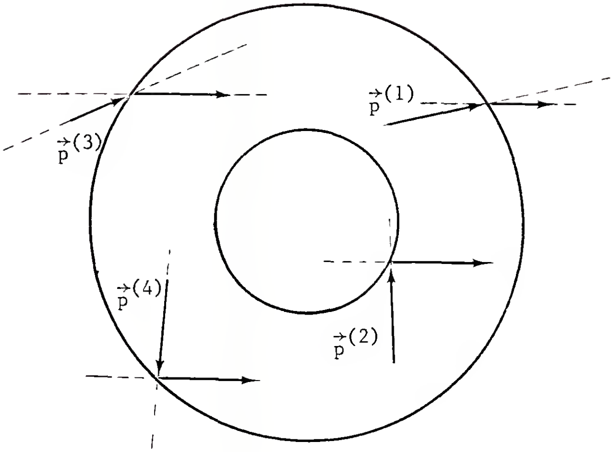
$\vec{p}^{(1)}$
$\vec{p}^{(3)}$
$\vec{p}^{(4)}$
$\vec{p}^{(2)}$

Using the conservation principles it is easily seen that

(1) For $\vec{p}\cdot\hat{r} > 0$ and $r \to R\sigma^{+}$

$$\vec{p}^{(1)} = \vec{p} + p\beta_1\hat{r}$$

$$\beta = a\left(1 - \left(\frac{x}{Ra}\right)^2\right)^{1/2} - \left(1 - \left(\frac{x}{R}\right)^2\right)^{1/2}$$

$$a = \left(1 + 1/y^2T*\right)^{1/2} \qquad \text{(C.2a)}$$

(2) For $\vec{p}\cdot\hat{r} > 0$ and $r \to \sigma^{+}$

$$\vec{p}^{(2)} = \vec{p} - p\beta_2\hat{r}$$

$$\beta_2 = 2\ (1 - x^2)^{1/2} \qquad \text{(C.2b)}$$

(3) For $\vec{p}\cdot\hat{r} < 0$ and $r \to R\sigma^{-}$ (scattering)

$$\vec{p}^{(3)} = \vec{p} + p\beta'\ \hat{r}$$

$$\beta_1' = \left(1 - \left(\frac{x}{R}\right)^2\right)^{1/2} - \alpha\left(1 - \left(\frac{x}{R\alpha}\right)^2\right)^{1/2}$$

$$\alpha = \left(1 - \frac{1}{y^2T^*}\right)^{1/2} \qquad \text{(C.2c)}$$

(4) For $\vec{p} \cdot \hat{r} < 0$ and $r \rightarrow R\sigma^-$ (bound)

$$\vec{p}^{(4)} = \vec{p} - p\beta_3 \hat{r}$$

$$\beta_3 = -2\left(1 - \frac{x^2}{R^2}\right)^{1/2} \qquad \text{(C.2d)}$$

For convenience, the scattering states and bound states will be considered separately.

1. Scattering states.

Using Equation (C.2) the distances a particle travels between momentum changes are easily seen to be

$$d_1 = R\left(1 - \left(\frac{x}{Ra}\right)^2\right)^{1/2} - \left(1 - \frac{x}{a}\right)^{1/2}$$

$$d_2 = R\left(1 - \left(\frac{x}{Ra}\right)^2\right)^{1/2}$$

$$d_3 = R\left(1 - \left(\frac{x}{R}\right)^2\right)^{1/2} - \left(1 - x^2\right)^{1/2}$$

$$d_4 = R\left(1 - \left(\frac{x}{R}\right)^2\right)^{1/2} \qquad \text{(C.3)}$$

Thus using Equations (C.2) and (C.3) one can find the eleven position and momentum vectors of Figure 4 in terms of the original vectors $\vec{p}$, $\hat{r}$:

$$\vec{p}_1 = \vec{p} + p\beta_1 \hat{r} \qquad |\vec{p}_1| = pa$$

$$\hat{r}_1 = \hat{r} \qquad \text{(C.4a)}$$

$$\vec{p}_2 = \left(1 - \frac{2d_2\beta_1}{Ra}\right) \vec{p} + p\beta_1 \left(2 - \frac{2\beta_1 d_2}{Ra}\right) \hat{r}$$

$$|\vec{p}_2| = p$$

$$\hat{r}_2 = \left(1 - \frac{2\beta_1 d_2}{Ra}\right) \hat{r} - \frac{2d_2}{Rpa} \vec{p} \qquad \text{(C.4b)}$$

--------

$$\vec{p}_3 = \left(1 + d_1\beta_2'\right) \vec{p} + p\beta_1 \left[1 - \frac{a\beta_2'}{\beta_1} \left(R - \frac{\beta_1 d_1}{a}\right)\right] \hat{r}$$

$$|\vec{p}_3| = pa$$

$$\hat{r}_3 = \left(R - \frac{\beta_1 d_1}{a}\right) \hat{r} - \frac{d_1}{pa} \vec{p} \qquad \text{(C.4c)}$$

--------

$$\vec{p}_4 = \left[1 + d_1\beta_2' - \frac{d_1\beta_1}{Ra} \left(2 + d_1\beta_2'\right)\right] \vec{p}$$

$$+ \, p \left[2\beta_1 - a\beta_2' R + 2\beta_1\beta_2' d_1 - \frac{d_1\beta_1^2}{Ra} \left(2 + d_1\beta_2'\right)\right] \hat{r}$$

$$|p_4| = p \qquad \text{(C.4d)}$$

$$\hat{r}_4 = \left[1 + d_1\beta_2' - \frac{d_1\beta_1}{Ra} \left(2 + d_1\beta_2'\right)\right] \hat{r}$$

$$- \frac{d_1}{Rpa} \left(2 + d_1\beta_2'\right)] \, \vec{p}$$

Note that in (C.4c) and (C.4d), $\beta_2' = 2 \left(1 - \frac{x^2}{a^2}\right)^{1/2}$.

$$\vec{p}_5 = \vec{p} - p\beta_2\,\hat{r} \qquad |\vec{p}_5| = p$$

$$\hat{r}_5 = r \qquad (C.4e)$$

$$\vec{p}_6 = \left(1 - \frac{d_3\beta_1'}{R}\right)\vec{p} + p\left(\frac{\beta_1'}{R}(1 + d_3\beta_2) - \beta_2\right)\hat{r}$$

$$|\vec{p}_6| = p\alpha$$

$$\hat{r}_6 = \left(\frac{1}{R} + \frac{d_3\beta_2}{R}\right)\hat{r} - \frac{d_3}{Rp}\vec{p} \qquad (C.4f)$$

--------

$$\vec{p}_7 = \left(1 - \frac{\beta_1' d_3}{R}\right)\vec{p} + \frac{p\beta_1'}{R}\hat{r} \qquad |\vec{p}_7| = p\alpha$$

$$\hat{r}_7 = \frac{1}{R}\hat{r} - \frac{d_3}{Rp}\vec{p} \qquad (C.4g)$$

--------

$$\vec{p}_8 = \vec{p} + p\beta_1'\,\hat{r} \qquad |\vec{p}_8| = p\alpha$$

$$\hat{r}_8 = \hat{r}$$

--------

$$\vec{p}_9 = \left(1 - \frac{2d_4\beta_1'}{R}\right)\vec{p} \qquad |\vec{p}_9| = p\alpha$$

$$\hat{r}_9 = r \qquad (C.4h)$$

--------

$$\vec{p}_{10} = (1 + d_3\beta_2)\,\vec{p} - pR\beta_2\,\hat{r} \qquad |\vec{p}_{10}| = p$$

$$\hat{r}_{10} = R\,\hat{r} - \frac{d_3}{p}\vec{p} \qquad (C.4i)$$

$$\vec{p}_{11} = \left[1 + d_3\beta_2 - \frac{\beta_1' d_3}{R}\left(2 + d_3\beta_1'\right)\right]\vec{p}$$

$$- p\left[R\beta_2 - \beta_1'\left(1 + d_3\beta_2\right)\right]\hat{r}$$

$$|\vec{p}_{11}| = p\alpha$$

$$\hat{r}_{11} = \left(1 + d_3\beta_2\right)\hat{r} - \frac{d_3}{Rp}\left(2 + d_3\beta_2\right)\vec{p} \qquad \text{(C.4j)}$$

In the calculation of the transport coefficients the functions

$$L_i = \frac{\vec{p}\cdot\vec{p}_i}{p^2}$$

$$K_i = \frac{\hat{r}\cdot\vec{p}_i}{p} \qquad \text{(C.5)}$$

are needed for the asymptotic states $\vec{p}_i$, $i = 2, 4, 6, 7, 8, 9$ and 11. Defining

$$K_0 = \left(1 - \frac{x^2}{R^2}\right)^{1/2}$$

$$K_0' = \left(1 - x^2\right)^{1/2}, \qquad \text{(C.6)}$$

it is seen that for initial conditions $r \to R\sigma^{\pm}$ and $\vec{p}\cdot\hat{r} > 0$, $\frac{\vec{p}\cdot\hat{r}}{p} = K_0$, for $r \to R\sigma^{-}$ and $\vec{p}\cdot\hat{r} < 0$, $\frac{\vec{p}\cdot\vec{r}}{p} = -K_0$, for $r \to \sigma^{+}$ and $\vec{p}\cdot\hat{r} > 0$, $\frac{\vec{p}\cdot\hat{r}}{p} = K_0'$, and finally for $r \to \sigma^{+}$ and $\vec{p}\cdot\hat{r} < 0$, $\frac{\vec{p}\cdot\hat{r}}{p} = -K_0'$.

Therefore the functions determining the Boltzmann and cross coefficients for scattering states are given by

$$L_2 = \left(1 - \frac{2d_2\beta_1}{Ra}\right) + 2\beta_1 \left(1 - \frac{\beta_1 d_2}{Ra}\right) K_0$$

$$K_2 = \left(1 - \frac{2d_2\beta_1}{Ra}\right) K_0 + 2\beta_1 \left(1 - \frac{\beta_1 d_2}{Ra}\right) \tag{C.7a}$$

--------

$$L_4 = \left[1 + d_1\beta_2' - \frac{d_1\beta_1}{Ra}\left(2 + d_1\beta_2'\right)\right]$$

$$+ \left[2\beta_1 - Ra\beta_2' + 2\beta_1\beta_2' d_1 - \frac{d_1\beta_1^2}{Ra}\left(2 + d_1\beta_2'\right)\right] K_0$$

$$K_4 = \left[1 + d_1\beta_2' - \frac{d_1\beta_1}{Ra}\left(2 + d_1\beta_2'\right)\right] K_0$$

$$+ \left[2\beta_1 - Ra\beta_2' + 2\beta_1\beta_2' d_1 - \frac{d_1\beta_1^2}{Ra}\left(2 + d_1\beta_2'\right)\right] \tag{C.7b}$$

--------

$$L_6 = \left(1 - \frac{d_3\beta_1'}{R}\right) + \left(\frac{\beta_1'}{R}\left(1 + d_3\beta_2\right) - \beta_2\right) K_0'$$

$$K_6 = \left(1 - \frac{d_3\beta_1'}{R}\right) K_0' + \left(\frac{\beta_1'}{R}\left(1 + d_3\beta_2\right) - \beta_2\right) \tag{C.7c}$$

--------

$$L_7 = \left(1 - \frac{d_3\beta_1'}{R}\right) - \frac{\beta_1'}{R} K_0'$$

$$K_7 = -\left(1 - \frac{d_3\beta_1'}{R}\right) K_0' + \frac{\beta_1'}{R} \tag{C.7d}$$

--------

$$L_8 = 1 - \beta_1' K_0$$

$$K_8 = -K_0 + \beta_1' \tag{C.7e}$$

--------

$$L_9 = \left(1 - \frac{2d_4\beta_1'}{R}\right) - \beta_1' K_0$$

$$K_9 = -\left(1 - \frac{2d_4\beta_1'}{R}\right) + \beta_1' \qquad \text{(C.7f)}$$

--------

$$L_{11} = \left[1 + d_3\beta_2 - \frac{d_3\beta_1'}{R}\,(2 + d_3\beta_1')\right]$$

$$- \left[R\beta_2 - \beta_1'\,(1 + d_3\beta_2)\right] K_0$$

$$K_{11} = \left[1 + d_3\beta_2 - \frac{d_3\beta_1'}{R}\,(2 + d_3\beta_1')\right] K_0$$

$$- \left[R\beta_2 - \beta_1'\,(1 + d_3\beta_2)\right]. \qquad \text{(C.7g)}$$

Although it is not obvious from the form given here, $L_{11} = L_6$ and $L_7 = L_8 = L_9$. The $L_i$'s can be shown after some tedious algebra to be equivalent to the functions of Marchetti and Dufty (Equation (B.31) of Reference 29), except for $L_7$, $L_8$ and $L_9$, where the first term in their expression should be $\frac{x^2}{R^2\alpha}$.

2. Bound states

The time dependence of the trajectories shown in Figure C.2 can be expressed as an infinite sum using the impulse function, $I(t_1,t_2)$, defined by

$$I(t_1,t_2) = \begin{cases} 0 & t < t_1 \\ 1 & t_1 < t < t_2 \\ 0 & t_2 < t\ . \end{cases} \qquad \text{(C.8)}$$

For the trajectories which miss the core, the momentum changes are spaced apart by a time $T_4$ given by

$$T_4 = \frac{1}{\sqrt{T^*}} \frac{R}{y} \left(1 - \frac{x^2}{R^2}\right)^{1/2} , \tag{C.9}$$

and those which hit the core by a time $T_3$ given by

$$T_3 = \frac{1}{\sqrt{T^*}} \frac{2}{y} \left(R\left(1 - \frac{x^2}{R^2}\right)^{1/2} - (1 - x^2)^{1/2}\right). \tag{C.10}$$

Note that the definitions of the other reduced variables specifies the units of time to be $\left(\frac{m\sigma^2}{\varepsilon_0}\right)^{1/2}$. It is neither convenient nor necessary to find the momentum or position in any time interval in terms of the initial $\vec{p}$ and $\hat{r}$, instead the functions needed for the bound state contribution to the transport coefficients, $\vec{p}\cdot\vec{p}(t)/p^2$ and $\hat{r}\cdot\vec{p}(t)/p$, can be found directly from the initial value of $\hat{r}\cdot\vec{p}/p$ and the cumulative angle changes in $\vec{p}(t)$ due to collisions at the core and the outer edge of the well. From (C.2d) it is seen that the angular change in the direction of $\vec{p}(t)$ for collisions at $R\sigma$ is given by

$$\cos\theta_1 \equiv \frac{\vec{p}_i\cdot\vec{p}_{i+1}}{p^2} = 2\frac{x^2}{R^2} - 1, \tag{C.11a}$$

and from (C.2b), collision at the core cause an angular change given by

$$\cos\theta_2 = 2x^2 - 1 . \tag{C.11b}$$

Thus the time dependence of $\hat{r}\cdot\hat{p}(-t)/p$ and $\vec{p}\cdot\vec{p}(-t)/p^2$ for the six classes of bound trajectories can be written in the following manner

(I.)

$$\frac{\vec{p}\cdot\vec{p}_I}{p^2} = \sum_{n=0}^{\infty} I(nT_4,(n+1)T_4)\cos n\,\theta_2$$

$$\frac{\hat{r}\cdot\hat{p}_I}{p} = \sum_{n=0}^{\infty} I(nT_4,(n+1)T_4)\cos(n\,\theta_2 - \gamma)$$

$$\text{where } \cos\gamma = \left(1 - \frac{x^2}{R^2}\right)^{1/2} \tag{C.12}$$

(II.)

$$\frac{\vec{p}\cdot\vec{p}_{II}}{p^2} = \sum_{n=0}^{\infty} I(nT_4,(n+1)T_4)\cos((n+1)\,\theta_2)$$

$$\frac{\hat{r}\cdot\vec{p}_{II}}{p} = \sum_{n=0}^{\infty} I(nT_4,(n+1)T_4)\cos((n+1)\,\theta_2 - \gamma')$$

$$\text{where } \cos\gamma' = -\left(1 - \frac{x^2}{R^2}\right)^{1/2} \tag{C.13}$$

(III.)

$$\vec{p}\cdot\vec{p}_{III}/p^2 = \sum_{n=0}^{\infty} I(2nT_3,(2n+1)T_3)\cos(n\alpha) + \sum_{n=1}^{\infty} I((2n-1)T_3,2nT_3)\cos(n\alpha - \theta_2)$$

$$\hat{r}\cdot\vec{p}_{III}/p = \sum_{n=0}^{\infty} I(2nT_3,(2n+1)T_3)\cos(n\alpha - \gamma) + \sum_{n=1}^{\infty} I((2n-1)T_3,2nT_3)\cos(n\alpha - \theta_2 - \gamma)$$

$$\text{where } \alpha = \theta_2 - \theta_1, \tag{C.14}$$

(IV.)

$$\vec{p}\cdot\vec{p}_{IV}/p^2 = \sum_{n=0}^{\infty} I(2nT_3,(2n+1)T_3)\cos(n\alpha + \theta_2) + \sum_{n=1}^{\infty} I((2n-1)T_3,2nT_3)\cos(n\alpha)$$

$$\frac{\hat{r}\cdot\vec{p}_{IV}}{p} = \sum_{n=0}^{\infty} I(2nT_3,(2n+1)T_3)\cos(n\alpha + \theta_2 - \gamma')$$

$$+ \sum_{n=1}^{\infty} I((2n-1)T_3,2nT_3)\cos(n\alpha - \gamma'), \qquad (C.15)$$

(V.)

$$\frac{\vec{p}\cdot\vec{p}_V}{p^2} = \sum_{n=0}^{\infty} I(2nT_3,(2n+1)T_3)\cos(n\alpha - \theta_1)$$

$$+ \sum_{n=1}^{\infty} I((2n-1)T_3,2nT_3)\cos(n\alpha)$$

$$\frac{\hat{r}\cdot\vec{p}_V}{p} = \sum_{n=0}^{\infty} I(2nT_3,(2n+1)T_3)\cos(n\alpha - \theta_1 - \delta)$$

$$+ \sum_{n=1}^{\infty} I((2n-1)T_3,2nT_3)\cos(n\alpha - \delta)$$

where $\cos\delta = (1 - x^2)^{1/2}$ (C.16)

(VI.)

$$\frac{\vec{p}\cdot\vec{p}_{VI}}{p^2} = \sum_{n=0}^{\infty} I(2n+1)T_3)\cos(n\alpha)$$

$$+ \sum_{n=1}^{\infty} I((2n-1)T_3,2nT_3)\cos(n\alpha - \theta_1)$$

$$\frac{\hat{r}\cdot\vec{p}_V}{p} = \sum_{n=0}^{\infty} I(2nT_3,(2n+1)T_3)\cos(n\alpha - \delta')$$

$$+ \sum_{n=1}^{\infty} I((2n-1)T_3,2nT_3)\cos(n\alpha - \theta_1 - \delta')$$

where $\cos\delta' = -(1 - x^2)^{1/2}$ (C.17)

From Equations (C.12) - (C.17) the time dependence of any function of $\hat{r}\cdot\vec{p}(-t)$ and $\vec{p}\cdot\vec{p}(-t)$ can be found; the I-functions ensure that only terms with same argument in I are non-zero. The series can be transformed term by term, and the limit $\varepsilon \to 0$ can be taken after the series is summed into a closed form.

For the shear viscosity, the $\varepsilon \to 0$ limit of the following must be found for the bound state contribution to $\eta_{\phi k,1}$:

$$\lim_{\varepsilon \to 0} \varepsilon \int_0^\infty e^{-\varepsilon t} \left[ \left( \frac{\hat{r} \cdot \vec{p}(-t)}{p} \right) \left( \frac{\vec{p} \cdot \vec{p}(-t)}{p^2} \right) - \frac{1}{3} \frac{\hat{r} \cdot \vec{p}}{p} \right] \tag{C.18}$$

Forming the product in the brackets and taking the transform gives each case (I – VI) as a series of exponentials and cosines; e.g., for cases I and II:

$$\text{(I.)} \quad \lim_{\varepsilon \to 0} \sum_{n=0}^{\infty} \left(1 - e^{\varepsilon T_4}\right) e^{\varepsilon n T_4} \cos(n\theta_2) \cos(n\theta_2 - \gamma) - \frac{1}{3} \cos\gamma$$

$$\text{(II.)} \quad \lim_{\varepsilon \to 0} \sum_{n=0}^{\infty} \left(1 - e^{-\varepsilon T_4}\right) e^{-\varepsilon n T_4} \cos((n+1)\theta_2) \cos((n+1)\theta_2 - \gamma') - \frac{1}{3} \cos\gamma' \tag{C.19}$$

Similar results hold for cases III – VI. Although it appears that the series are zero term by term in the limit $\varepsilon \to 0$, expressing the series in a closed form allows one to identify a piece which is non-zero in that limit. The series can be summed by representing the cosines as exponentials and summing the resultant exponential series. By example consider case (I):

$$\lim_{\varepsilon \to 0} \left\{ \left(1 - e^{-\varepsilon T_4}\right) \sum_{n=0}^{\infty} e^{-n\varepsilon T_4} \frac{1}{4} \left(e^{in\theta_2} + e^{-in\theta_2}\right) \left(e^{i(n\theta_2 - \gamma)} + e^{-i(n\theta_2 - \gamma)}\right) \right\}$$

$$- \frac{1}{3} \cos\gamma =$$

$$\lim_{\varepsilon \to 0}\left\{\left(1-e^{-\varepsilon T_4}\right) \frac{1}{4} \sum_{n=0}^{\infty} \left[e^{n(2i\theta_2-\varepsilon T_4-i\gamma)} + e^{-n\varepsilon T_4} 2 \cos \gamma + e^{-n(2i\theta_2+\varepsilon T_4-i\gamma)}\right]\right\}$$

$$- \frac{1}{3} \cos \gamma =$$

$$\lim_{\varepsilon \to 0}\left\{\frac{1-e^{-\varepsilon T_4}}{4}\left[\left(1-e^{-\varepsilon T_4+i(2\theta_2-\gamma)}\right)^{-1} + \left(1-e^{-\varepsilon T_4-i(2\theta_2-\gamma)}\right)^{-1}\right]\right.$$

$$\left. + \frac{1}{2} \cos \gamma\right\} - \frac{1}{3} \cos \gamma =$$

$$\lim_{\varepsilon \to 0} \frac{1-e^{-\varepsilon T_4}}{2} \left[\frac{1+e^{-\varepsilon T_4} \cos(2\theta_2-\gamma)}{1-2e^{-\varepsilon T_4} \cos(2\theta_2-\gamma)+e^{-2\varepsilon T_4}}\right] + \frac{1}{6} \cos \gamma = \frac{1}{6} \cos \gamma \qquad (C.20)$$

Similar results can be found for the other cases, giving the general result for the bound states as

$$\lim_{\varepsilon \to 0} \varepsilon \int_0^\infty e^{-\varepsilon t}\left[\left(\frac{\hat{r}\cdot\vec{p}(-t)}{p}\right)\left(\frac{\vec{p}\cdot\vec{p}(-t)}{p}\right) - \frac{1}{3} \frac{\hat{r}\cdot\vec{p}}{p}\right]$$

$$= \frac{1}{6} \frac{\hat{r}\cdot\vec{p}}{p} . \qquad (C.21)$$

This surprisingly simple result leads to the bound state contribution to $n_{\phi k,1}$ evaluated in Chapter V.

# REFERENCES

1. J. E. Mayer and M. G. Mayer, Statistical Mechanics (John Wiley and Sons, New York, 1940).

2. J. R. Dorfman and H. van Beijeren, in Statistical Mechanics, Part B, ed. B. J. Berne (Plenum Press, New York, 1977). An extensive review of literature on the kinetic theory of gases is included here.

3. J. R. Dorfman and E. G. D. Cohen, J. Math. Phys. 8, 282 (1967).

4. J. V. Sengers, D. T. Gillespie, and J. J. Perez-Esandi, Physica 90A, 365 (1978); D. T. Gillespie and J. V. Sengers, Three-Particle Collision Integrals for Thermal Conductivity, Viscosity and Self-Diffusion of a Gas of Hard Spherical Molecules. Part II. Calculations, Technical Report AEDC-TR-73-171 (Arnold Engineering Development Center, Tennessee, 1973);Triple Collision Effects in the Thermal Conductivity and Viscosity of Moderately Dense Gases. Part II. Technical Report AEDC-TR-71-51 (Arnold Engineering Development Center, Tennessee, 1971); in Proc. 5th Symposium on Thermophysical Properties, C. F. Bonilla, ed. (American Society of Mechanical Engineers, New York, 1970); J. V. Sengers, M. H. Ernst and D. T. Gillespie, J. Chem. Phys. 56, 5583 (1972); W. R. Hoegy and J. V. Sengers, Phys. Rev. A2, 2461 (1970); J. V. Sengers, D. T. Gillespie and W. R. Hoegy, Phys. Lett. 32A, 387 (1970); J. V. Sengers, Acta Physica Austriaca, Suppl. X, 177 (1973); in Kinetic Equations, R. L. Liboff and N. Rostoker, eds. (Gordon and Breach, New York, 1971); Triple Collision Effects in the Thermal Conductivity and Viscosity of Moderately Dense Gases, Technical Report AEDC-TR-69-68 (Arnold Engineering Development Center, Tennessee, 1969); in Boulder Lectures in Theoretical Physics, Vol. 9C, Kinetic Theory, W. E. Britten, ed. (Gordon and Breach, New York, 1967); Phys. Fluids 9, 1333 (1966).

5. D. McQuarrie, Statistical Mechanics (Harper and Row, Pub., Inc., New York, 1976). A comparison of different potential models for virial coefficients and low density transport coefficients can be found here and in many other standard texts.

6. J. P. J. Michels and N. J. Trappeniers, Physica 101A, 156 (1980).

7. Y. Kan and J. R. Dorfman, Phys. Rev. A 16, 2447 (1977) and references listed therein.

8. J. H. Ferziger and H. G. Kaper, Mathematical Theory of Transport Processes in Gases, (North-Holland Pub. Co., Amsterdam, 1972).

9. R. W. Zwanzig, Ann. Rev. Phys. Chem. 16, 67 (1965).

10. J. A. McLennan, J. Stat. Phys. 28, 257 (1982).

11. J. P. J. Michels and N. J. Trappeniers, Chem. Phys. Lett 33, 195 (1975); Physica 104A, 243 (1980); 107A, 158, 299 (1981); 116A, 516 (1982).

12. M. H. Ernst, J. R. Dorfman, and E. G. D. Cohen, Physica 31, 493 (1965).

13. J. L. Lebowitz, J. K. Percus and J. Sykes, Phys. Rev. 188, 487 (1969).

14. P. A. Egelstaff, W. Glaser, D. Litchinsky, E. Schneider, and J. B. Suck, Phys. Rev. A 27, 1106 (1983).

15. S. Yip, W. Alley, and B. Alder, J. Stat. Phys. 27, 201 (1982).

16. J. J. Ullo and S. Yip, Phys. Rev. A, to be published.

17. H. J. M. Hanley, R. D. McCarty and D. G. D. Cohen, Physica 60, 322 (1972).

18. J. P. Hansen and I. R. McDonald, Theory of Simple Liquids, (Academic Press Inc., London, 1976).

19. B. J. Alder, D. M. Gass, and T. E. Wainwright, J. Chem. Phys. 53, 3813 (1970).

20. J. V. Sengers, Int. J. Heat Mass Transfer 8, 1103 (1965).

21. M. C. Marchetti and J. W. Dufty, Chem. Phys. Letters 70, 539 (1980).

22. D. K. Hoffman and C. F. Curtiss, Phys. Fluids 8, 667 (1965).

23. R. Zwanzig, Phys. Rev. 129, 486 (1961).

24. J. W. Dufty, M. J. Lindenfeld and G. E. Garland, Phys. Rev. A 24, 3212 (1981).

25. M. H. Ernst, J. R. Dorfman, W. R. Hoegy, and J. M. J. van Leuwen, Physica 45, 127 (1969).

26. M. H. Ernst, L. K. Haines, and J. R. Dorfman, Rev. Mod. Phys. 41, 296 (1969).

27. D. B. Boercker and J. W. Dufty, Phys. Rev. A 23, 1952 (1981).

28. J. A. McLennan, Prog. Theoret. Phys. (Kyoto) 30, 408 (1963).

29. M. C. Marchetti and J. W. Dufty, Phys. Rev. A 24, 2116 (1981).

30. E. M. Holleran and H. M. Hulbert, J. Chem. Phys. 129, 232 (1951).

31. S. G. Brush and J. D. Lawrence, Report U.C.R.L. - 7376, Lawrence Radiation Laboratory, University of California, Livermore, CA (1963).

32. J. Karkeck and G. Stell, to be published.

33. W. M. Haynes, Physica 67, 440 (1973); 76, 1 (1974).

34. J. A. Barker, in Rare Gas Solids, Volume I, M. L. Klein and J. A. Venables, eds. (Academic Press, London, 1976).

35. D. E. Stogryn and J. O. Hirschfelder, J. Chem. Phys. 31, 1531 (1959).

36. G. E. Garland and J. W. Dufty, Int. Jour. Quant. Chem. 16, 91 (1982).

# BIOGRAPHICAL SKETCH

Gregory Ellis Garland was born on November 6, 1955, in Rayville, Louisiana. He graduated from Start High School, in Start, Louisiana, in May of 1973. He received the Bachelor of Science degree in physics from Northwestern State University of Louisiana in Natchitoches, Louisiana, in May of 1977. He has been in graduate studies at the University of Florida since September, 1977. He is a member of Phi Kappa Phi and Sigma Pi Sigma.

I certify that I have read this study and that in my opinion it conforms to acceptable standards of scholarly presentation and is fully adequate, in scope and quality, as a dissertation for the degree of Doctor of Philosophy.

James W. Dufty, Chairman
Professor of Physics

I certify that I have read this study and that in my opinion it conforms to acceptable standards of scholarly presentation and is fully adequate, in scope and quality, as a dissertation for the degree of Doctor of Philosophy.

Charles F. Hooper, Jr.
Professor of Physics

I certify that I have read this study and that in my opinion it conforms to acceptable standards of scholarly presentation and is fully adequate, in scope and quality, as a dissertation for the degree of Doctor of Philosophy.

J. R. Buchler

J. Robert Buchler
Professor of Physics

I certify that I have read this study and that in my opinion it conforms to acceptable standards of scholarly presentation and is fully adequate, in scope and quality, as a dissertation for the degree of Doctor of Philosophy.

Gary G. Ihas

Gary G. Ihas
Associate Professor of Physics

I certify that I have read this study and that in my opinion it conforms to acceptable standards of scholarly presentation and is fully adequate, in scope and quality, as a dissertation for the degree of Doctor of Philosophy.

K.Y. Chen

K. W. Chen
Professor of Astronomy

This dissertation was submitted to the Graduate Faculty of the Department of Physics in the College of Liberal Arts and Sciences and to the Graduate School, and was accepted as partial fulfillment of the requirements for the degree of Doctor of Philosophy.

April 1984

Madelyn Lockhart

Dean for Graduate Studies and
Research

UNIVERSITY OF FLORIDA
3 1262 08666 349 8